WADD TECHNICAL REPORT 60-699
VOLUME X

ENERGY CONVERSION SYSTEMS REFERENCE HANDBOOK

VOLUME X — REACTOR SYSTEM DESIGN

Atomics International

Electro-Optical Systems, Inc.

SEPTEMBER 1960

Flight Accessories Laboratory
Contract Nr. AF 33(616)-6791
Project Nr. 4769
Task Nr. 61048

WRIGHT AIR DEVELOPMENT DIVISION
AIR RESEARCH AND DEVELOPMENT COMMAND
UNITED STATES AIR FORCE
WRIGHT-PATTERSON AIR FORCE BASE, OHIO

700 — May 1961 — 30-1134

ABSTRACT

This report discusses various aspects of reactor design with respect to inherent limitations and system requirements and outlines in some detail many problems which are common to all nuclear systems such as shielding, reliability, heat rejection, and safety.

This report was prepared by Atomics International, a Division of North American Aviation, under contract to the Missiles Project Branch of the Atomic Energy Commission. It was made available to Electro-Optical Systems, Inc., for inclusion in this Energy Conversion Systems Reference Handbook.

ENERGY CONVERSION SYSTEMS REFERENCE HANDBOOK

LIST OF VOLUME AND SECTION TITLES WITH AUTHORS

ENERGY CONVERSION SYSTEMS REFERENCE HANDBOOK

LIST OF VOLUME AND SECTION TITLES WITH AUTHORS (CONT'D)

A complete detailed Table of Contents for all volumes of Energy Conversion Systems Reference Handbook is included in Volume I.

CONTENTS

VOLUME X

CONTENTS (cont.)

ILLUSTRATIONS

VOLUME X

Figures

Figures

Figures

Tables

Tables

VOLUME X

REACTOR SYSTEM DESIGN

Manuscript released by the author September 1960 for publication in this Energy Conversion Systems Reference Handbook.

SUMMARY

The high energy content of nuclear power systems (10^6 electrical watt-hr/lb) makes them an extremely attractive source of space power in the hundreds of watts to tens of kilowatt power range. The use of ion, plasma and other electrical propulsion devices proposed for space vehicles will require hundreds to thousands of kilowatts. Nuclear electrical power systems appear to be the only reasonable means of providing this power.

For significant electrical power loads, which are required for missions in excess of several days, only solar and nuclear systems can be considered. Batteries and other chemical systems are ruled out on the basis of the large weights associated with these systems. At power levels of the order of a few kilowatts, both the various solar and nuclear power systems offer their own specific advantages and disadvantages, and the selection of a particular solar or nuclear power system can only be accomplished in the context of specific mission requirements, payload considerations, reliability, costs, etc. As the power requirements are increased to the order of tens of kilowatts, the nuclear systems have an increasingly favorable weight, size, and cost advantage over any of the presently envisioned solar power systems. For power levels in the hundreds of kilowatts and for all powers above a nuclear system is the only one which appears at all feasible.

An estimate of the space power requirements versus time is shown in Fig. S-1. Also shown in this figure, as a function of availability and power level, are the nuclear power systems currently under development. Some typical space missions are listed as appropriate to the power level of these developmental systems.

At the present time there are three promising approaches to converting nuclear heat to electrical power. They are the turboelectric, thermoelectric, and thermionic conversion systems. The specific weights of nuclear systems employing these conversion schemes are shown in Fig. S-2 as a function of power level. From this it is seen that low specific weight nuclear power systems are obtainable. Specific weight is a major criterion for

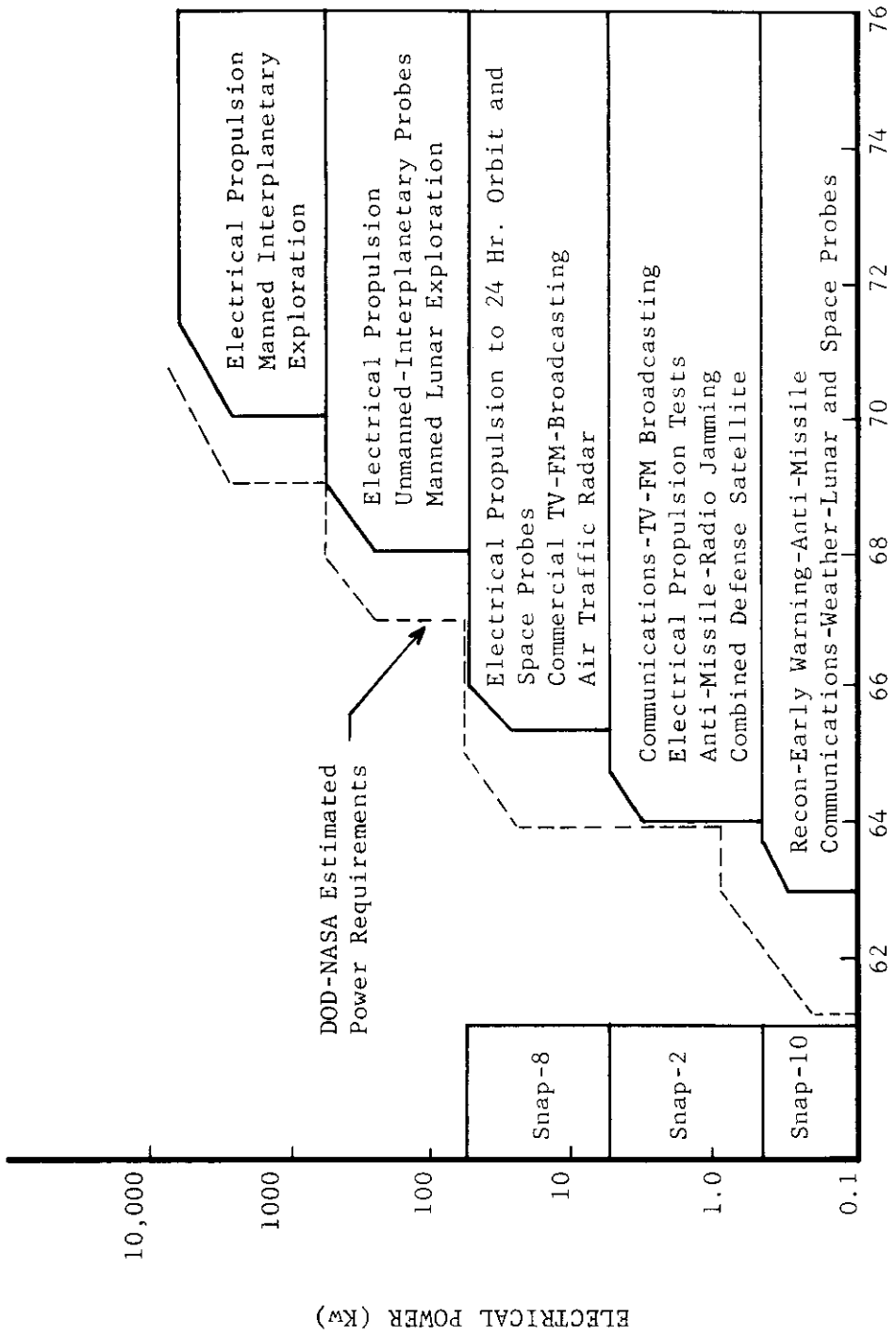

Figure S-1. Space Power Requirements and First Flight Availability

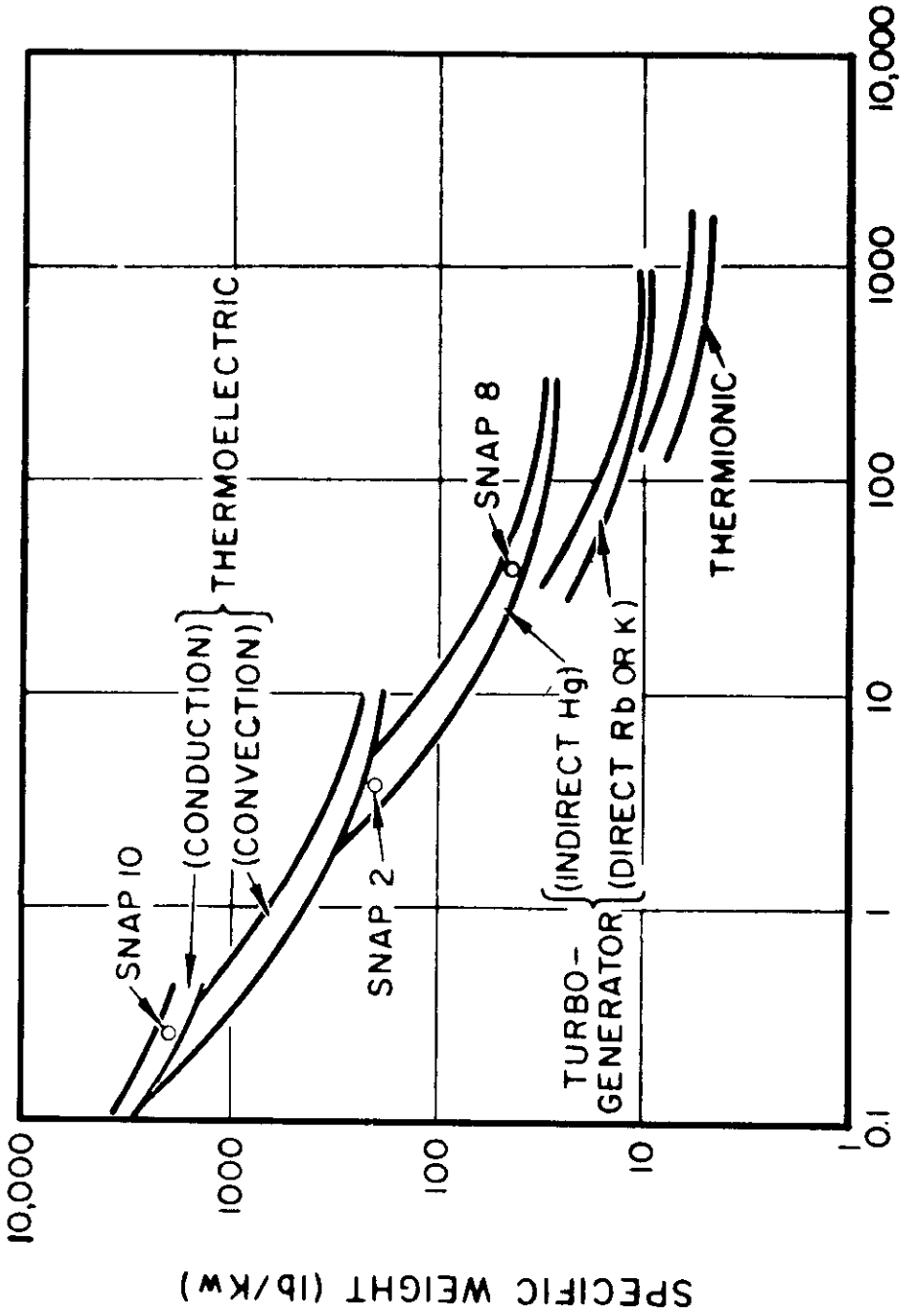

Figure S-2. Specific Weight vs Power Output for Nuclear Power Systems

the selection of a space power system, since every pound of weight associated with the power system subtracts from the available payload weight. For the very promising ion, plasma, and other electrical propulsion schemes, their desirability and usefulness will, to a large extent, be determined by the weight of their associated electrical generating systems.

The major advantages of nuclear space power plants lie in their ability to achieve low specific weights, long life, extremely small area requirements and independence of a changing space environment, (e.g., there is no need for orientation, energy storage when shaded from the sun and the associated sensing devices required for most solar powered systems). That nuclear power systems can make a significant contribution to meaningful space missions is undeniable. In fact, the ability to explore and ultimately utilize space may well be contingent upon the development of high power, light weight nuclear power systems.

1. INTRODUCTION

It is generally recognized that light weight nuclear systems will be required to furnish the increasing power demands of our future space programs. At the present time there is a vigorous and costly national program devoted to the development of extremely high thrust space vehicle booster systems. These large and expensive booster systems will have the capability of placing large vehicles and payloads into space. The successful utilization of these large payloads will only be realized with the concurrent availability of light weight, long-lived, high-power, reliable electrical generating systems.

In order to meet the need for space power, the Atomic Energy Commission currently has under development three space reactor power systems as part of the SNAP (Systems for Nuclear Auxiliary Power) program. These systems range from 500 watts to 60 kw in electrical power output. They are the SNAP 10A, a 500-watt static power unit utilizing thermoelectric conversion; the SNAP 2, a 3-kwe turbogenerator unit employing a high temperature mercury Rankine cycle; and the SNAP 8, a 30 to 60 kwe system which is a scale-up of the SNAP 2 unit. The SNAP 8 system is being developed in conjunction with the National Aeronautics and Space Administration. These systems are described in detail elsewhere.

A nuclear power supply for space vehicle applications is composed of three major subsystems: a nuclear reactor heat source, a power conversion system, and a heat rejection system. Some of the major requirements which are imposed on the power system are listed in Table 1-1.

Presently there are three available means of converting nuclear heat to electrical power. They are the turboelectric, the thermoelectric, and thermionic conversion systems. Each of these systems imposes different restrictions and operating conditions on the reactor. In addition to the requirement imposed by the particular power conversion system employed, there are some stringent requirements imposed upon the reactor design itself, if the total system is to meet the specifications of Table 1-1.

TABLE 1-1

NUCLEAR SPACE POWER SYSTEM REQUIREMENTS

Operation in space environment
Minimum weight and size
Long unattended life
High reliability
Completely automatic control
Safe handling and operation
Remote orbital startup capability
Minimum disturbing torques introduced into vehicle
Minimum vehicle modifications for installation

The reactor design considerations are treated elsewhere in this report. Discussion of nuclear power systems, weights, performance, etc., are presented in sections defined by the method of the power conversion system selected, i.e., thermoelectric, turboelectric and thermionic. Discussion of those items which are common to all nuclear space systems such as shielding, safety, reliability, heat rejection, are treated in separate sections.

While an attempt has been made to generalize the material presented, where it was necessary for illustrative purposes, information and numerical examples of the SNAP 2, 8, 10 systems are employed.

2. HEAT REJECTION SYSTEMS

2.1 Introduction

The heat rejection system for space power plants is a major weight item, and for high power systems may be the predominant one. For this reason considerable effort can profitably be expended to ensure the design of minimum weight systems.

The large number of variables involved in the design of a radiator condenser makes it impossible to prepare a single design curve. The different aspects of the radiator-condenser design problem are considered in the following sections. The data developed in these sections are then combined in Section 2.6 where a procedure leading to the determination of a minimum weight heat rejection system is developed. An example of the procedure is presented for the SNAP 2 radiator design point which requires the mercury working fluid to be condensed at $600^{\circ}F$. The example illustrates that minimum weight heat rejection systems can only be determined when all the design parameters are simultaneously considered.

2.2 Pressure Drop

2.2.1 Condensing Systems

Viscous drag is the mechanism by which condensate is removed from a radiative condenser. The working fluid enters the radiator-condenser as saturated vapor, and is condensed at substantially constant temperature by being subjected to a constant heat flux throughout the length of the tube. After the working fluid has been completely condensed it may be subcooled to reduce the possibility of pump cavitation, and in the case of turboelectric systems, to provide a low-temperature bearing and alternator coolant.

The design of a minimum weight condensing radiator requires an accurate prediction of the pressure drop associated with condensing in the radiator tubes. This must be done with some precision since a loss of static pressure in the condenser tubes lowers the (saturation) temperature of the working fluid, resulting in a drop in radiating power.

Many investigators have correlated pressure drop data for two-phase flow in tubes. Of these, the correlation of Lockhart and Martinelli[1] is probably the best and most widely used. They were able to correlate pressure drop for two-phase, two-component flow in the non-dimensional form:

$$\left(\frac{dP}{d\ell}\right)_{TPF} = \phi_g^2 \left(\frac{dP}{d\ell}\right)_g , \qquad (2\text{-}1)$$

where

$\left(\frac{dP}{d\ell}\right)_{TPF}$ = two phase frictional pressure gradient,

$\left(\frac{dP}{d\ell}\right)_g$ = pressure gradient per unit tube length of the gas (vapor) phase alone,

ϕ_g = dimensionless parameter which is a function only of $\frac{\left(\frac{dP}{d\ell}\right)_\ell}{\left(\frac{dP}{d\ell}\right)_g}$;

and

$\left(\frac{dP}{d\ell}\right)_\ell$ = pressure gradient per unit tube length of the liquid phase alone.

The experimental data of Lockhart and Martinelli were plotted in terms of

ϕ_g and $\sqrt{\left(\frac{dP}{d\ell}\right)_\ell \Big/ \left(\frac{dP}{d\ell}\right)_\ell}$ for different combinations of flow regimes,

e.g., viscous liquid-turbulent gas (viscous-turbulent), and turbulent liquid-turbulent gas. While these correlations were for two-component flow, extension of these correlations to boiling or condensing (i.e., two-phase one-component flow) has been suggested by Martinelli and Nelson[2] and has been tested with some success. In support of this extrapolation, McAdams[3] has found that friction arising from transfer of momentum between phases of a one-component system was of little importance under his experimental conditions. Furthermore, Lockhart and Martinelli stated that their

correlation was independent of flow mechanism, whether mist, annular or stratified flow existed. Unpublished experimental work being conducted by AI and its subcontractors indicates that these correlations predict reasonable values for condensing pressure drop in tubes.

The Lockhart and Martinelli correlation for viscous-turbulent flow is reproduced in Fig. 2-1. In the range of interest this can be represented by

$$\phi_g = 1.76\, X^{0.0825}, \qquad (2\text{-}2)$$

where

$$X = \sqrt{\frac{\left(\frac{dP}{d\ell}\right)_\ell}{\left(\frac{dP}{d\ell}\right)_g}} \qquad (2\text{-}3)$$

By combining Equations (2-1), (2-2), and (2-3) with the appropriate values of $(dP/d\ell)_g$ and integrating the resulting expression to account for the changing flow conditions throughout the length of the tube, an expression for the frictional pressure drop can be derived.[11] The result is given by:

$$\left(\frac{\Delta P}{L}\right)_{TPF} = \frac{0.402 W_T^{1.684} \mu_g^{0.316}}{N^{1.684} D^{4.684} \rho_g g_c} \left(\frac{\rho_g \mu_\ell}{\rho_\ell \mu_g}\right)^{0.0825} \qquad (2\text{-}4)$$

where

W_T = weight flow
μ_g = viscosity of vapor
μ_ℓ = viscosity of liquid
N = number of tubes
D = inside tube diameter
ρ_g = density of vapor
ρ_ℓ = density of liquid
g_c = gravitational constant

Any consistent system of units may be used.

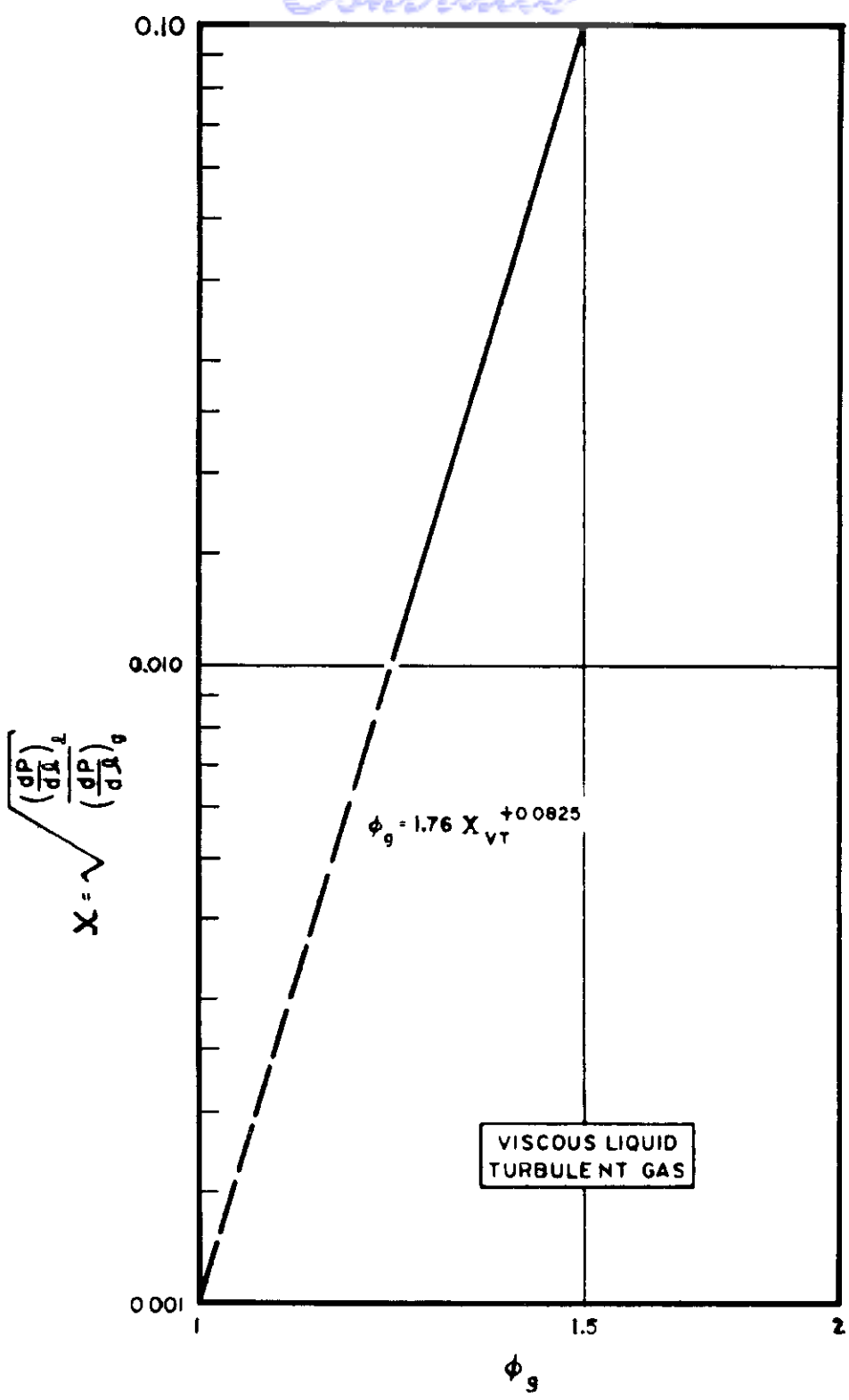

Figure 2-1. Correlation of Lockhart and Martinelli for Two-Phase Flow

In addition to the frictional pressure drop given by Equation 2-4 there is a pressure rise due to the momentum loss of the high velocity mercury vapor as it traverses the condenser tube. Since the fluid velocity is essentially zero at the exit of the condenser this is given by:

$$(\Delta P)_M = \int_{\text{inlet}}^{\text{outlet}} \rho u du = -\rho_g U_o^2 , \qquad (2\text{-}5)$$

or for parallel flow through N tubes

$$(\Delta P)_M = -\left(\frac{1.62 W_T^2}{\rho_g g_c D^4 N^2}\right), \qquad (2\text{-}6)$$

where the negative sign indicates a pressure rise. Equations 2-4 and 2-6 can be used to calculate the pressure drop in condensing radiators.

2.2.2 Noncondensing Systems

In noncondensing systems, which reject heat by cooling a liquid, the pressure drop is easily predicted by the Fanning friction equation:

$$\frac{dP}{d\ell} = \frac{2f u^2 \rho}{g_c D} \qquad (2\text{-}7)$$

where the friction factor, f, is given by

$$f = 0.079\ Re^{-0.25} \qquad (2\text{-}8)$$

For flow through N tubes in parallel:

$$\frac{\Delta P}{L} = 0.242\ \frac{W_T^{1.75}\ \mu^{0.25}}{N^{1.75} D^{4.75} \rho\ g_c} \qquad (2\text{-}9)$$

Equation 2-9 gives the pressure drop for a noncondensing radiator.

2.3 Heat Transfer

For most nuclear-system radiators the controlling thermal resistance is conduction and radiation in the fin itself. Condensing and forced convection coefficients are ordinarily orders of magnitude greater than radiator coefficients. Therefore the preliminary designer need only consider heat transfer in the fin.[4,11] Heat transfer from the working fluid to the fin is a second-order effect and of course must eventually be treated in some detail.

2.3.1 Temperature

Radiant heat transfer is described by the following equation:

$$Q = \epsilon\sigma A(T_o^4 - T_{sink}^4) , \qquad (2\text{-}10)$$

where

Q = radiative power (Btu/hr)

ϵ = surface emissivity

A = surface area (ft^2)

σ = Stephen Boltzman constant = 0.171×10^{-8} Btu/hr-ft^2-$^oR^4$

T_o = radiating surface temperature (^oR)

T_{sink} = radiative sink temperature (^oR)

The exact determination of T_{sink} is a complicated calculation requiring a detailed knowledge of the specific mission and conditions involved. A detailed study[5] for a satellite orbiting the earth at a 300-mile altitude, reveals that the effective radiative sink temperature is about 0^oF. This value is sufficiently low in comparison with the range of T_o under consideration for space applications as to permit the neglect of this term. With this assumption, Equation 2-10 is greatly simplified and reduces to

$$Q = \epsilon\sigma A T_o^4 \qquad (2\text{-}11)$$

Equation 2-11 is plotted in Fig. 2-2 for values of ϵ from 0.2 to 1.0.

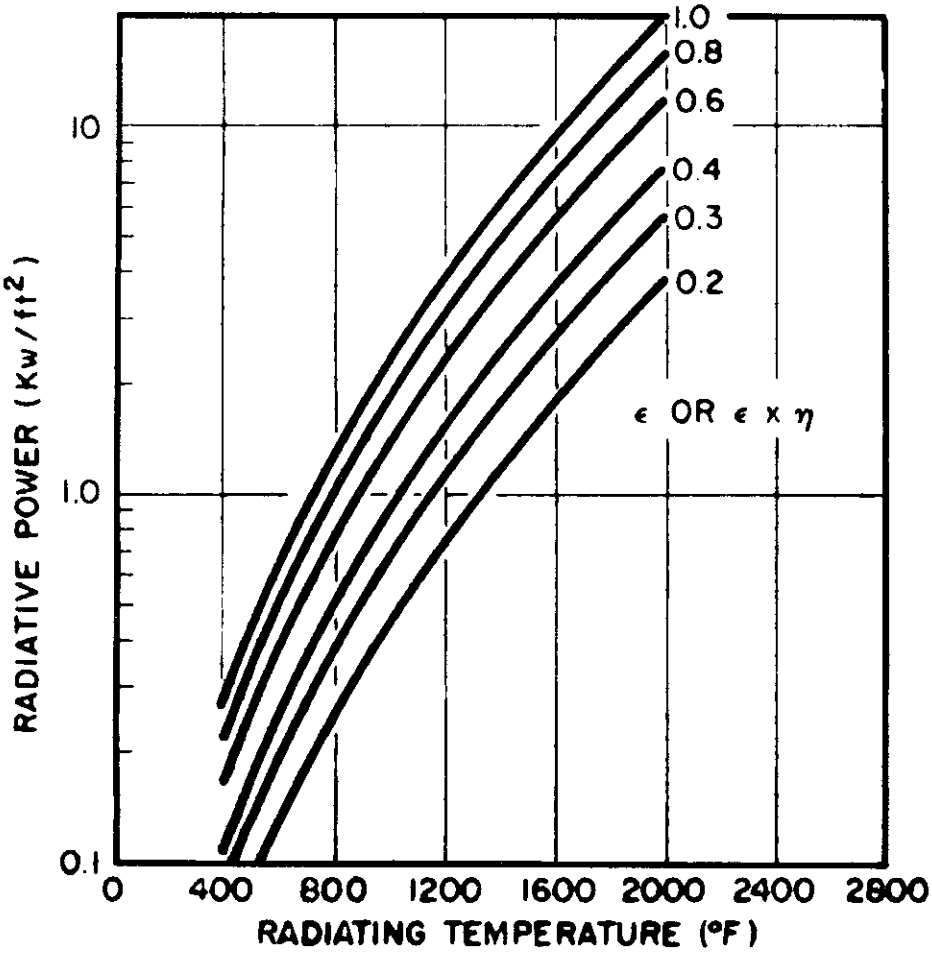

Figure 2-2. Radiative Heat Flux vs Temperature

2.3.2 Fin Effectiveness

A quantity termed the fin effectiveness is introduced to assist in the evaluation of the performance of the tube-and-fin radiator. It is defined as the ratio of the heat rejected by the fin to that which would be rejected if the entire fin were maintained at the base temperature. The model used to calculate the fin effectiveness is shown in Fig. 2-3. Expressed mathematically:

$$\eta = \frac{\int_0^{B/2} T_x^4 dx}{\frac{B}{2} T_o^4} \qquad (2\text{-}12)$$

where

η = fin effectiveness
B = tube spacing
T_x = temperature at a point on the fin
x = distance along fin

This equation was derived by Coombs[11] et al., and was solved numerically on an IBM-704 computer. The results are given in Fig. 2-4 as a function of the dimensionless parameter M_r, defined as:

$$M_r = \frac{B^2 \epsilon \sigma T_o^3}{kt} \qquad (2\text{-}13)$$

where

k = conductivity of fin material
t = fin thickness

By using the curve in Fig. 2-4, the fin effectiveness may be evaluated for a given material, geometry, and base temperature (T_o).

2.3.3 Radiator Area Requirements

2.3.3.1 Condensing Systems

For condensing radiators, the tube temperature remains constant until the fluid is completely condensed. This will be true only if the static pressure drop is kept small since the condensate

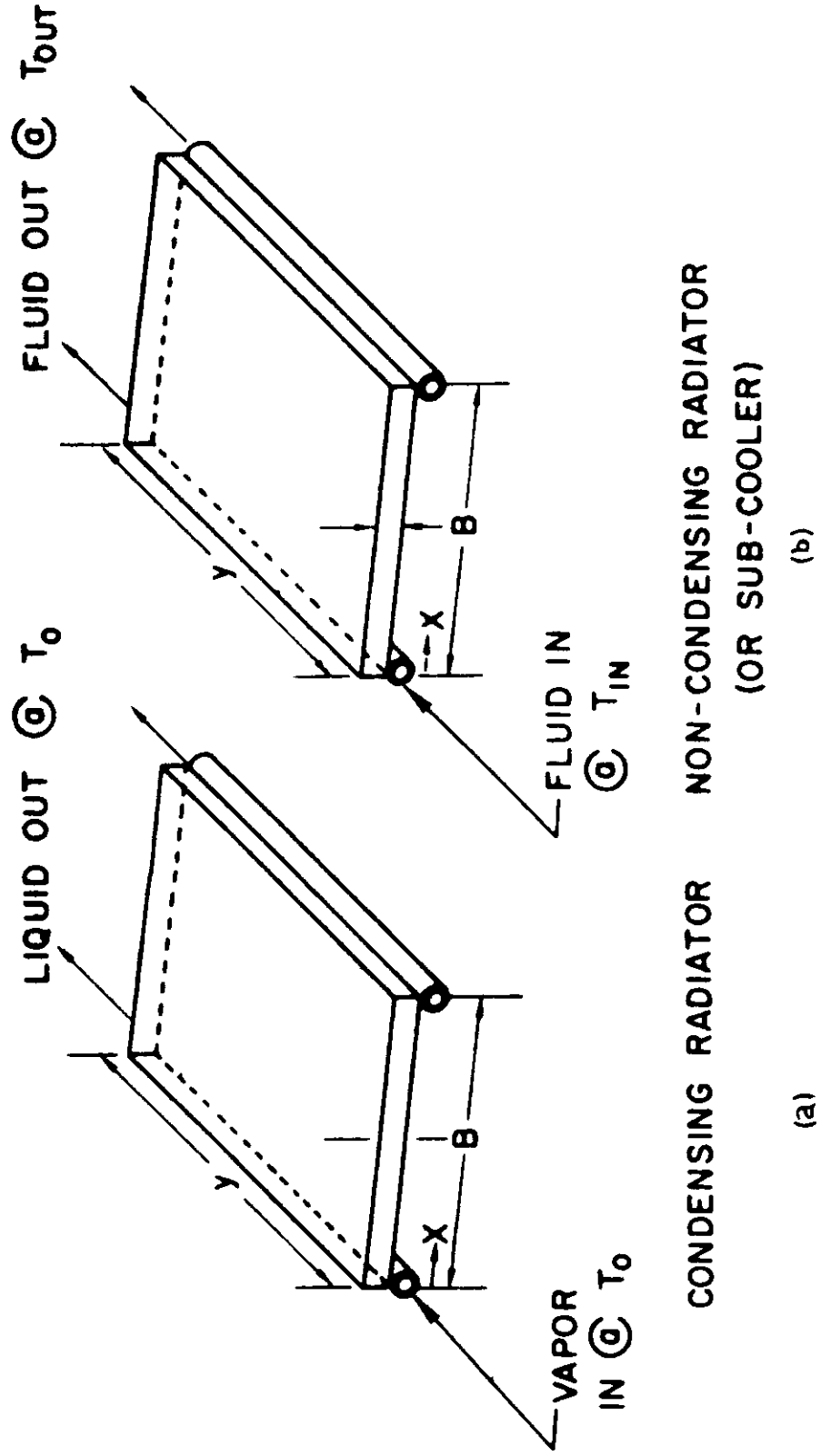

Figure 2-3. Tube and Fin Radiator

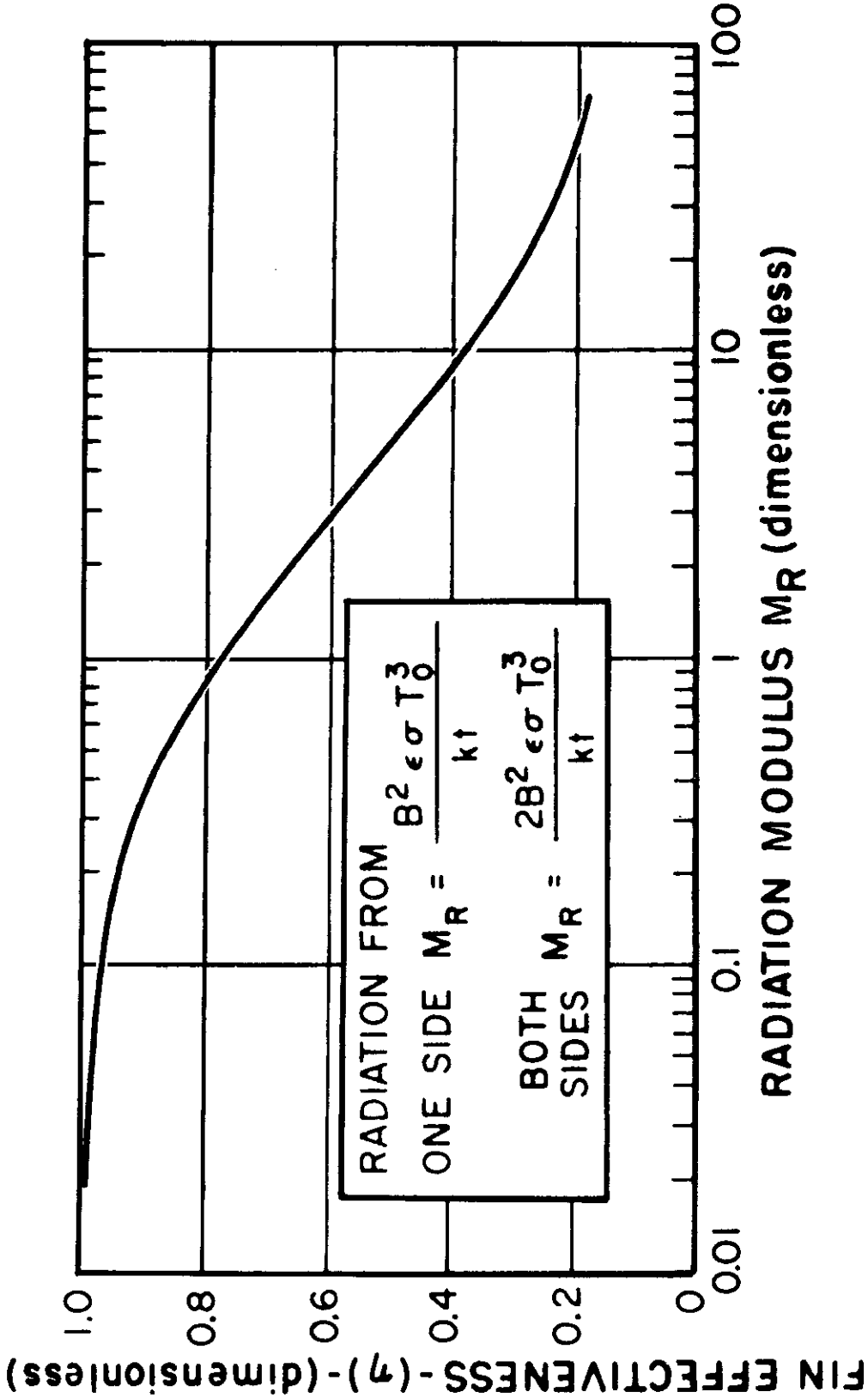

Figure 2-4. Fin Effectiveness vs Radiation Modulus

and condensing vapor are always in thermal equilibrium. If this condition is met, the area requirements for the condensing portion of the radiator can be obtained by combining Equation 2-4 with the definition of fin effectiveness.

$$Q = \epsilon\sigma\eta\ AT_o^4 \qquad (2\text{-}14)$$

Figure 2-2 can be used directly to obtain the required area if the ϵ as shown is considered to be equal to the product, e x η.

2.3.3.2 Noncondensing Systems

In noncondensing systems (or in the subcooling section of condensing systems) the radiant heat rejection is accompanied by a sensible heat loss of the fluid. The temperature decrease of the fluid results in temperature gradients both perpendicular and parallel to the direction of fluid flow. This complicates the analysis, but by combining the model of the condensing (constant temperature) fin with that of a radiator which experiences a coolant temperature drop (Fig. 2-3b), an expression can be derived to give the area requirements for the tube-fin configuration.[11] The result is given by:

$$Q = \eta\sigma\epsilon AT_{eff}^4 \qquad (2\text{-}15)$$

where

Q = radiative power (Btu/hr)

A = area required (ft^2)

T_{in} = fluid temperature into radiator (^oR)

T_{out} = fluid temperature out of radiator (^oR)

$$T_{eff} = \left[\frac{3T_{in}^3 T_{out}^3}{T_{in}^2 + T_{in}T_{out} + T_{out}^2}\right]^{1/4}$$

and

η = fin effectiveness (evaluated at T_{eff}. Figure 2-4 can be used as in the case of the condensing radiator, with M_R also based on T_{eff}.

Equation (2-15) is plotted in Fig. 2-5 for various values of T_{in} and ΔT. This figure can be used to determine the area requirements for the non-condensing radiator.

2.3.4 Emissivity

Since metals in general have low emissivities, they are not good radiating surfaces. To reduce weight, it may become necessary to apply a surface coating of a high-emissivity material. A survey of the literature indicates that certain ceramic coatings, such as Al_2O_3, ZrO_2, and ZrS_iO_4, are attractive from the standpoint of high-emissivity.

Figure 2-6 presents emissivity data for various oxidized metals as a function of temperature.[6] The curve for mild steel shows this material to be attractive but the high weight associated with steel fins precludes them from consideration in this temperature range.

2.4 Meteoroid Protection

At the present time there is considerable doubt associated with the methods used to calculate the amount of armor required to provide adequate meteoroid protection. The best effort to date to correlate the small amount of experimental data with a reasonable analytical model has been by Bjork.[7,8] While admittedly his results are probably conservative, his approach appears justifiable in view of the meager experimental data available. It is essentially an extension of this procedure which is briefly outlined here and leads to the determination of the armor requirements for meteoroid protection of the radiator.

There are two methods by which meteoroids may damage the radiator. The first is puncture of fluid lines, causing loss of working fluid. The second is erosion of the radiator surface or surface coatings, causing a change in surface emissivity. Both of these effects must be considered in the design of a space radiator, and both are quite sensitive to the assumed flux density of meteoroids.

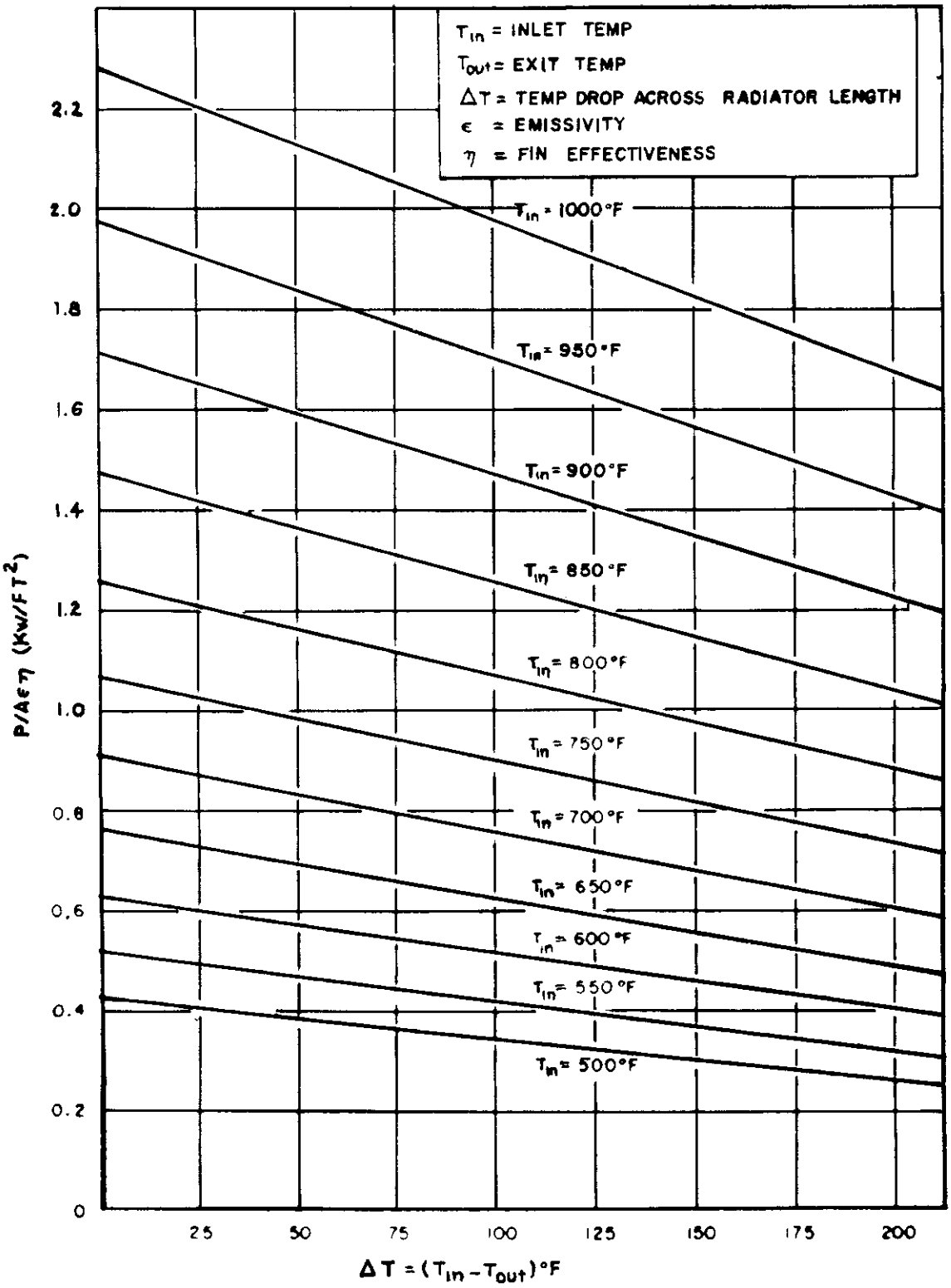

Figure 2-5. Radiator Area Requirements for Subcooler Section

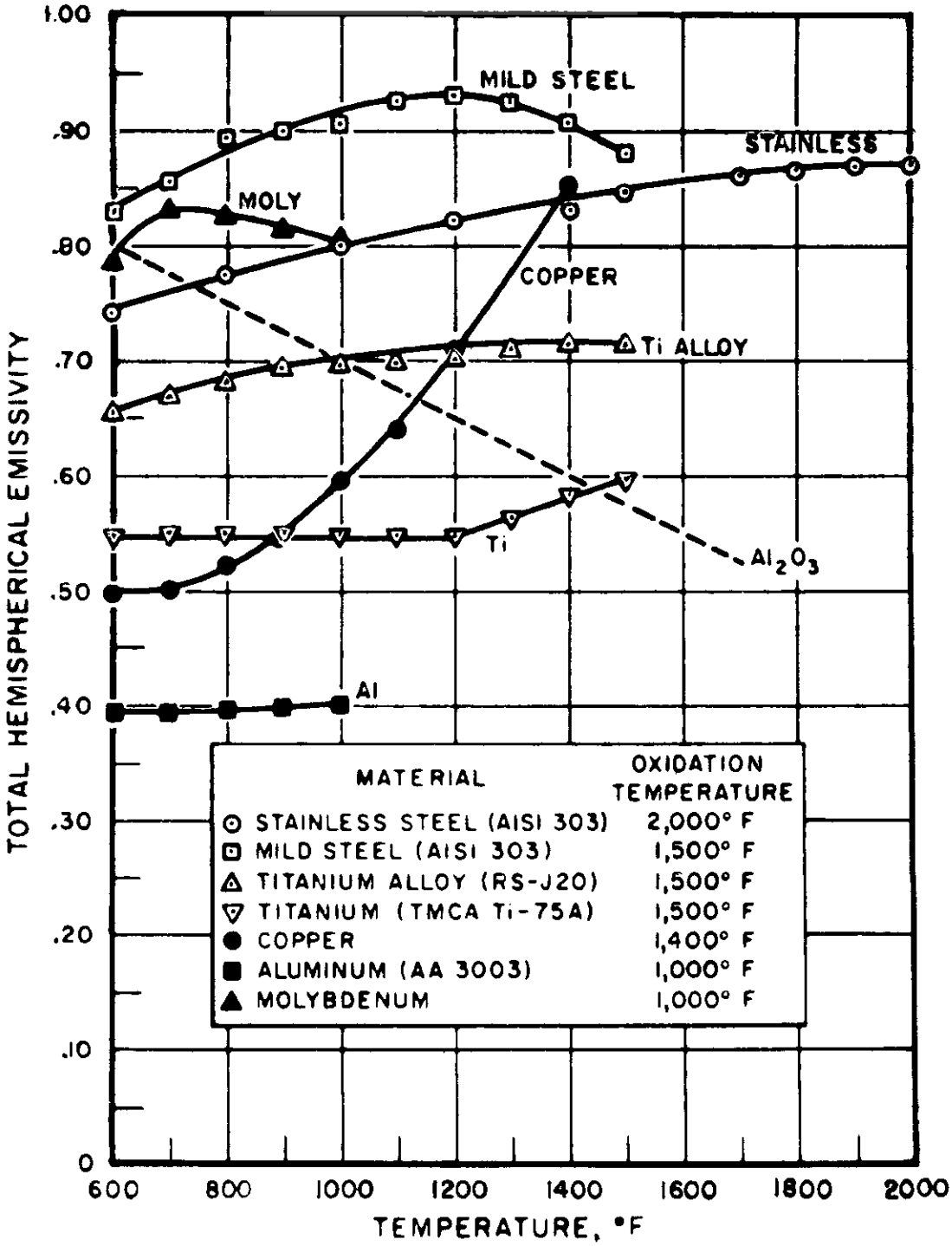

Figure 2-6. Emissivity vs Temperature
(Data from NACA-TN-4206)

2.4.1 Meteoroid Flux

The flux of meteoroids given in Reference 8 is:

$$\phi = 10^{-12} M^{-10/9} , \qquad (2\text{-}16)$$

where

ϕ = number of particles of mass greater than M per square meter per second

M = mass of particle in grams

This expression is plotted in Fig. 2-7, along with experimental points derived from satellite data. This curve is in agreement with that predicted by Whipple from visual observations if one accepts a mass of 30 grams as the mass of zero magnitude meteor.[8]

2.4.2 Meteoroid Penetration

The theoretical model postulated by Bjork[7] predicts the depth of penetration of projectiles impinging upon thick targets at hypersonic velocities. The calculations based on this model agree in both size and shape (hemispherical) with experimental craters produced in aluminum at 6.3 km/sec and in iron at 6.8 km/sec. The results of the theoretical analysis are summarized by the equation:

$$p = K'(Mv)^{1/3} \qquad (2\text{-}17)$$

where

p = penetration depth (cm)

M = mass of projectile (grams)

v = projectile velocity in (km/sec)

and

K' = constant depending upon materials;

for aluminum projectiles impinging on aluminum targets - K' = 1.09

for iron projectiles impinging on iron targets - K' = 0.606.

The modification of Equation 2-17 to account for projectiles which have densities different than the target material is uncertain,[11] as is the value of the meteoroid density itself. Some evidence

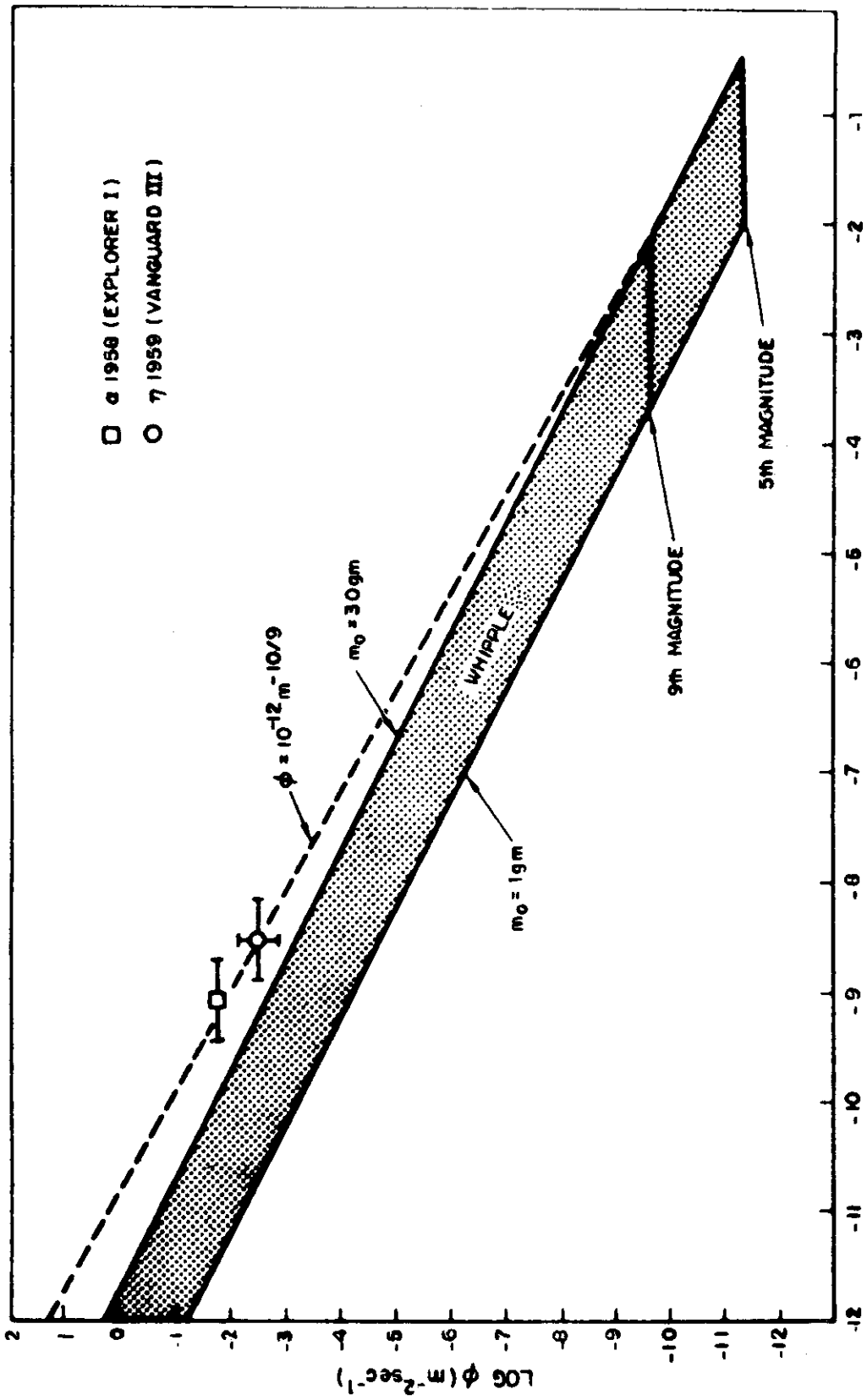

Figure 2-7. Meteoroid Flux vs Mass Near Earth (Data from Reference 10)

exists which indicates that the meteoroid density may be that of stone, ~2.3 g/cc. Hence, Equation 2-17 will be a good approximation for stone meteoroids inpinging upon aluminum, but will predict too high a value for the depth of penetration in materials which have a density significantly greater than that of aluminum.

While Equation (2-17) was derived for thick targets, enough information was obtained from Bjork's[10] analysis to deduce that if a projectile penetrates a depth, p, in a thick target it will just penetrate a sheet of the same target material which is 1.5 p thick, thus:

$$t_i = 1.5\ p \qquad (2\text{-}18)$$

where

t_i = required thickness of material (cm)

Equations (2-16) and (2-17) may be combined to obtain a penetrating flux which is given as:

$$\Psi = 10^{-12} t_i^{-10/3} K^{10/3} v^{10/9} \qquad (2\text{-}19)$$

where

Ψ = the number of penetrations of target thickness t_i per square meter per second

and

$K = 1.5K'$.

This relationship is shown in Table 2-1 for the velocity distribution stated by Whipple.[8]

2.4.3 Armor Requirements

The meteoroid punctures may be expected to follow a Poisson distribution which is given as:

$$P(n) = \frac{(\Psi A'\tau')^n}{n!} \exp^{-(\Psi A'\tau')} \qquad (2\text{-}20)$$

where

P(n) is the probability that n punctures will occur in time τ' of a sensitive area A'.

TABLE 2-1

METEOROID PENETRATION

Visual Magnitude	Mass (gm)	Velocity (km/sec)	Aluminum Thickness (cm)	Steel Thickness (cm)	Penetrating Flux (Penetrations/m^2-sec)
0	25.0	28.0	14.5	8.06	2.80×10^{-14}
1	9.95	28.0	10.7	5.93	7.79×10^{-14}
2	3.96	28.0	7.85	4.36	2.17×10^{-13}
3	1.58	28.0	5.78	3.21	6.02×10^{-13}
4	0.628	28.0	4.25	2.36	1.68×10^{-12}
5	0.250	28.0	3.13	1.74	4.67×10^{-12}
6	9.95×10^{-2}	28.0	2.30	1.28	1.30×10^{-11}
7	3.96×10^{-2}	28.0	1.69	0.940	3.62×10^{-11}
8	1.58×10^{-2}	27.0	1.23	0.684	1.00×10^{-10}
9	6.28×10^{-3}	26.0	0.894	0.496	2.80×10^{-10}
10	2.50×10^{-3}	25.0	0.649	0.360	7.78×10^{-10}
11	9.95×10^{-4}	24.0	0.471	0.261	2.17×10^{-9}
12	3.96×10^{-4}	23.0	0.341	0.190	6.03×10^{-9}
13	1.58×10^{-4}	22.0	0.248	0.138	1.67×10^{-8}
14	6.28×10^{-5}	21.0	0.179	9.96×10^{-2}	4.67×10^{-8}
15	2.50×10^{-5}	20.0	0.130	7.21×10^{-2}	1.30×10^{-7}
16	9.95×10^{-6}	19.0	9.38×10^{-2}	5.21×10^{-2}	3.61×10^{-7}
17	3.96×10^{-6}	18.0	6.78×10^{-2}	3.76×10^{-2}	1.01×10^{-6}
18	1.58×10^{-6}	17.0	4.90×10^{-2}	2.72×10^{-2}	2.79×10^{-6}
19	6.28×10^{-7}	16.0	3.53×10^{-2}	1.96×10^{-2}	7.78×10^{-6}
20	2.50×10^{-7}	15.0	2.54×10^{-2}	1.41×10^{-2}	2.17×10^{-5}
21	9.95×10^{-8}	15.0	1.87×10^{-2}	1.04×10^{-2}	6.03×10^{-5}
22	3.96×10^{-8}	15.0	1.37×10^{-2}	7.63×10^{-3}	1.68×10^{-4}
23	1.58×10^{-8}	15.0	1.01×10^{-2}	5.62×10^{-3}	4.66×10^{-4}
24	6.28×10^{-9}	15.0	7.44×10^{-3}	4.13×10^{-3}	1.30×10^{-3}
25	2.50×10^{-9}	15.0	5.47×10^{-3}	3.04×10^{-3}	3.61×10^{-3}
26	9.95×10^{-10}	15.0	4.03×10^{-3}	2.24×10^{-3}	1.01×10^{-2}
27	3.96×10^{-10}	15.0	2.96×10^{-3}	1.64×10^{-3}	2.80×10^{-2}
28	1.58×10^{-10}	15.0	2.18×10^{-3}	1.21×10^{-3}	7.77×10^{-2}
29	6.28×10^{-11}	15.0	1.60×10^{-3}	8.90×10^{-4}	0.217
30	2.50×10^{-11}	15.0	1.18×10^{-3}	6.55×10^{-4}	0.603
31	9.95×10^{-12}	15.0	8.67×10^{-4}	4.82×10^{-4}	1.68

For the case of the fluid type radiator under consideration, the allowable number of punctures of the tube walls is zero, hence Equation (2-20) reduces to:

$$P(o) = \exp^{-\psi A'\tau'} \qquad (2\text{-}21)$$

where

$P(o)$ = the probability that no punctures will occur in time τ' of a sensitive area A'.

Combining Equations (2-19) and (2-21) yields

$$t_1 = \frac{2.5 \times 10^{-4} Kv^{1/3} (A'\tau')^{3/10}}{\ln\left[\frac{1}{P(o)}\right]^{3/10}} \qquad (2\text{-}22)$$

For values of $P(o)$ > than 0.90 there is little error incurred by making the following approximation:

$$t_1 = 2.5 \times 10^{-4} Kv^{1/3} \left[\frac{A'\tau'}{1 - P(o)}\right]^{3/10} \qquad (2\text{-}23)$$

Assuming an average meteoroid velocity of 30 km per second and converting to engineering units, Equation (2-23) reduces to:

for aluminum,

$$t' = 43.6 \left[\frac{A\,\tau}{1 - P(o)}\right]^{0.3} \qquad (2\text{-}24)$$

for steel,

$$t' = 24.2 \left[\frac{A\,\tau}{1 - P(o)}\right]^{0.3} \qquad (2\text{-}25)$$

where

t' = required thickness in mils

A = area in ft^2

τ = time of exposure in years

and

$P(o)$ = probability that no punctures will occur in time $\underline{\tau}$ of area $\underline{A}$.

These equations are plotted in Figs. 2-8 and 2-9 for aluminum and steel respectively for various values of P(o) from 0.90 to 0.99 for τ equal to one year. These curves can then be used to determine the tube armor thickness required.

Another interesting approach to the meteoroid protection problem is that of the meteoroid "bumper." The usual concept has a piece of material placed around, and at some distance from the point to be protected. The meteoroid, by passing through this light piece of material, shatters and its mass is dispersed over a larger area. Preliminary calculations indicate that this is indeed the case but insufficient analytical techniques or experimental evidence exist at the present time to base radiator designs on this approach.

2.4.4 Erosion

The surface of the radiator will likely be subjected to an erosion process from the meteoroids. If high emissivity surface coatings are employed they may be gradually worn away by the eroding action of the meteoroids. An approximate measure of the magnitude of the erosion problem may be deduced from Equation 2-19 . Since the collisions produce a hemispherical crater of radius p, the amount of area removed by such punctures is:

$$da = 10^{-4}\pi p^2 dn \qquad (2\text{-}26)$$

where

da = area removed

p = penetration depth in cm

and

dn = number of hits with penetration between p and p + dp.

The number of hits with penetration greater than p is given by multiplying Equation 2-19 by the area and the exposure time which yields;

$$n = 10^{-12} p^{-10/3} v^{10/9} A' \tau' K'^{10/3} \qquad (2\text{-}27)$$

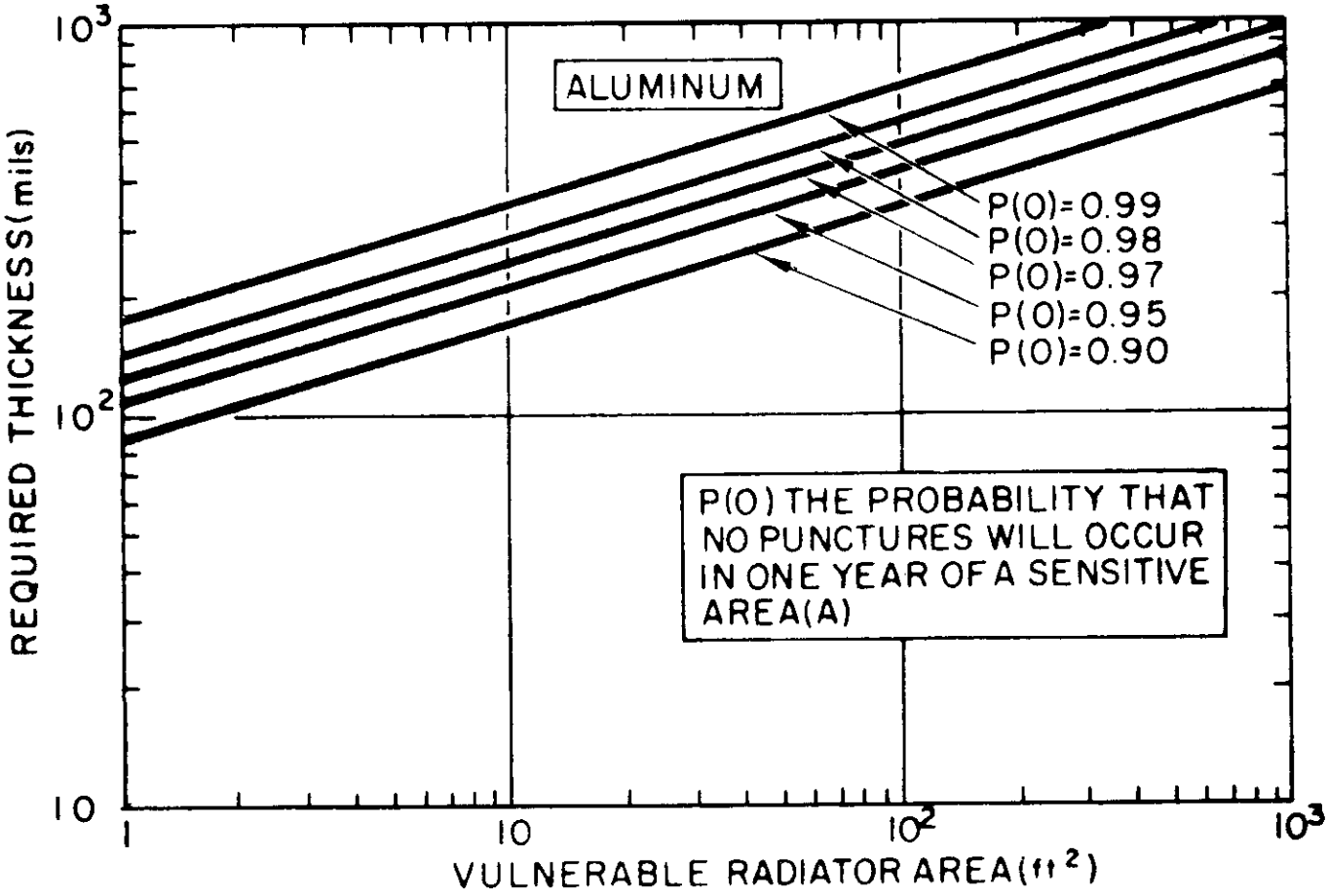

Figure 2-8. Material Thickness vs Radiator Area (Aluminum)

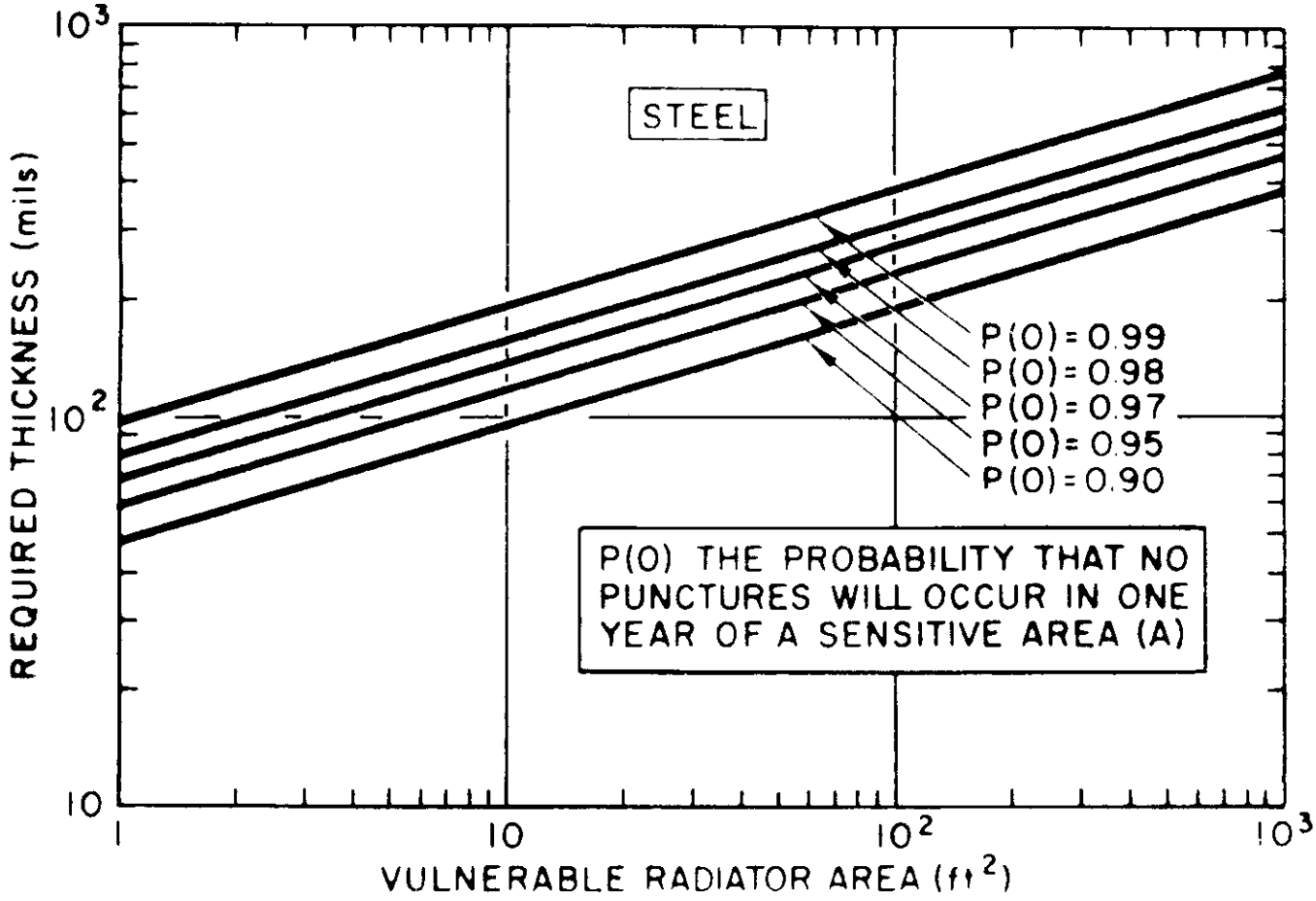

Figure 2-9. Material Thickness vs Radiator Area (Steel)

so that

$$dn = -1/3\ 10^{-11} p^{-13/3} v^{10/9} A'^{\tau'} K'^{10/3} dp \qquad (2\text{-}28)$$

The area removed by hits of penetration exceeding p is:

$$a = \int_p^{\infty} \pi 10^{-4} p^2 dn = \pi/4\ 10^{-15} v^{10/9} A'^{\tau'} K'^{10/3} p^{-4/3} \qquad (2\text{-}29)$$

For small values of a/A', multiple hits on the same area may be neglected. The ratio, a/A', which is the fraction of the original surface coating of thickness p that has been removed after a time τ', may be calculated from Equation 2-29 . $T_{1/10}$, the time required for removal of one-tenth of the original surface, is shown in Fig. 2-10 as a function of surface-coating thickness.

This calculation shows that there should be a negligible effect on the radiator surface. If high emissivity coatings are employed, it is possible that they may be eroded slightly. However, a hole which is just the depth of the coating thickness should not result in any loss in emissivity since the product of the view factor and the increased area (due to the formation of the hole) should be approximately unity. Other effects such as spallation of the coatings could seriously effect the thermal characteristics of the radiator surface. (It should be noted that this could have a severe effect on optical reflecting surfaces such as mirror collectors.)

2.5 Reactor-Radiator Configuration

2.5.1 Scattered Radiation

The large area of the radiator serves as a scattering medium for the radiation emanating from the reactor, and deflects a portion of this radiation into the payload section. This requires additional shielding over and above that required if the radiator were absent. Since the shield weights represent a sizeable fraction of the total system weight, in the low power range (<30 kwe unmanned and <1000 kwe manned), it is important to select configurations where this scattering problem is minimized. This is usually done

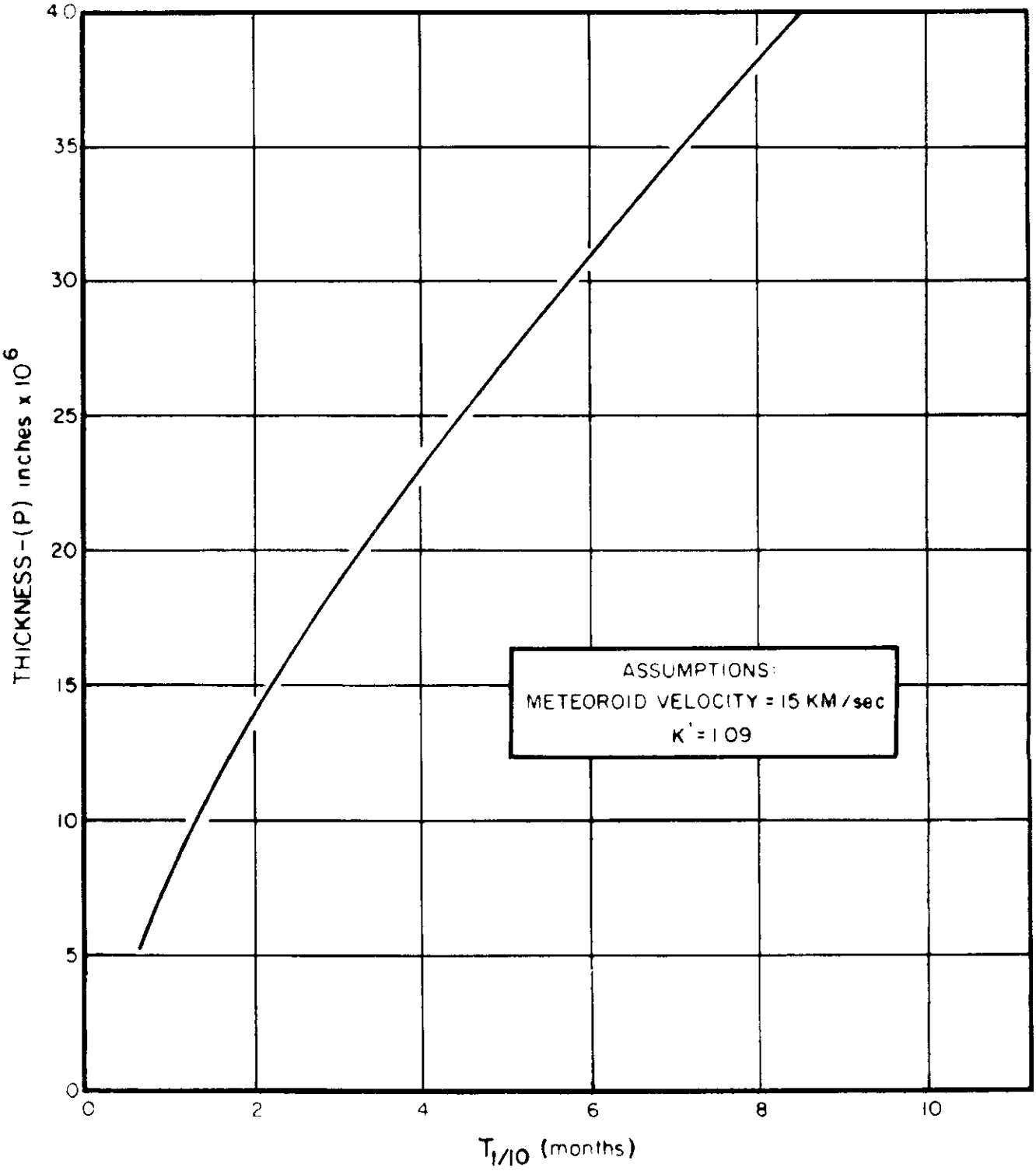

Figure 2-10. Time for 10 percent Loss of Area vs Material Thickness

by selecting a radiator configuration so as to have it lie within the shadow of the reactor shield. The reactor shield shadow is determined by the separation distance between the reactor and payload, the reactor size and shape, and the projected area of the payload section. Several radiator-shield configurations, designed with the scattered radiation problem in mind, are shown in Fig. 2-11. What has been said concerning the radiator is applicable for the vehicle structure since this also will serve as radiation scattering or activation centers.

It is impossible at this time to do more than indicate configurations where the scattering problem is at least minimized. This is because the shielding requirements can only be established in terms of a specific payload and mission. Payloads may range from hard tubes, which will probably require no shielding, to manned vehicles which will require a large amount of shielding. In general, the scattered radiation problem increases with increasing payload radiation sensitivity. The particular shape, configuration, or geometry of the radiator will be further influenced by the vehicle employed and the installation, structural, and aerodynamic requirements imposed by the vehicle or mission.

2.5.2 Activation

For systems which employ boiling directly in the reactor core and condensing in the radiator, neutron activation of the working fluid could be a problem since it introduces an extended diffuse source of radiation which could require significant payload shielding depending on the allowable dose-rates, fluid activation cross section, and type of radiation emitted. In general, this problem only arises when manned systems are considered, since the allowable radiation levels are lowest for manned missions. It is possible that the payload shielding required for Van Allen or cosmic radiation may mitigate this particular consideration.

2.6 Weight Optimization

Heat transfer, fluid flow, and meteoroid protection characteristics of the radiator-condenser are all closely interrelated, and any one of them can be improved only at the expense of the others. For example, a reduction in condensing pressure drop requires an increase in the number

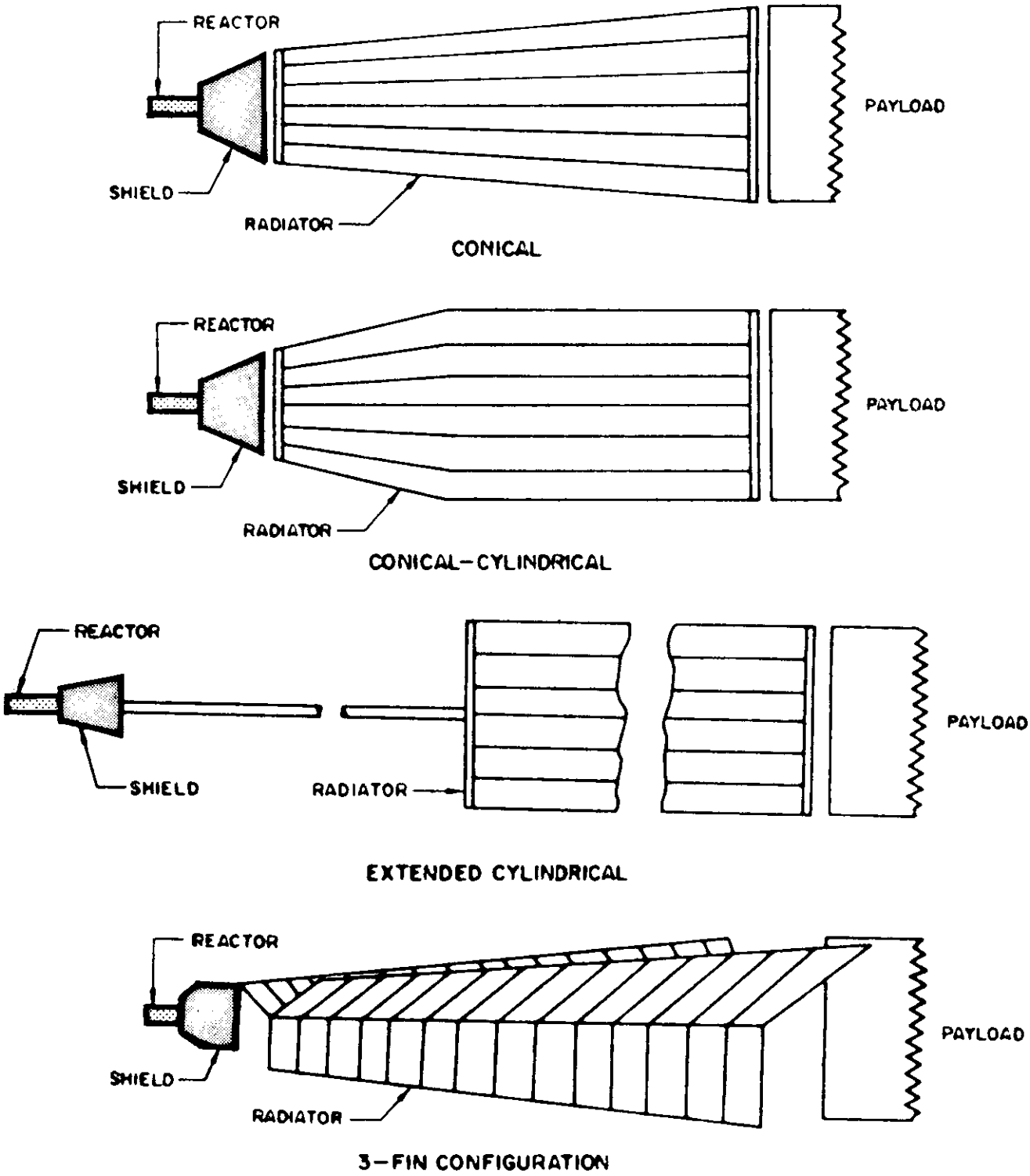

Figure 2-11. Several Radiator-Shield Configurations

of tubes, or tube diameter, thus increasing tube weight and meteoroid armor requirements; increasing pressure drop permits decreasing tube weight, but at the cost of lowering the radiating temperature. Similarly, increasing fin thickness raises the effectiveness of the fins and allows a reduction in number of tubes, but only at the expense of pressure drop and fin weight.

To illustrate how the various design variables are combined to determine a minimum weight heat rejection system, a specific example is presented. The conditions selected correspond to the design point of the SNAP-2 power system and are listed below:

1. Power - 3-kw electrical,
2. Working fluid - mercury,
3. Cycle overall efficiency - 6.0 percent
4. Condensing temperature - 600°F,
5. Vehicle skin geometry - 3.8 ft equivalent-diameter truncated cone
6. Required subcooling T = 180°F,
7. Surface emissivity - 0.90,
8. Condenser static pressure drop - 1.75 psi,
9. Meteoritic protection - 90% probability of no puncture for one-year life, and
10. Materials - fins: aluminum
    tubes: steel, eccentric bore (20-mil- minimum wall thickness)

The radiator geometry selected is a conical nose-cone configuration. The shape was selected so as to have the radiator lie entirely within the shadow of the reactor shield, thus minimizing the shield weights. The small diameter of the cone was set by the reactor and its shield dimensions at 2-1/2 ft; the large diameter was set by the missile diameter which was taken as 5 ft. Such a geometry may be adequately described in terms of an equivalent cylinder with a diameter equal to $D_1 + D_2/2$.

The tube and fin detail are shown in Fig. 2-12. The meteoroid armor is made up of the fin material and the steel tubes containing the condensate. The steel tubes are made eccentric so as to provide the necessary meteoroid armor in one direction only. Meteoroids which enter from the

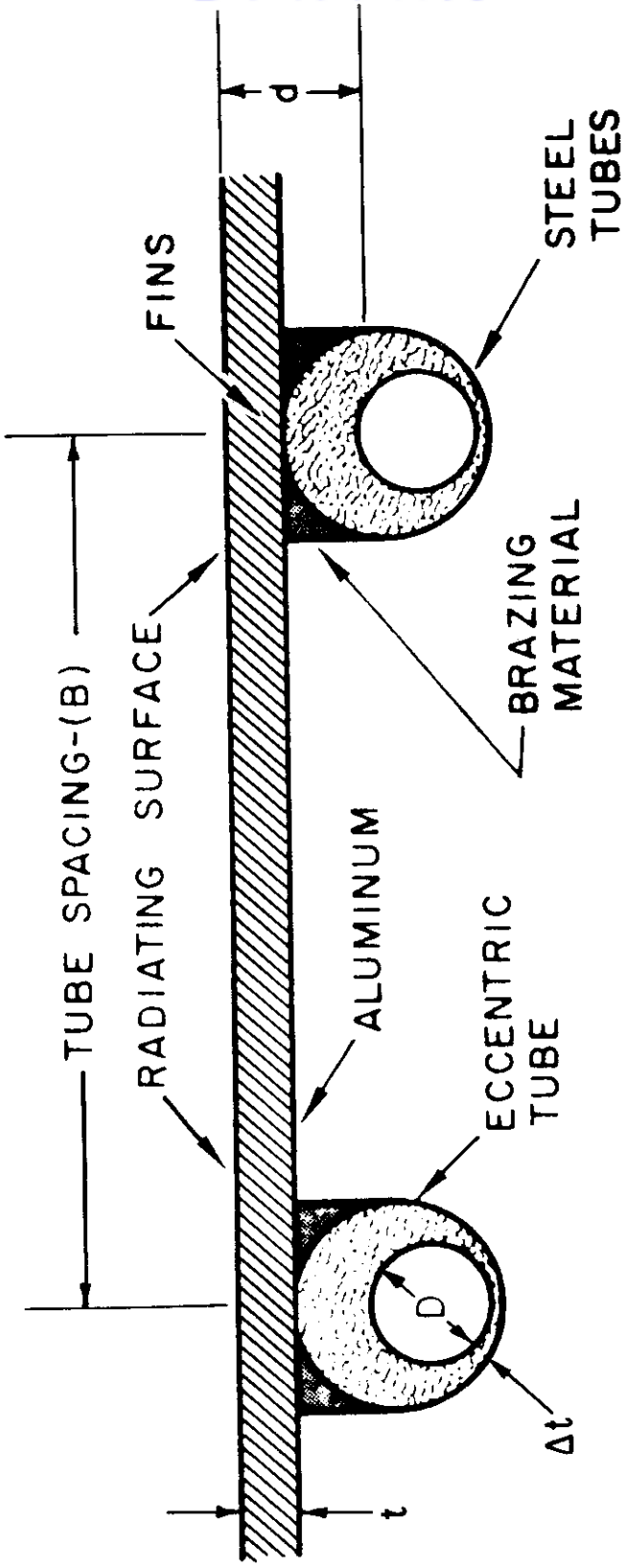

Figure 2-12. Detail of SNAP 2 Tube and Fin Arrangement

opposite side of the radiator were assumed to be sufficiently dispersed[10] so as to require no armor and the minimum thickness of tube wall was set by corrosion and strength considerations at 20 mils.

A system of equations was then developed, expressing analytically the heat transfer, fluid flow, and meteroid protection requirements of the radiator. Weights were calculated by a digital computer for wide ranges of pressure drop, number of tubes, and fin effectiveness. A typical result is shown in Fig. 2-13, for a constant value of fin effectiveness equal to 0.83. From Fig. 2-13 it is seen that the weight curve passes through a broad minimum at about 114 pounds and 36 tubes. Figure 2-14 illustrates the effect of varying fin effectiveness and shows the radiator weight going through a minimum for a fin effectiveness of 0.79. However, system requirements dictate a maximum area of 110 ft^2, corresponding to $\eta = 0.83$. It is seen that the weight penalty imposed by the arbitrary area restriction is small.

The minimum-weight design specifications for the SNAP-2 system are listed in Table 2-2.

TABLE 2-2

SNAP-2 RADIATOR SPECIFICATIONS

Area	110 ft^2
Geometry	Truncated Cone, 5 ft diameter tapered to 2-1/2 ft (9.4 ft long)
Shell Thickness (Fins)	28 mils (aluminum)
Number of Tubes	36 (steel)
Tube Dimensions	0.366 in. OD 0.273 in. ID
Fin Effectiveness	0.83
Weight	114 lb

2.7 Radiator Specific Weights

The procedure of Section F was applied to condensing systems over a power range of 100 to 300 kwe, with system boiling temperatures from 1600 to 2200°F and sodium, potassium, and rubidium working

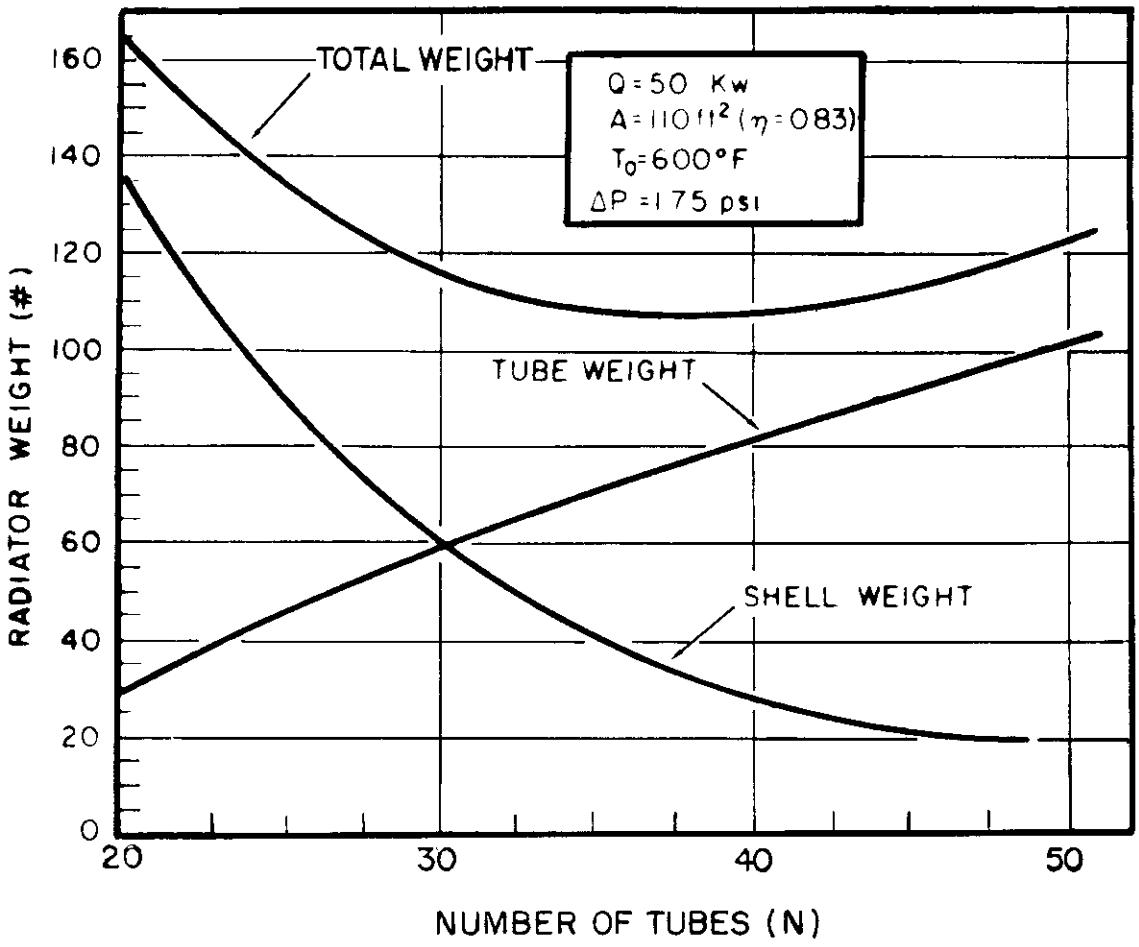

Figure 2-13. Radiator Weight vs Number of Tubes

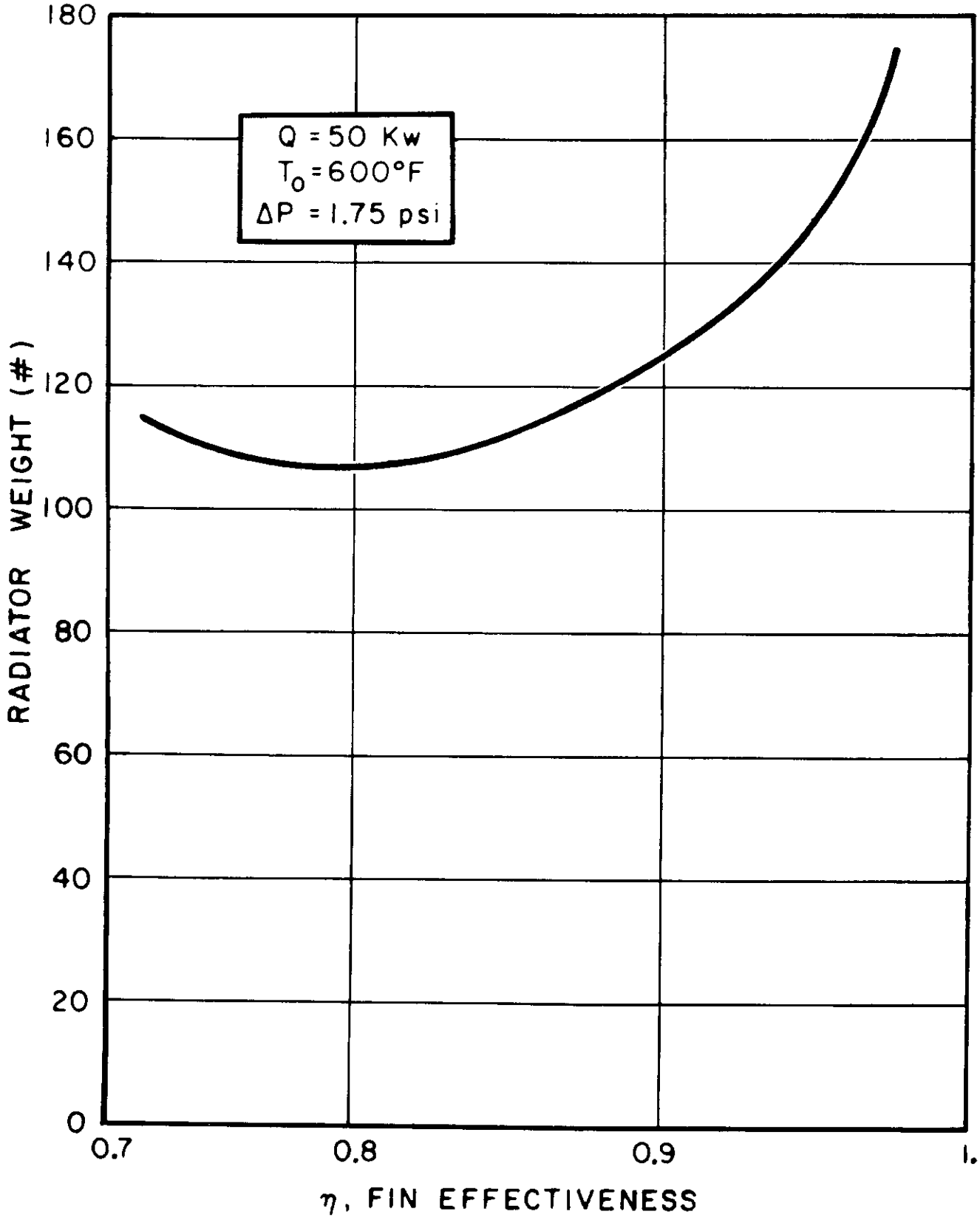

Figure 2-14. Minimum Radiator Weight vs Fin Effectiveness

fluids. The condensing temperature was taken to be three-quarters of the boiling temperature. This is the condition of minimum required radiator area.

The specific weights of the resultant optimized radiators are shown in Fig. 2-15.

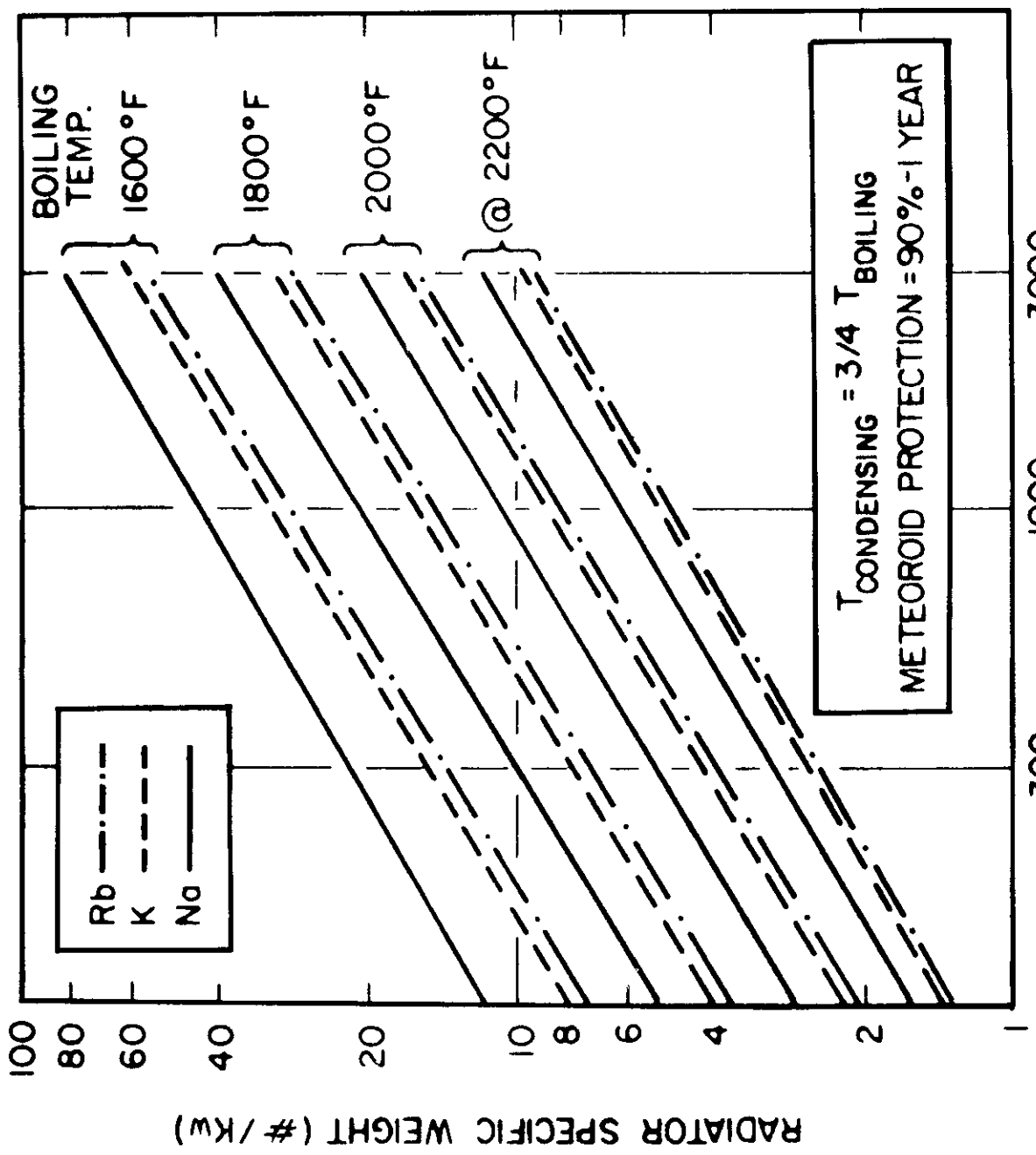

Figure 2-15. Specific Weights of Alkali Metal Direct Condensing Radiators

REFERENCES

Section 2

1. R.W. Lockhart and R.C. Martinelli, "Chemical Engineering Progress," 45, 39-48 (1949)

2. R.C. Martinelli and D.B. Nelson, "Trans. ASME," 70, 695-702 (1948)

3. W.H. McAdams, W.K. Woods, and R.L. Bryan, "Trans. ASME," 63, 545-552 (1941)

4. B. Misra and C. Bonnilla, "Heat Transfer in the Condensation of Metal Vapors: Mercury and Sodium up to Atmospheric Pressure," Presented at the Heat Transfer Symposium, March 20-23, 1955

5. NAA-SR-1840A, Classified Report (Secret RD)

6. W.R. Wade, "Measurements of Total Hemispherical Emissivity of Various Oxidized Metals at High Temperatures," NACA-TN-4206

7. R.L. Bjork, "Effects of a Meteoroid Impact on Steel and Aluminum in Space," Tenth International Astronautical Congress, London, England, August 28, 1959

8. R.L. Bjork, "Meteoroids vs Space Vehicles," Semi-Annual Meeting, American Rocket Society, Los Angeles, California, May 9-12, 1960

9. M.G. Coombs, "A Design Procedure for a Minimum Weight Mercury Radiative Condenser," SNAP Sponsored Meteorite Penetration Conference, Washington D.C., December 1-2, 1959

10. R.L. Bjork, SNAP Sponsored Meteoroid Penetration Conference, Washington D.C., December 1-2, 1959

11. M.G. Coombs, R.A. Stone, and T. Kapus, "The SNAP 2 Radiative Condenser Analysis," NAA-SR-5317, July 1960

12. "Interim Report on the SNAP 2 Radiator-Condenser Development Program" NAA-SR-5458

3. SHIELDING

3.1 Introduction

The use of nuclear power necessitates the design of a radiation shielding system to protect personnel and/or equipment from the damaging effects of radiation. This section has been prepared with the objective of presenting simple methods and data used in shielding calculations as they may be encountered in a system for use in space.

There are five major steps required in the design of a radiation shielding system:

1. Determine the ground rules for the shield design; i.e., which geometry, what is to be shielded, what is the mission, etc.
2. Establish the acceptable radiation levels for personnel and/or equipment.
3. Determine the various sources of radiation important to the shielding problem, and their absolute energy spectrum and spatial distribution.
4. Select shield materials on the basis of their shielding, structural, and chemical properties. In cases where a minimum weight shield is desired, cost may be of secondary importance if a definite improvement can be realized.
5. Perform shielding calculations and determine optimum shield design.

It should be emphasized that a complete shield design involves following the above five steps, not just once, but many times each using a different set of design parameters. Finally, a compromise design has to be established which will be the design of the shield.

3.2 Radiation Units and Permissible Radiation Levels

The use of nuclear reactors as power sources and experimental tools has introduced the serious problem of protecting personnel and equipment from harmful effects of radiation. For the proper evaluation of the effects and hazards of radiation, the various units of radiation have to be understood. In addition, safe or permissible radiation levels for personnel and equipment must be known in order that designs maintain a minimum of over-shielding and certainly no under-shielding.

3.2.1 Radiation Units

The knowledge of radiation effects, unfortunately, suffers on account of lack of proper standardization of units. The commonly accepted definitions are presented below but it is still wise to ascertain the definitions employed when analyzing any data concerning radiation.

The roentgen (r) is defined as that quantity of X — or gamma radiation which will produce, as a result of ionization, one electrostatic unit of charge of either sign in 1 cubic centimeter (0.001293 gram) of dry air at standard conditions of temperature and pressure (0 °C and 760 mm Hg). This is equivalent to the absorption of about 83 ergs per gram of air.

The roentgen equivalent physical (rep) is a measure of the energy absorbed by the human body rather than the energy absorbed by air. It is defined as the amount of any type of ionizing radiation which expends 93 ergs per gram on passing through soft body tissue. Originally, a rep was associated with the absorption of 83 ergs per gram of body tissue.

The rad is defined as the absorption of 100 ergs of ionizing radiation per gram in any material. Note that neither the kind of ionizing radiation nor the absorbing material are specified.

The roentgen equivalent man (rem) is not a directly measurable physical quantity as are the roentgen and the rep, but, rather, it is an index of the damage effects produced in the human body by the various types of radiation. The varying biological effects of the various types of radiation are frequently correlated by a coefficient called the relative biological effectiveness (RBE). The RBE is defined as the ratio of body damage from a given type of radiation to that caused by the same (physical units) dose of gammas. The rem is defined as the dosage in rad multiplied by the RBE for the type of radiation involved.

Table 3-1 shows the relationship of radiation units.

In space systems substantial fluxes of natural radiations will be encountered. These natural radiations will be comprised of high-energy charged particles — mainly protons, some heavier particles, and in some cases, energetic electrons. There is little substantial information available for estimating the RBE of fast protons and alphas. Presently a value of about 1 for the RBE of these particles has some general acceptance. Should further work suggest a

TABLE 3-1

RELATIONSHIP OF RADIATION UNITS

Type of Radiation	RBE	Rad	Roentgen	Rem
X or gamma (0-3 Mev)	1	1	1	1
Beta	10	1	Not applicable	1
Protons ~ 20 Mev	10	1	Not applicable	10
Alphas ~ 20 Mev	20	1	Not applicable	20
Protons >> 20 Mev	1	1	Not applicable	1
Alphas >> 20 Mev	1	1	Not applicable	1
Fast neutron (0.1-10 Mev)	10	1	Not applicable	10
Intermediate neutrons (10^2-10^5 ev)	7	1	Not applicable	7
Slow neutrons (0-10^2 ev)	5	1	Not applicable	5

value of the RBE more comparable with that of the lower energy charged particles (10 to 30 Mev), then cosmic radiation on missions of about one year duration will pose a serious radiological threat.

3.2.2 Permissible Radiation Levels

3.2.2.1 Human Beings

Any significant departure from the natural radiation environment in which man has evolved may introduce some risk. It is, however, possible to define a permissible dose that, in light of the present knowledge, is not expected to cause appreciable bodily injury to a person at any time during his normal span of life. The following is a summary of recommendations by the National Committee on Radiation Protection:

1. The maximum permissible dose (MPD), shall not exceed 3 rem per 13 weeks.
2. The MPD shall not exceed 5 times the age minus 18; i.e., 5 (age - 18), rem during lifetime.
3. The MPD shall not exceed 200 rem during normal span of life.
4. Maximum accidental or emergency exposure occuring only once in the lifetime of a person should not exceed 25 rem.

It is also recommended that the 3 rem per 13 weeks be taken at a slow rate rather than all 3 rem in a very short time.

It has been customary, in designing shields for reactors in terrestrial application, to observe these standards of radiological tolerance rigidly.

The realities of rocket technology, of weight lifting capacity, of the incident of highly penetrating radiations in space, make it very unlikely that such rigid tolerances can be satisfied in the near future. Current recommendations are for a mission dose of about 5 rem excluding solar flares with the possibility of about 20 rem from one solar flare. Such a tolerance evidently applies to rather short missions — one to two weeks.

3.2.2.2 Components and Materials

When materials are subjected to an environment of radiation, their properties are changed in ways that could not necessarily be anticipated from previous experience with nonradiation environments. Thus, component performance will be altered when these materials are subjected to nuclear radiation. Two of the observed effects of radiation on materials are important to component life:

1. Permanent changes in the chemical and physical properties of materials.
2. Instantaneous or transient changes in their properties.

Permanent changes that result, usually from prolonged exposures, affect all types of components. Instantaneous changes affect the performance of sensitive circuits in electronic systems, by producing noise.

Ionization and lattice dislocation are the two principal mechanisms of damage. Either of these mechanisms can produce noise or can lead to permanent damage. Most noise induced by radiation is caused by ionization. Further dissipation of radiative energy in lattice dislocation processes is far more effective in producing permanent damage than is dissipation in ionization. Since neutrons cause lattice dislocations much more frequently than photons of comparable energy content, and since most space payloads now under active consideration tend to be limited more by permanent radiation damage than by radiation-induced noise, the current problems in unmanned payload shielding are much more concerned with neutron-induced damage than with that caused by photons.

Table 3-2 gives thresholds of radiation damage to electronic components which have extremely low thresholds of radiation damage.

TABLE 3-2

APPROXIMATE THRESHOLDS OF RADIATION DAMAGE OF ELECTRONIC COMPONENTS

Component	Gamma Dose (Rads)	Integrated Fast Neutron Flux (nvt)
Photocells affected	$\sim 10^5$	$\sim 10^5$
Transistors and diodes affected	$10^6 - 10^7$	$10^{11} - 10^{12}$
Transistors and diodes seriously affected	$10^7 - 10^8$	$10^{12} - 10^{13}$
Transistors and diodes destroyed	$10^8 - 10^9$	$10^{13} - 10^{15}$
Electron tubes	$\sim 10^8$	$10^{15} - 10^{18}$
Capacitors affected	$10^8 - 10^9$	$10^{15} - 10^{17}$
Resistors affected	$10^8 - 10^9$	$10^{16} - 10^{18}$
Capacitors and resistors seriously affected	$10^9 - 10^{10}$	$10^{17} - 10^{19}$

It is common current practice to allow existing conventional transistor tolerances to establish the payload tolerance. The generally used tolerance numbers are 10^{12} nvt fast neutrons (tenths of Mev and higher energies), and 10^7 roentgen photon exposure. Some of the radiation damage literature suggests a transistor tolerance of 10^{13} nvt. This number is often based on an epicadmium flux whose fast component (> 0.1 Mev) may approximate 10^{12} nvt.

Work is now being carried on to develop components with high radiation tolerance to replace conventional transistors. Other work is in progress to develop circuitry capable of useful operation, even with heavily damaged components. There is, consequently, good prospect that at least in some applications, the present tentatively set tolerances may be substantially relaxed.

3.3 Features of Reactor Shielding Peculiar to Space Application

Many of the problems of reactor shielding are largely independent of the application to which the reactor system is put. In space application, however, some

features require a different treatment, some a different emphasis. The principal conditions encountered in space which tend to alter reactor shielding considerations are:

1. The absence of a surrounding gaseous medium
2. The general, though not universal, elongated shape of systems with reactor and payload opposed
3. The substantial number of missions which will be unmanned
4. The absence of need, in many cases, to dispose of or to consider the reactor after the end of its useful life
5. The necessity to reject heat by radiation to space.

The absence of a surrounding gaseous medium makes it possible to leave extensive surfaces of the reactor completely unshielded. This, in turn, makes it highly desirable to hold to a minimum the total solid angle of system, payload or scattering components, viewed by any part of the reactor. In short, it makes vehicle integration, the disposition of payload and components with respect to the reactor, the most significant aspect of shield design. Further, the materials most suitable for reactor shielding in space application have vapor pressures such that exposure to vacuum would cause them to dissipate and disperse in short order. It is necessary, therefore, to design a shield container sufficiently rugged to maintain its integrity, even against pinhole leaks, under all the conditions to which it will be subjected.

Most space nuclear systems under consideration are of elongated shape, generally conical in the neighborhood of the reactor. Such shape has evident inverse- square and solid-angle advantages in shielding. Moreover, in a sufficiently long system, the conical angle is quite small. Hence, the system diameter increases only slightly as one moves a moderate distance from the reactor toward the payload. In circumstances where protection against secondary photons is required, lamination of neutron and photon shielding materials can therefore be accomplished without the excessive weight penalties encountered in a system whose dimensions increase with distance from the reactor.

The unmanned mission causes, in general, the dose tolerance to be established by transistor tolerance rather than by human tolerance. Transistors are more sensitive to neutrons than to photons by orders of magnitude, if the particles

are compared on an equal energy basis. Consequently, the shielding emphasis is heavily on neutron shielding. Secondary photons constitute a less important problem in many systems, and are often negligible.

The absence of need, in many cases, to handle or dispose of a spent reactor core eliminates the requirement of after-shutdown shielding and permits a greater degree of freedom in the disposition of shield materials.

The necessity to reject heat to space by thermal radiation implies a fairly high temperature shield and therefore restricts considerably the choice of materials available. The nature of the space heat sink makes desirable, if not necessary, a somewhat different approach to shield cooling mechanisms.

3.4 Sources of Radiation

One of the first steps in designing a shield is the determination of the energy distribution, spatial distribution, and intensity of radiation sources. If the primary source of radiation is a reactor, only neutron and gamma rays are considered, since they are the most penetrating forms of radiation. This section gives the methods for calculating the intensity and spectral distribution of this radiation.

3.4.1 During Reactor Operation

The sources of radiation during reactor operation are given in Table 3-3. The following sections give a brief method of calculating these sources of radiation.

TABLE 3-3

SOURCES OF RADIATION DURING REACTOR OPERATION

Where Produced	Gamma Rays	Neutrons
Reactor core	Prompt-fission gammas Fission-product gammas Neutron-capture gammas Gammas from neutron inelastic scattering Decay gammas of neutron activated materials in core	Fission neutrons Delayed neutrons Photoneutrons
Coolant, structural materials and reactor shield	Neutron-capture gammas Gammas from neutron inelastic scattering Coolant-activation gammas	Photoneutrons

3.4.1.1 Gamma Rays

In the computation of the core gamma-ray strength, the most important contributions are the prompt-fission gammas, the fission-product gammas, and the neutron-capture gammas. The gamma rays from neutron inelastic scattering and decay of neutron-activated materials in the core are a small contribution; thus they may be neglected unless great accuracy is desired. Table 3-4 gives the gamma-ray energy spectra from fission of U^{235}. The neutron-capture gamma rays from other materials in the core should be added to the spectrum given in Table 3.4.

TABLE 3-4

GAMMA RAY ENERGY SPECTRA FROM FISSION OF URANIUM-235

(Mev per Fission)

Average Gamma Ray Energy	Prompt Fission Gamma Ray	Equilibrium Fission Product Gamma Ray	Capture Gamma Ray* in U-235 in Thermal Reaction	Total
1	3.450	5.16	0.520	9.130
2	2.360	1.737	0.356	4.453
3	1.175	0.322	0.177	1.674
4	0.477		0.072	0.549
5	0.203		0.031	0.234
6	0.136		0.020	0.156
7	0.026		0.004	0.030
TOTAL	7.827	7.219	1.18	16.226

*Capture gamma-ray spectrum is assumed to have the same spectral distribution as that of the prompt fission gamma rays.

Table 3-5 gives the neutron-capture gamma-ray spectra for various elements.[1] The total gamma-ray source strength at a point is computed by the following equation:

$$S(\vec{r}, E) = \sum_i \chi_i(E) \int_0^\infty \Sigma_i(\vec{r}, E')\phi(E', \vec{r})dE' \qquad (3\text{-}1)$$

TABLE 3-5

THERMAL-NEUTRON-CAPTURE GAMMA RAY ENERGY SPECTRA

(Gamma Ray Energy, Mev per Radiative Capture)

Energy of Emitted Gamma Ray	0-1	1-2	2-3	3-4	4-5	5-6	6-7	7-8	8-9	9-10
Aluminum			0.60	1.29	1.29	0.51	0.42	1.90		
Antimony				0.78	0.64	0.45	0.28			
Arsenic				1.01	0.93	0.65	0.64	0.17		
Barium				1.89	1.08	0.69	0.10	0.01	0.01	0.01
Beryllium				1.70			5.12			
Bismuth					4.17					
Boron-10					5.10		1.88		0.50	0.09
Cadmium	0.46	0.34	0.40			0.52	0.13	0.11	0.03	0.02
Calcium	0.07	0.94	0.41	1.08	1.96	1.28	2.32	0.07		
Carbon				1.10	3.47					
Chlorine	0.40		1.57	1.07	1.57	1.45	1.89	1.06	0.12	
Chromium				0.26	0.29	0.62	0.75	1.87	3.93	1.11
Cobalt	0.34	0.25	0.08	0.77	0.87	1.57	1.70	0.57		
Copper					0.61	0.62	0.94	3.13	0.016	
Fluorine					1.83	3.20	2.82			
Gadolinium				0.64	0.30	0.15	0.06			
Gold				0.01	1.53	1.31	1.10	0.01		
Hafnium					0.50	0.51	0.17	0.0026		
Hydrogen			2.23							
Indium				0.76	0.55	0.26				
Iron	0.05	0.30	0.20	0.37	0.45	0.84	0.67	2.66	0.25	0.20
Lead								7.40		
Lithium-6							2.90	4.15		
Magnesium			0.62	2.68	0.25	0.31	0.27	0.01	0.26	0.05
Manganese		0.21	0.38	0.25	1.24	0.98	1.11	1.78		
Mercury	0.21	0.50	0.56	1.35	1.94	1.91	0.63	0.04		
Molybdenum				1.93	1.41	0.90	0.66	0.16	0.05	

TABLE 3-5 (Continued)

Energy of Emitted Gamma Ray	0-1	1-2	2-3	3-4	4-5	5-6	6-7	7-8	8-9	9-10
Nickel	0.07	0.06	0.04	0.20	0.51	0.81	1.32	1.35	4.57	0.98
Niobium				1.22	0.88	0.68	0.20	0.04		
Nitrogen				1.07	0.72	4.77	1.07	0.66	0.35	0.09 1.08
Phosphorus				2.17	1.51	0.66	1.04	0.58		
Platinum				1.07	0.71	0.75	0.08	0.06		
Potassium	0.24	0.61	0.83	1.80	1.86	1.99	0.24	0.39	0.01	
Praseodymium				0.76	0.59	0.45				
Rhodium				0.82	0.68	0.45	0.17			
Samarium	0.53	0.21	0.77	1.21	0.55	0.28	0.08	0.07		
Silicon		0.37	1.61	2.14	3.89	0.47	0.92	0.62	0.14	0.02
Silver			0.24	1.52	1.28	0.81	0.23	0.04		
Sodium	0.80	0.39	1.44	1.05		0.33	0.83			
Strontium				1.46	1.03	0.91	2.18	0.79	0.29	0.02
Sulphur	0.40		1.77	1.62	1.92	4.64	0.29	0.22	0.09	
Tantalum					0.05	0.10	0.04			
Thallium				0.94	2.15	2.68	0.96			
Tin				3.64	1.89	1.24	0.65	0.25		0.04
Titanium	0.14	1.59	0.08	0.37	0.72	0.09	6.58	0.11	0.02	0.01
Vanadium	0.16	0.21	0.15	0.39	0.50	1.33	2.16	1.07	0.008	
Tungsten				1.28	0.77	0.58	0.33	0.03		
Zirconium				2.52	1.71	1.07	1.15	0.15	0.11	

where

$S(\vec{r}, E)$ = gamma ray source density per unit energy at $\vec{r}$

i = subscript denoting i^{th} process for production of gamma rays

$\Sigma_i(\vec{r}, E')$ = macroscopic cross section at $\vec{r}$ for production of gammas through the i^{th} process of neutron interaction, neutron energy E'

$\phi(E', \vec{r})$ = neutron flux density at $\vec{r}$, energy E'

$\chi_i(E)$ = energy spectrum of gamma rays produced in the i^{th} process.

As capture gamma rays are usually high in energy, for thick shields they may be very important. Gamma ray sources outside the reactor are due to (1) activated coolant, and (2) secondary photons produced as a result of neutron interactions with materials predominantly in the shield.

Table 3-5 shows the gamma ray spectra in various elements for the emission of photons emitted following thermal neutron capture. One can use the same spectra with little error to describe the (n, γ) spectra in the same materials for capture of epithermal neutrons.

3.4.1.2 Neutrons

For thermal reactors using U^{235}, 2.47 ± 0.03 neutrons are emitted per fission. The energy spectrum of these neutrons is given in Table 3-6. Delayed neutrons and photoneutrons in the core may be ignored in the shielding calculations, since they represent a very small fraction of the total neutrons produced.

TABLE 3-6

NEUTRON SPECTRUM FROM FISSION OF U^{235} BY THERMAL NEUTRONS

Energy of Neutrons, E (Mev)	Fraction of Neutrons Above Energy, E
0	1.000
0.5	0.8531
1.0	0.7024
2.0	0.4024
3.0	0.2131
4.0	0.1076
5.0	0.05259
6.0	0.02505
7.0	0.01169
8.0	5.372×10^{-3}
9.0	2.434×10^{-3}
10.0	1.092×10^{-3}

3.4.2 After Reactor Shutdown

After the reactor is shut down, the fission products decay results in the emission of beta and gamma rays. The following equation gives the approximate power generated in a reactor by beta and gamma rays after shutdown:

$$P \approx 5.9 \times 10^{-3} P_o \left[(t - t_o)^{-0.2} - t^{-0.2} \right] \qquad (3\text{-}2)$$

where

P = power generated in reactor at time t days after reactor startup, in watts

P_o = operating power of reactor, in watts

t = time after reactor startup, in days

t_o = time the reactor has operated, in days.

The activity of fission products after reactor shutdown is given by the following approximate equation:

$$C \approx 1.4 P_o \left[(t - t_o)^{-0.2} - t^{-0.2} \right] \qquad (3\text{-}3)$$

where

C = activity of fission products at time t days after reactor startup in curies (1 curie = 3.7×10^{10} disintegrations/sec)

P_o, t, and t_o are defined above.

It should be noted that in both Equations (3-2) and (3-3), $(t - t_o)$ is the number of days after shutdown. These two equations should only be used when $(t - t_o)$ is considerably greater than 10 seconds.

In order to calculate after-shutdown shielding requirements, the gamma-ray intensity and energy spectrum should be known. Figures 3-1a and b show the rate of gamma-ray energy emitted per watt of reactor power, as a function of time after shutdown, for various energy groups and for a reactor operation time of 10^3 hours. It should be noted that the gamma-ray energy spectrum does not vary appreciably for operating times from a few days to one year. However, the total gamma-ray energy emitted per watt as a function of time after a shutdown, varies with the reactor operation time, as shown in Figure 3-2. Thus, the

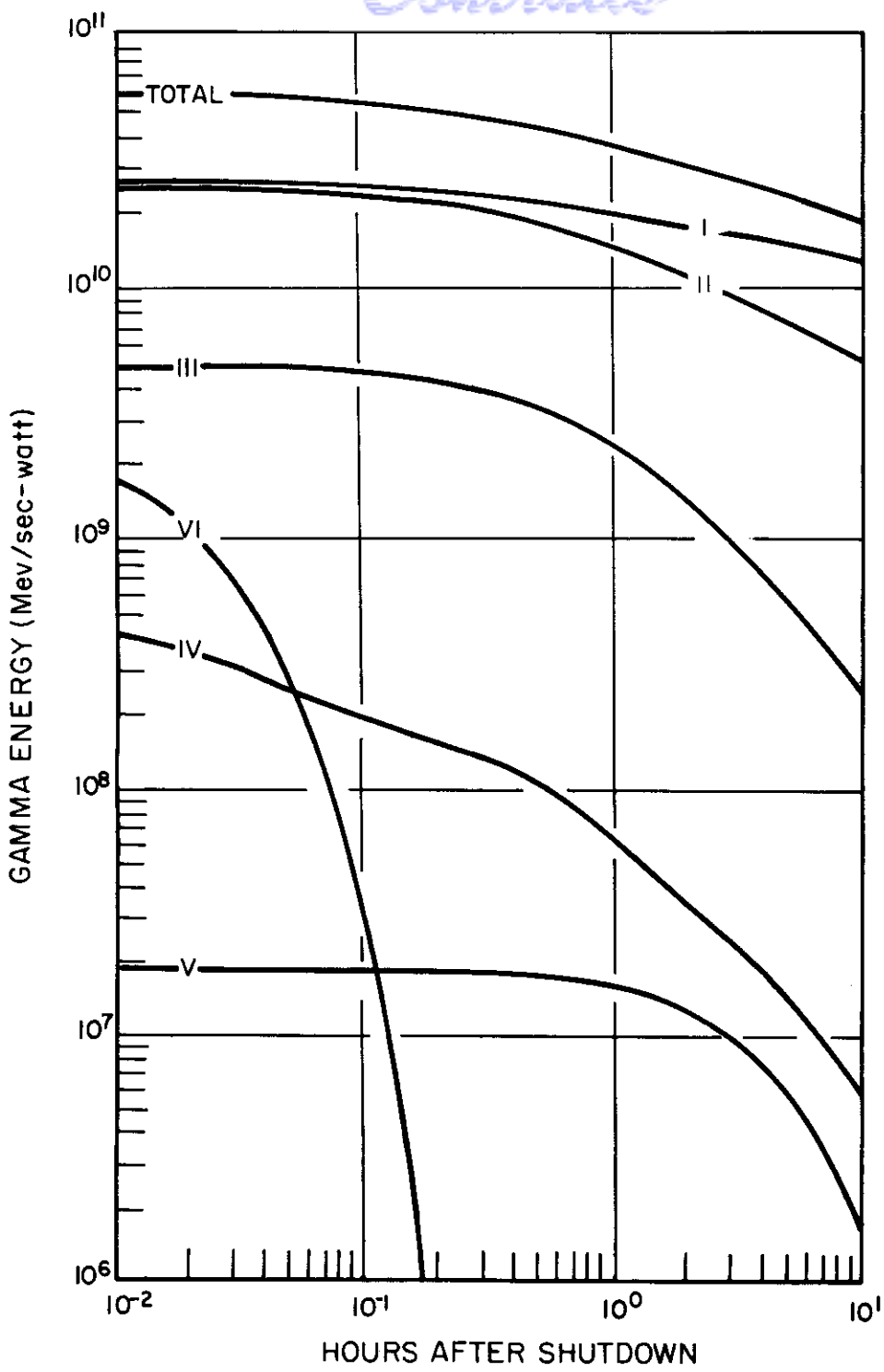

Figure 3-1a. Gamma Ray Energy — 10^3-Hour Reactor Operation

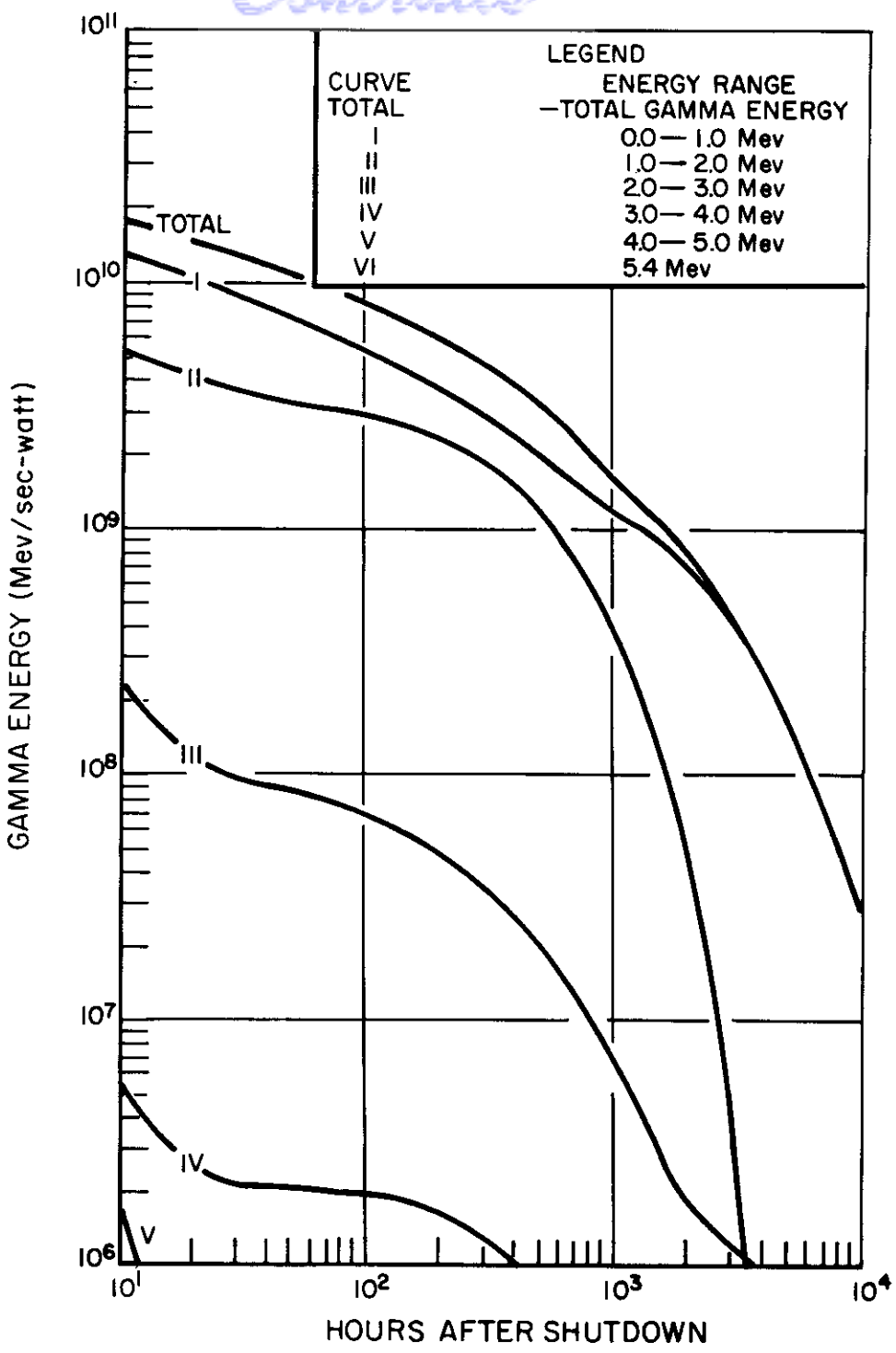

Figure 3-1b. Gamma Ray Energy — 10^3-Hour Reactor Operation

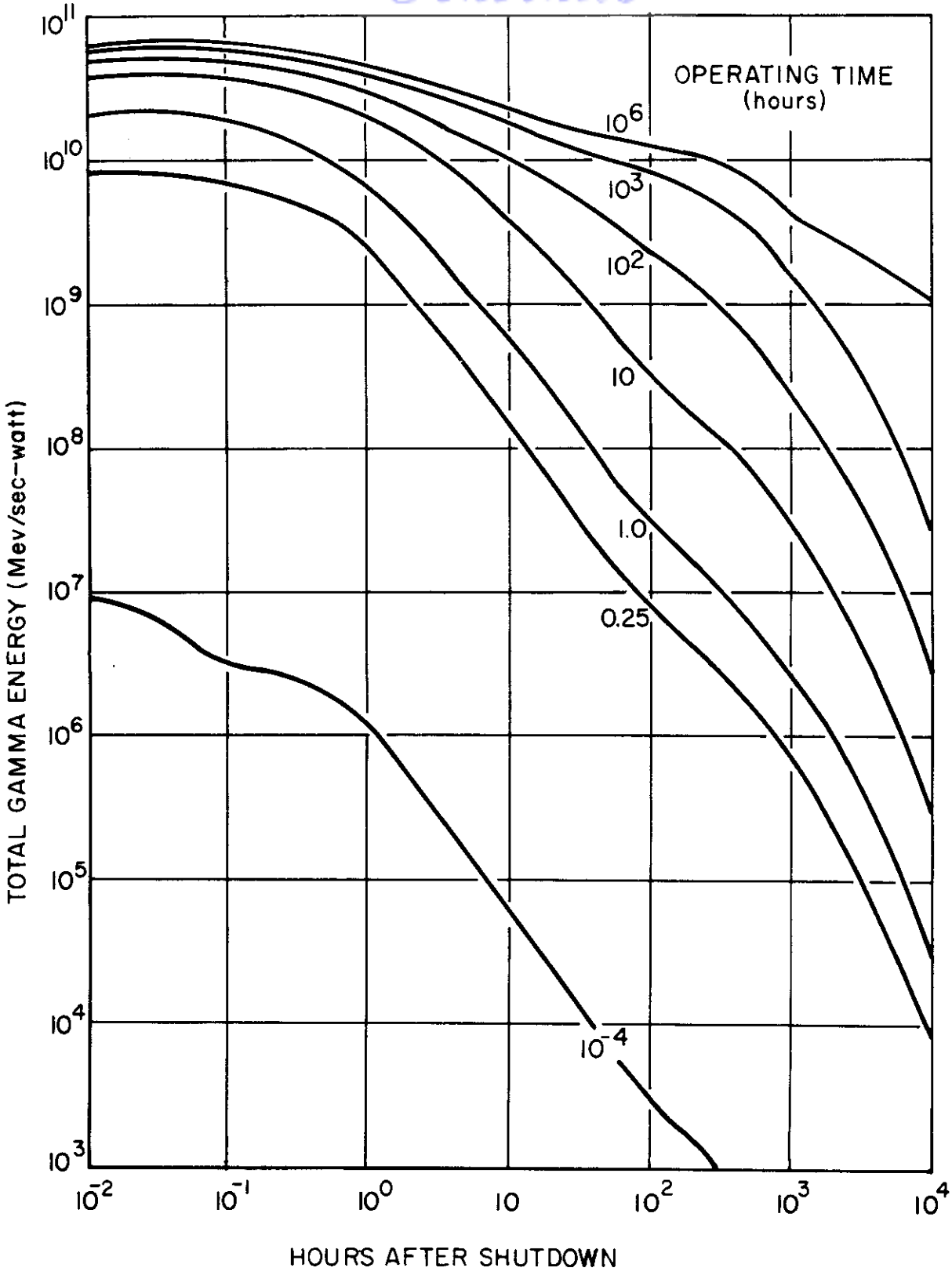

Figure 3-2. Total Energy for Various Reactor Operation Times

gamma-ray energy spectrum in Figures 3-1a, b (operating time 10^3 hours) may be used, and the total power may be normalized to that in Figure 3-2, if operating times other than 10^3 hours are required.

3.5 Calculation of Penetration of Radiation

The general considerations governing the penetration of radiation through matter are presented in this section along with a few convenient recipes for rough calculations. The presentation of recipes here is not intended to endow them with any preference over other recipes not presented. More refined calculations will require resort to more extensive and specialized literature. It is generally true for shielding calculations that results with any degree of refinement require the development of computing schemes tailored closely to the needs of the particular system. This is due to the great sensitivity of leakage currents to the boundary conditions and irregularities which are unique to each system. More extensive treatment of shielding problems can be found in References 2, 4, and 11, and in the specialized literature.

3.5.1 Gamma Rays

In generalized form the equations for computing dose from any class of radiation can be represented by

$$D^*(\vec{r}, E) = \int_{\substack{\text{all phase} \\ \text{space}}} S(\vec{r}, E, \vec{\Omega}) F(\vec{r}, \vec{r}', \vec{\Omega}, E' E) dV \qquad (3\text{-}4)$$

$$D(\vec{r}) = \int_0^\infty \frac{D^*(\vec{r}, E)}{K(E)} \, dE \qquad (3\text{-}5)$$

$\vec{r}$ = spatial coordinates of detector

$\vec{r}'$ = spatial coordinates of source

E' = energy coordinate of source

$\vec{\Omega}$ = angular coordinate of source

E = energy coordinate of dose at detector

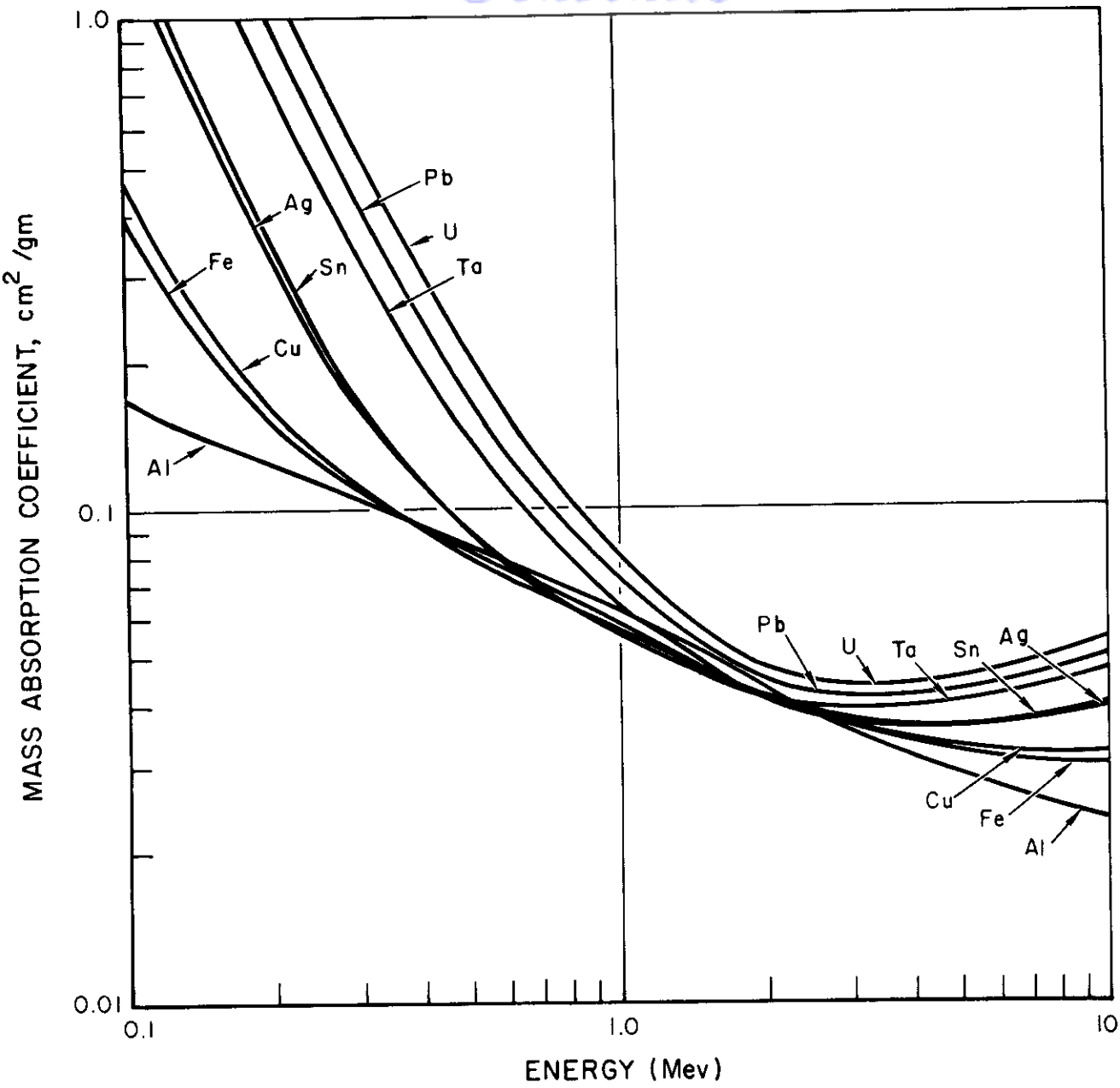

Figure 3-3a. Gamma-Ray Mass Absorption Coefficient for Various Materials

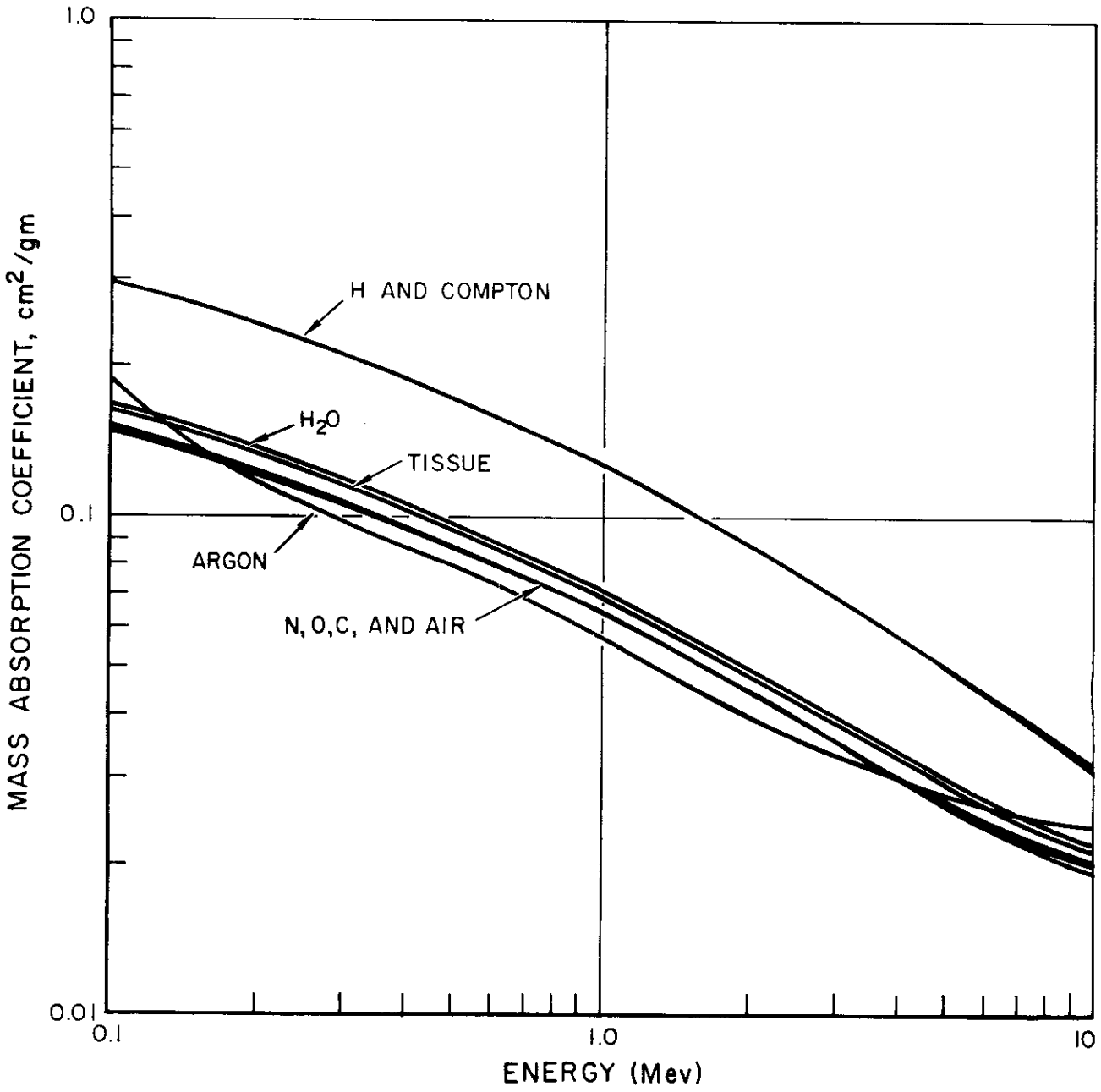

Figure 3-3b. Gamma-Ray Mass Absorption Coefficient for Various Materials

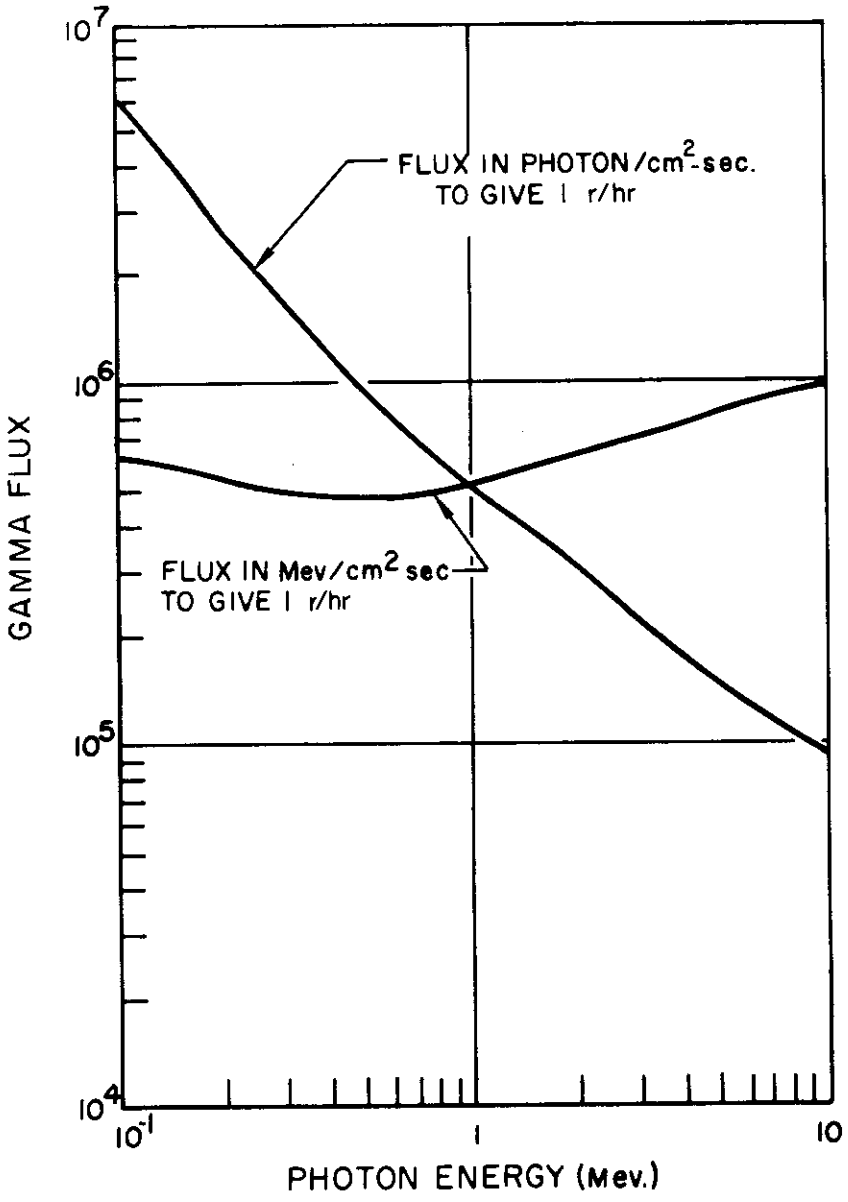

Figure 3-4. Gamma Ray Flux Equivalent to 1 Roentgen Per Hour as a Function of Gamma Ray Energy

S = source distribution function

$D^*(\vec{r}, E)$ = dose spectrum at detector in physical units

$D(\vec{r})$ = dose at detector in suitable energy-integrated dose units

K(E) = dose unit conversion function

$F(\vec{r}, \vec{r}', \vec{\Omega}, E'E)$ is a kernel which yields the dose at r, E attributable to a unit source at $\vec{r}', \vec{\Omega}, E'$.

Phase space is comprised of the entire range of variation of $\vec{r}'$, E', and $\vec{\Omega}$.

In no practical situation are equations of the generality of Equation 3-4 solved. They serve only to exhibit the problem compactly in all its generality. The more elaborate schemes of computation generally simplify geometry by requiring bounding surfaces to be easily-expressible analytic forms; smooth the physical data to a convenient form; ignore one or more possible dimensions of variation; and employ approximate integration techniques, frequently Monte Carlo. Methods which are practical for producing rough answers without resort to high-speed computing machinery generally rely on a ray-tracing scheme. That is, the effects of the attenuating media and all boundaries are considered only by counting the number of mean free paths traversed in each material in a straight line trajectory from source point to detector. Additional assumptions are frequently made on top of this basic one.

Some of the forms in simple geometries which serve as a useful basis for gamma ray calculation are described below.

3.5.1.1 Point Source

$$\overline{D}(r, E) = \frac{\overline{S}(E)\, e^{-\mu(E)t}\, B(E, \mu t)}{4\pi r^2 \overline{K}(E)} \qquad (3\text{-}6)$$

where

$\overline{D}(r, E)$ = dose rate at point r cm from source due to gamma rays of source energy E, in roentgens/hr

$\overline{S}(E)$ = source strength of gamma ray of energy E, in Mev/sec

$\mu(E)$ = linear absorption coefficient for gamma rays of energy E of particular shield material,[4,5] in cm^{-1} (see Figures 3-3a, and b)

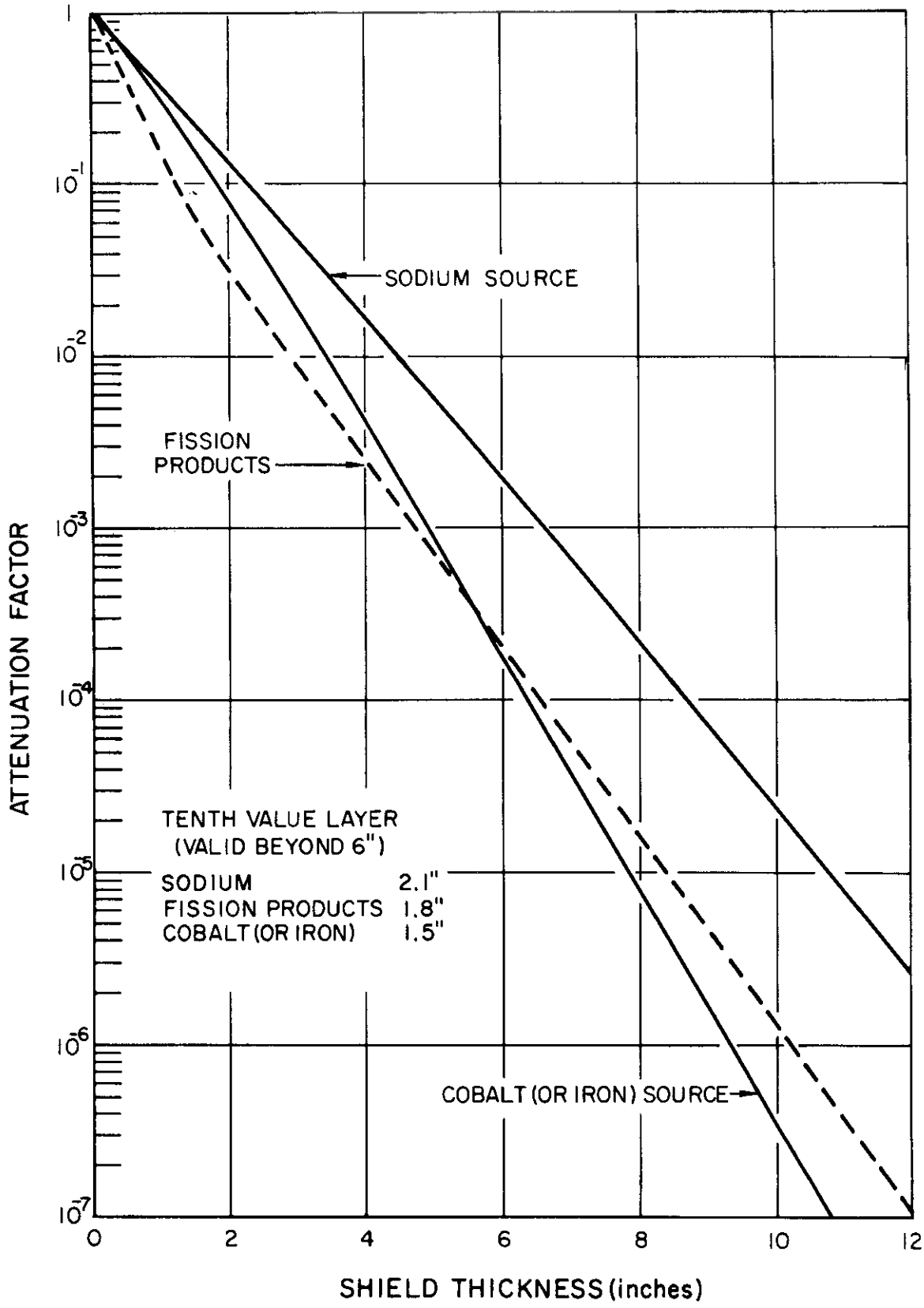

Figure 3-5. Attenuation of Point Source Gamma Rays in Lead

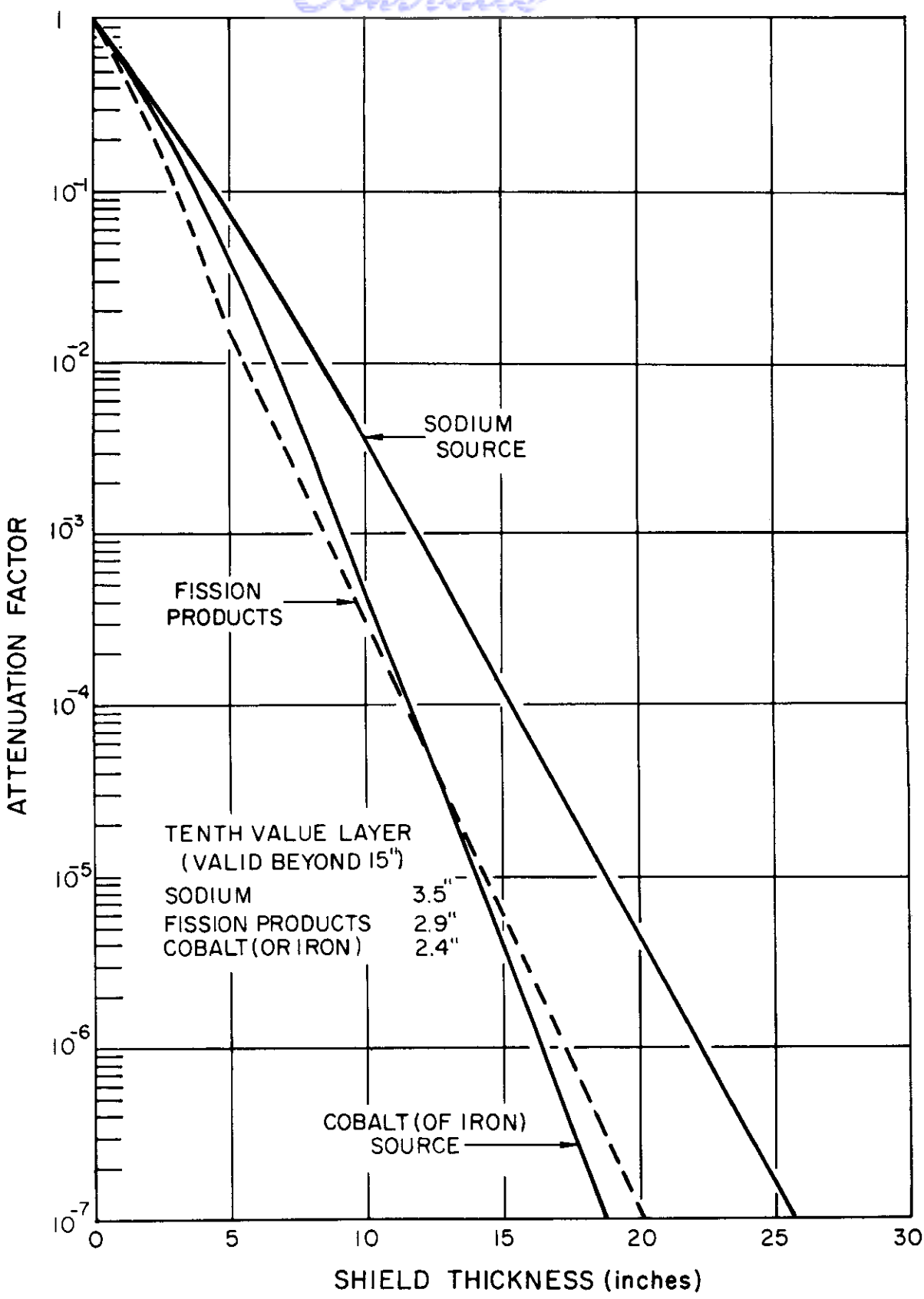

Figure 3-6. Attenuation of Point Source Gamma Rays in Iron

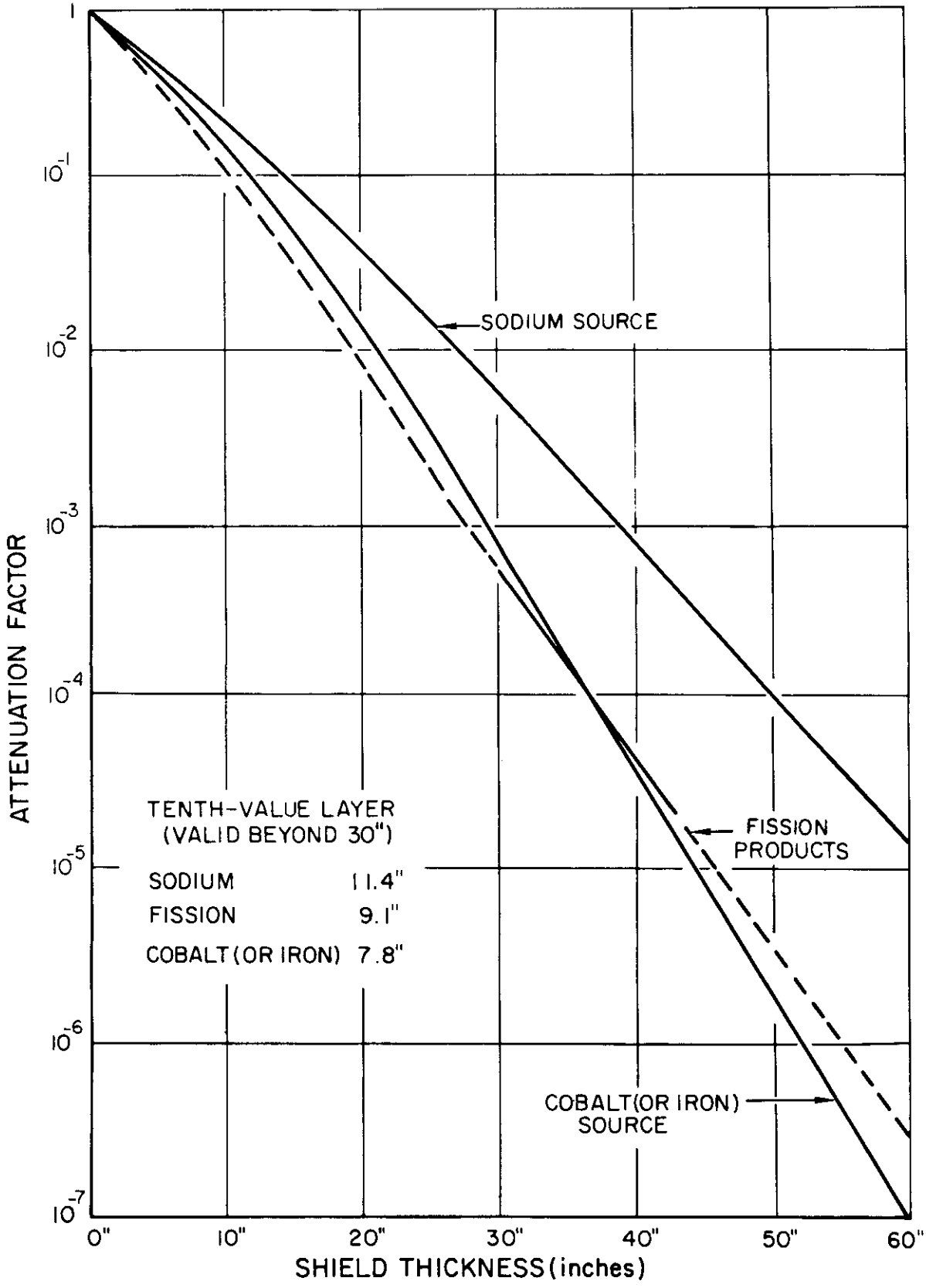

Figure 3-7. Attenuation of Point Source Gamma Rays in Ordinary Concrete

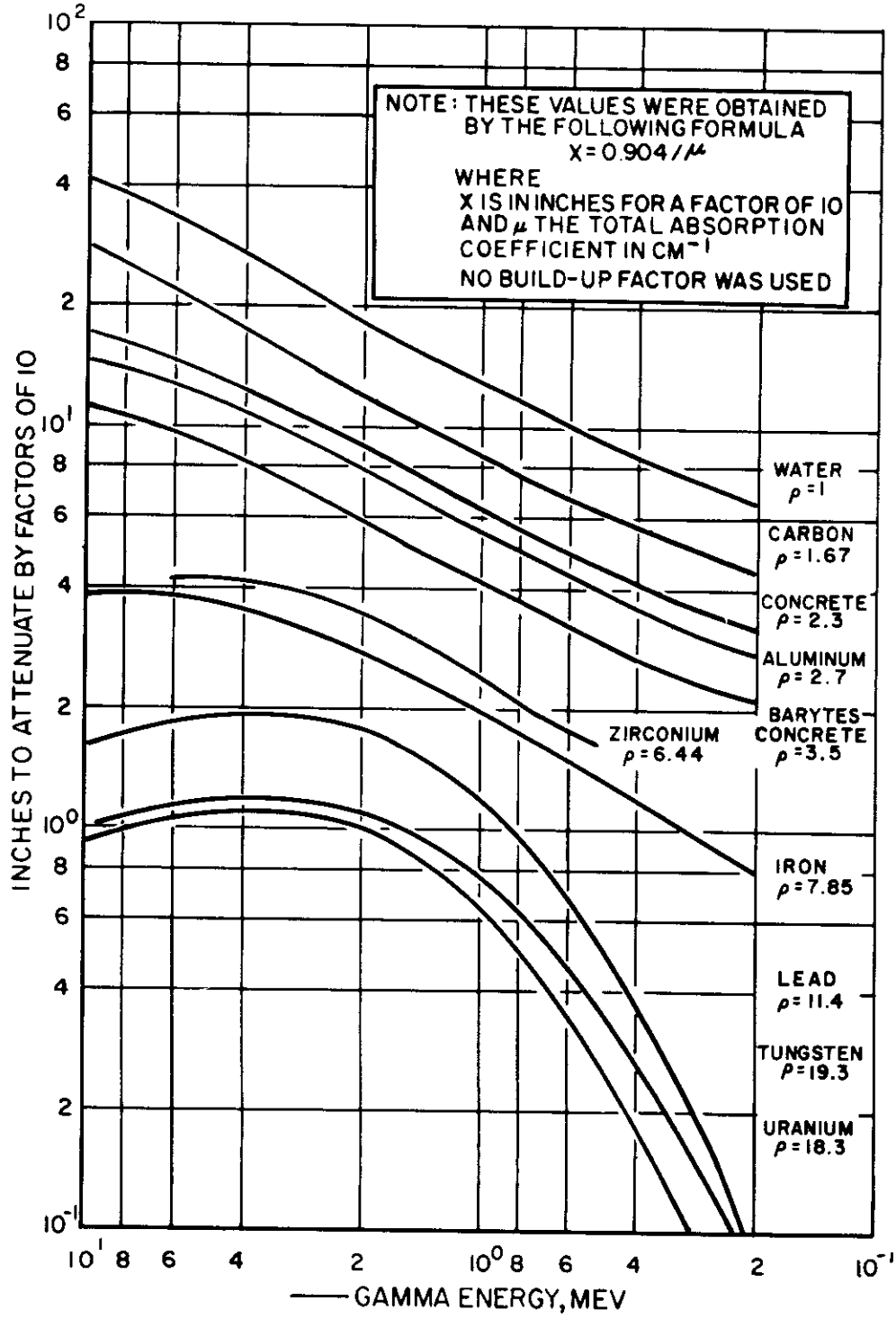

Figure 3-8. Inches to Attenuate by Factor of Ten in Common Shield Materials for Narrow Beam Geometry

t = thickness of shield, in cm

$B(E, \mu t)$ = dose buildup factor for shield material at energy E and penetration of μt mean free paths[6] (a tabulated function)

r = distance between source and detector, in cm

$\bar{K}(E)$ = energy flux to dose rate conversion factor at energy E in $\frac{\text{Mev}}{\text{cm}^2\text{-sec}} \Big/ \frac{\text{r}}{\text{hr}}$ (see Figure 3-4)

The quantity μt is the total number of narrow beam absorption mean free paths measured along a ray from a source point to a detector point. Note that $B(E, \mu t)$ is a function also of the medium traversed. It therefore does not strictly apply to a multimedium configuration. Various devices are used to fit an effective B to multimedium systems. The simplest is to choose the B appropriate to the last dense medium. This leads to quite reasonable results if the last dense medium is hydrogenous and is several mean free paths thick.

When shield calculations are performed for fission products, the following approximation may be used;

$$D = \frac{S}{4\pi r^2} A \times 2 \times 10^{-6} \qquad (3\text{-}7)$$

where

D = dose rate at detector, in r/hr

S = source strength in Mev/sec

r = distance from source, in cm

$A = Be^{-\mu t}$, as defined in Equation 3-6

In cases where radioactive isotopes are handled and high accuracy is not required, the following approximation may be used:

$$D = (6CE)\frac{A}{r^2} \qquad (3\text{-}8)$$

where

C = source strength, in curies

E = total energy of gamma rays in Mev/disintegration (see Table 3-7)

r = distance from source, in feet.

Equation 3-8 is a convenient equation to use, because for an unshielded case, the dose rate is 6CE r/hr at 1 foot from the source. It can be noted that a geometry attenuation of $1/r^2$ is used as in Equations 3-6 to 3-8. Figures 3-5 to 3-8 give values of A in Equations 3-7 and 3-8 for various shield materials.

3.5.1.2 Line, Plane, and Cylindrical Sources

For distributed sources such as line, plane, or cylinder sources, the geometry factor is no longer $1/r^2$, as in the point source case. Special functions will have to be used to correct for geometry as given in Reference 3. However, a distributed source, whose largest dimension is less than 1/3 the source-to-detector separation distance, can be adequately represented by a point source. This approximation yields results within 20% accuracy.

3.5.2 Neutrons

Neutron shielding calculations are much more complicated than those for gamma rays. This is because (a) no analytic form of the cross-section comparable to the Klein-Nishina formula for Compton scattering of photons exists, and (b) cross-section data are known much less accurately than for photons. As a consequence, it has not been possible to produce for neutrons tabulated functions like the buildup factors for photons.

A widely used device for the estimation of neutron attenuation is the removal cross-section. In an infinite homogeneous medium with an infinite plane source of fission neutrons, and in the absence of materials capable of producing neutrons by secondary processes, the fast neutron spatial distribution tends to become asymptotically exponential. This picture is very much an oversimplification if the neutron interaction cross section of the medium has a pronounced variation over the fission spectrum. At least for the simpler media the lower energy neutrons in the penetration spectrum are dominated in their spatial distribution by the higher energies. This is because they are determined mathematically by a convolution of the higher energy neutrons with a kernel characteristic of the medium. If the medium is hydrogenous, the half width of the kernel

to thermal energies will be quite small. Since neutron shields are invariably provided with heavy thermal poisoning, the result is roughly that removal of a neutron from the fast-flux component is tantamount to absorption. The asymptotic exponential spatial distribution is analyzed to associate a cross-section, called the removal cross-section, with the medium. Subsequently, slabs of other material are placed in front of the source and the additional diminution of the asymptotic fluxes is associated with a removal cross-section of the slab material.

The neutron quantity measured in the asymptotic region is a flux of high directionality. For practical purposes, that is for use of this quantity in conventional calculations, the angular flux is essentially equivalent to the neutron current, and not at all suitable, in most contexts, for use in expressions which call for the flux.

In view of the nature of the removal cross-section, its domain of justifiable applicability is limited. It is desirable to restrict its use to shields which are thick and whose final regions consist of several mean free paths (to fast neutrons) of hydrogenous material. The meaning of "thick" is that sufficient attenuation is provided to reduce neutrons of primary energy less than ~6 Mev to proportions negligible when compared with neutrons of greater primary energies. Then, from an isotropic point source of fission neutrons, the attenuated current at sufficiently large distances is given by

$$j(r) = \alpha S_o \frac{e^{-\int_o^r \Sigma_r(x)dx}}{4\pi r^2} \qquad (3\text{-}9)$$

where

$j(r)$ = fast neutron current (n/cm^2-sec) at deep penetration

S_o = point source strength (fission neutrons/sec)

$\Sigma_r(x)$ = macroscopic removal cross-section in region of x

α = fraction of fission spectrum above ~6 Mev

For distributed sources, this expression is integrated over the source region. These methods lead to rough but reasonable evaluations of the fast neutron dose, within the restrictions stated. It is sometimes required to have more neutron information than this for a crude preliminary shielding estimate. Two

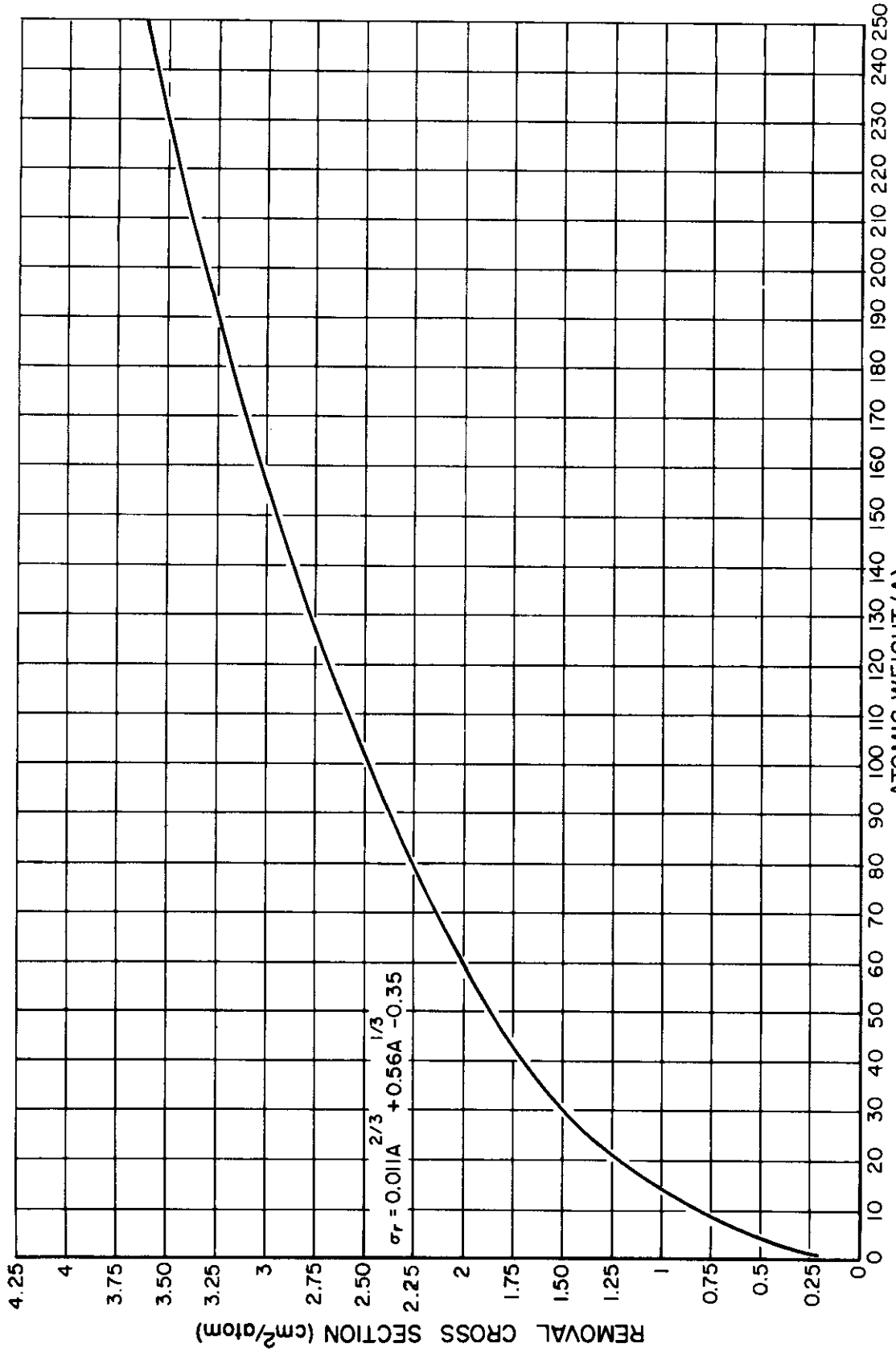

Figure 3-9. Neutron Removal Cross Section as a Function of Atomic Weight

demands which frequently arise are (a) fast neutron dose from a thin shield, and (b) neutron penetration spectrum for the purpose of evaluating secondaries.

For the fast neutron dose from a thin shield, one may examine the data applicable to the dominant hydrogenous medium, from which the medium removal cross section was determined. This will, in general, be data measured at the ORNL Lid Tank or computed by Goldstein et al. with moments. It is a neutron dose in the infinite hydrogenous medium given as a function of distance from a fission source. Reduced to a point kernel, K(r), the data can be used in the analog of Equation 3-9 as follows:

$$j(r) = S_o K(r) \tag{3-10}$$

The kernel K(r) is sometimes explicitly fit for a particular medium with an expression of the form

$$K(r) = \sum_i \frac{a_i e^{-\mu_i r}}{4\pi r^2} \tag{3-11}$$

It is customary, in any event, to represent K(r) by

$$K(r) = \frac{f(r)}{4\pi r^2} \tag{3-12}$$

Then, in cases where other material is placed heterogeneously into the hydrogenous medium, one sometimes uses in place of K

$$K'(r) = f(u) \frac{e^{-\Sigma_r^I v}}{4\pi r^2} \tag{3-13}$$

where

u = track length through hydrogenous medium

v = track length through other material

Σ_r^I = macroscopic removal cross-section of other material

r = u + v

TABLE 3-7

NUCLEAR PROPERTIES OF MATERIALS

Material	Z	A	ρ (gm/cm^3)	σ_r (barns)	Σ_r (1/cm)	Σ_r/ρ (cm^2/gm)
H	1	1.008	0.000084	1.00	0.0000503	0.598
D	1	2.015	0.00018	0.88	0.0000538	0.299
Li	3	6.940	0.53	1.01	0.0466	0.0879
Be	4	9.013	1.82	1.07	0.131	0.0717
B	5	10.82	2.3	0.97	0.124	0.054
C	6	12.011	1.62	0.81	0.066	0.0407
O	8	16.000	0.00133	0.99	0.0000495	0.0372
F	9	19.00	0.00158	1.29	0.0000647	0.0409
Na	11	22.991	0.97	1.20	0.0032	0.033
Mg	12	24.32	1.74	1.29	0.0557	0.032
Al	13	26.98	2.70	1.31	0.0788	0.0292
Si	14	28.09	2.33	1.37	0.0688	0.0295
P	15	30.975	1.82	1.53	0.0456	0.0298
S	16	32.066	2.07	1.55	0.0602	0.0291
Cl	17	35.457	0.00324	1.2	0.0000648	0.020
A	18	39.944	0.00166	1.71	0.0000428	0.0258
K	19	39.10	0.86	1.59	0.0211	0.0245
Ca	20	40.08	1.55	1.60	0.0372	0.024
Ti	22	47.90	4.5	1.82	0.103	0.0229
Cr	24	52.01	6.92	1.77	0.142	0.0205
Mn	25	54.94	7.2	1.84	0.146	0.0202
Fe	26	55.85	7.8	1.98	0.154	0.0214
Co	27	58.94	8.71	2.0	0.178	0.0204
Ni	28	58.71	8.83	1.89	0.168	0.0190
Cu	29	63.54	8.93	2.04	0.173	0.0194
Y	39	88.92	3.8	2.31	0.059	0.0155
Zr	40	91.22	6.4	2.35	0.10	0.0155
Nb	41	92.91	8.4	2.36	0.129	0.0154
Mo	42	95.95	10.2	2.39	0.153	0.015
Ba	56	137.36	3.5	2.83	0.0435	0.0124
W	74	183.86	18.8	2.51	0.154	0.00821
Pb	82	207.21	11.3	3.53	0.1163	0.0103
Bi	83	209.00	9.8	3.49	0.099	0.0101
U	92	238.07	18.8	3.6	0.171	0.0091
H_2O	-	18.00	1.0	-	0.103	0.103
D_2O	-	5.038	1.1	2.76	0.101	0.0921
B_4C	-	55.29	1.82	5.1	0.101	0.0555
LiH	-	7.948	0.775	2.01	0.1182	0.1525
$ZrH_{1.5}$	-	92.72	5.9	3.86	0.148	0.0251

Other somewhat similar approximations are available to apply removal theory to this problem. The application of removal theory is not, however, well justified because of the obvious variation in penetration spectra encountered from system to system.

To estimate a penetration spectrum, the simplest thing one can do is to fit a 1/E tail to the removal-computed fast flux. There is necessarily a considerable arbitrariness in this. If it is required to estimate thermal populations, one can say that it is roughly the ratio of the thermal lifetime to the time of occupancy of some energy interval of known population, multiplied by that known population. This rule works fairly well if there is no substantial loss by leakage or absorption in slowing down from the known group to thermal.

Table 3-7 and Figure 3-9 give some useful fast neutron data. Table 3-8 provides some conversion rules relating neutron currents to dose units.

TABLE 3-8

CONVERSION BETWEEN NEUTRON FLUX AND PHYSICAL AND BIOLOGICAL DOSE RATE

Neutron Energy (Mev)	Physical Dose Rate (rad/hr-n/cm^2-sec)	Biological Dose Rate (rem/hr-n/cm^2-sec)
Thermal	0.115×10^{-5}	0.0375×10^{-4}
0.001	0.25	0.0484
0.005	0.205	0.044
0.02	0.205	0.090
0.1	0.396	0.30
0.5	0.86	0.83
1.0	1.37	1.36
2.5	1.55	1.25
5.0	2.10	1.35
7.5	2.56	1.5
10.0	2.52	1.5

3.6 Neutron-Induced Activity

Certain nuclei become radioactive upon neutron absorption, and emit beta and/or gamma radiation. This source of radiation may sometimes be important, as in the case of reactor coolants, presenting an additional shielding problem to the shield designer. In order to perform the shielding calculations, the source strength of activated material has to be determined. The following equation is general and may be used for nearly all cases:

$$S_i(E_j, T) = \left[\frac{N\rho f_i E_{ij} n_{ij}}{A_i} \int_E \phi(E)\sigma_i(E)dE\right] \frac{(1 - e^{-\lambda_i t_r})(1 - e^{-n\lambda_i t_c})\, e^{-\lambda_i T}}{(1 - e^{-\lambda_i t_c})} \qquad (3\text{-}14)$$

where

$S_i(E_j)$ = source strength of radioactive isotope i per unit volume of activated material emitting gamma rays of energy E_j, in Mev/cm^3-sec

N = Avogadro's number, 6.025×10^{23} atoms/mole

ρ = density of material, in gm/cm^3

f_i = weight fraction of parent isotope of radioactive isotope i. This is equal to the product of the weight fraction of element i and the isotopic abundance of the parent isotope of i.

A_i = atomic weight of parent isotope of i, grams/mole

E_{ij} = decay gamma ray energy of isotope i, in Mev/photon (Reference 7)

N_{ij} = fraction of photons emitted by isotope i at energy E_j, in photons/disintegration

$\phi(E)$ = differential neutron flux, in neutrons/cm^2-sec-Mev

$\sigma_i(E)$ = energy dependent absorption cross section[8] of parent isotope i, in cm^2/atom

λ_i = decay constant of isotope i, in units of inverse time

= 0.693/half life

t_r = amount of time that the parent isotope is being irradiated per cycle

t_c = amount of time for one cycle

n = number of cycles

T = time after material being activated is out of neutron flux

and $$H \equiv \left[\frac{N\rho f_i E_{ij} n_{ij}}{A_i} \int_E \phi(E)\sigma_i(E)dE\right] .$$

It should be noted that the products $\lambda_i t_r$, $n\lambda_i t_c$, $\lambda_i T$, and $\lambda_i t_c$ are all dimensionless; i.e., if T is in seconds, λ_i is sec^{-1}, etc.

For one cycle activation (n = 1): Equation 3-14 reduces to

$$S_i(E_j, T) = H(1 - e^{-\lambda_i t_r}) e^{-\lambda_i T} \tag{3-15}$$

This is the basic equation for activation of stationary materials.

The following approximation is convenient in activation calculations.

$$1 - e^{-x} \approx x, \text{ if } x \text{ is less than } 0.1 \tag{3-16}$$

or

$$e^{-x} \approx 1 - x, \text{ if } x \text{ is less than } 0.1 \tag{3-17}$$

Thus in Equation 3-15, if $\lambda_i t_r$ is less than 0.1,

$$S_i(E_j, T) \approx H\lambda_i t_r e^{-\lambda_i T} . \tag{3-18}$$

Again in Equation 3-15, if $\lambda_i t_r$ is large, i.e., greater than about 3,

$$S_i(E_j, T) \approx H\, e^{-\lambda_i T} . \tag{3-19}$$

For many cycle activations, (n very large): Equation 3-14 reduces to

$$S_i(E_j, T) = H \frac{\left(1 - e^{-\lambda_i t_r}\right)}{\left(1 - e^{-\lambda_i t_c}\right)} e^{-\lambda_i T} \qquad (3\text{-}20)$$

In in addition $\lambda_i t_c$ (and Hence $\lambda_i t_r$) is a small number, i.e., less than about 0.1, Equation 3-20 reduces to

$$S_i(E_j, T) \approx H \frac{t_r}{t_c} e^{-\lambda_i T} \quad . \qquad (3\text{-}21)$$

Equations 3-20 and 3-21 are usually used for calculating reactor coolant activities. In this case:

t_r = time coolant spends in core, i.e., in high neutron flux

t_c = coolant cycle time

T = time after reactor shutdown.

During reactor operation, Equation 3-21 reduces to,

$$S_i(E_j, T) \approx H \frac{t_r}{t_c} \qquad (3\text{-}22)$$

Coolant cycle times seldom exceed one minute, thus for radioactive sodium (Na^{24}), which has a half life of 15.0 hours, Equation 3-22 could be used, and the source strength calculated would be quite accurate.

In thermal reactors, most of the activation results from thermal neutrons, for which the following approximation may be used:

$$\int_E \phi(E)\sigma_i(E)dE \approx \phi(th)\sigma_i(th) \qquad (3\text{-}23)$$

where

$\phi(E)$ and $\sigma_i(E)$ are defined in Equation 3-14

$\phi(th)$ = average thermal flux in the core, in neutrons/cm^2-sec

$\sigma_i(th)$ = thermal neutron absorption cross section of parent isotope i, in cm^2/atom.

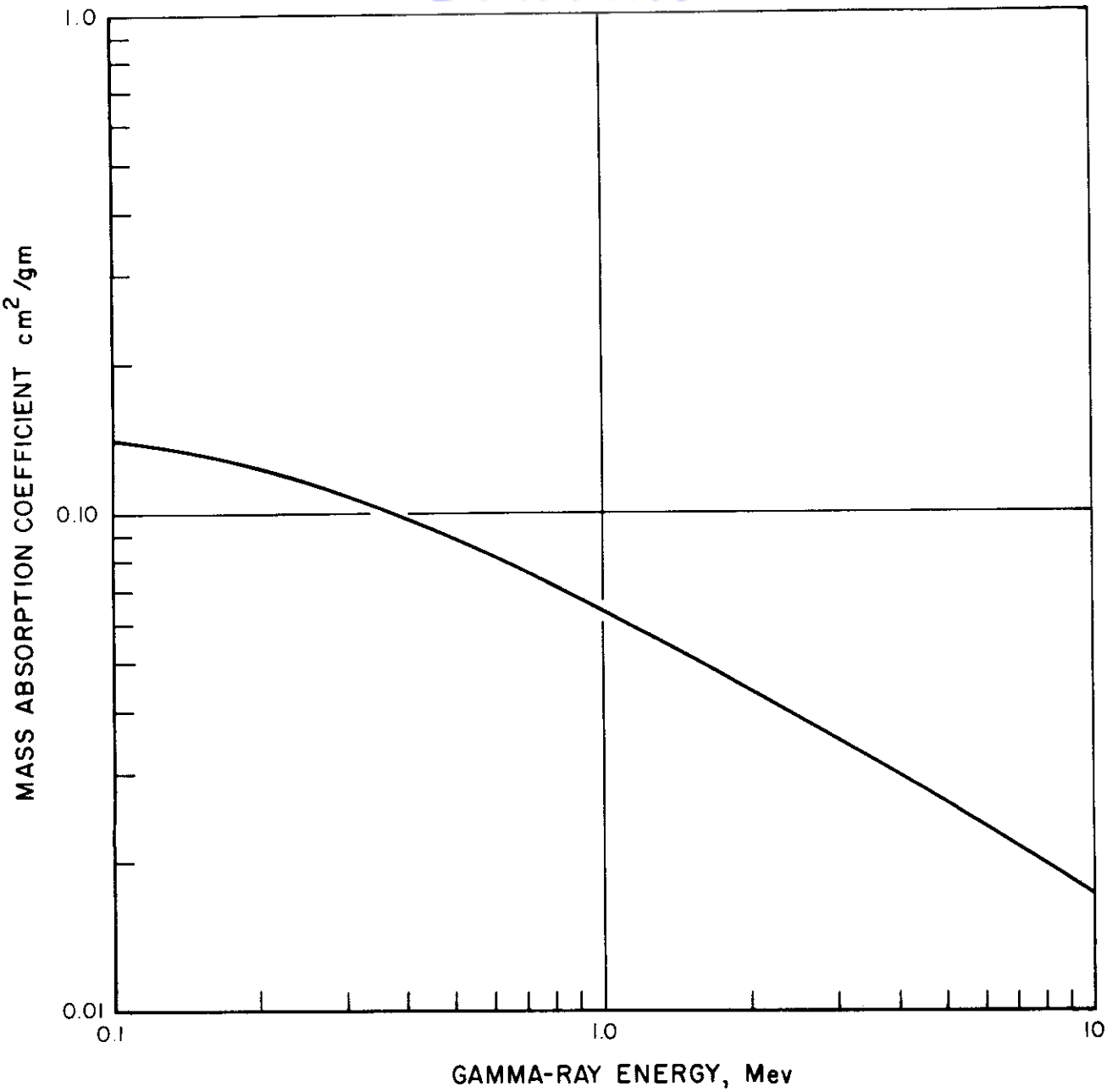

Figure 3-10. Gamma-Ray Mass Absorption Coefficient for Lithium Hydride

In some cases, the fast-neutron activation may be important. In these, cases, the radioactive isotopes are produced by (n, γ), (n, p), (n, α), and (n, 2n) reaction. (n, γ) cross sections may be obtained from BNL-325 (Reference 8), and cross sections for the other fast reactions may be obtained from References 9 and 10.

In manned space applications it will probably be desirable to avoid the need for shielding the crew from the extensive radiator system. This may be accomplished by providing shielding for the heat exchanger or by immersing the heat exchanger in the primary shield. Without a heat exchanger, the radiator would almost certainly contain a considerably activated coolant. In shielding the heat exchanger one must simultaneously provide adequate neutron shielding between heat exchanger and reactor to protect the secondary coolant from activation; and at the same time provide adequate photon shielding between the heat exchanger and the crew to protect the crew from excessive exposure to the activated primary coolant.

3.6.1 Secondary Gamma Rays

Calculation of production and attenuation of secondary gamma rays is one of the most difficult of all shielding problems. The expression for the dose from such gamma rays may be written as

$$D(E,\vec{r}) = \iiint \sigma(E'')\phi(\vec{r}', E'')N(E')Q\left[E', E, \vec{r}', \vec{r}\right] d\vec{r}'dE'dE'' \qquad (3\text{-}24)$$

where

$D(E,\vec{r})$ = dose deposited per unit energy about E at the receiver location $\vec{r}$

$\sigma(E'')$ = secondary photon production cross section for neutrons of energy E''

$\phi(\vec{r}', E'')$ = neutron flux density about energy E'' at location $\vec{r}'$

$N(E')$ = density of photons produced at energy E' from the neutron interaction characterized by $\sigma(E'')$

$Q\left[E',E,\vec{r}',\vec{r}\right]$ = amount of dose at energy E deposited at $\vec{r}$ when a gamma of energy E' is produced isotropically at $\vec{r}'$

The kernel Q is only a formal representation of the photon penetration problem described in a previous section. Apart from complexities

introduced by geometry in any particular situation — and these must be treated by ad hoc devices — the most difficult evaluation in Equation 3-20 may be the integral

$$\int \sigma(E'')\phi(\vec{r}', E'')dE''$$

In the high energy region and the thermal region the integral may frequently be evaluated with a one-energy approximation. If the shield is a hydrogenous medium with laminar inserts of resonance absorbing materials, evaluation of the integral at resonance energies may be quite difficult. For materials whose resonances tend to be low and broad, one might use the tabulated resonance integrals to determine effective average cross sections — with the possibility of some manner of self shielding refinement. For high, narrow resonances one might roughly set

$$\int_{\substack{\text{Resonance}\\ \text{Region}}} \sigma(E'')\phi(\vec{r}, E'')dE'' = \sum_k \int_{E_k^-}^{E_k^+} j(\vec{r}', E)dE \qquad (3\text{-}25)$$

where

E_k^- and E_k^+ bound a region in which the photon production cross section is greater than some appropriately high value

k is summed over all significant resonances

$j(\vec{r}', E)$ = current spectrum flowing into the resonance material at the interface $\vec{r}'$.

This approximation causes all neutrons to be absorbed in energy ranges where the photon production cross section lies above some value, and none absorbed elsewhere. It further causes the source of secondary photons to be a delta function at region interfaces — a reasonably realistic representation.

The crudeness of these evaluations is apparent. We are dealing in this manual only with rough and rapid estimation techniques. It might be well to note, however, that even the most refined and expensive methods developed for handling secondary photons have led to unsatisfactory results in most complex systems.

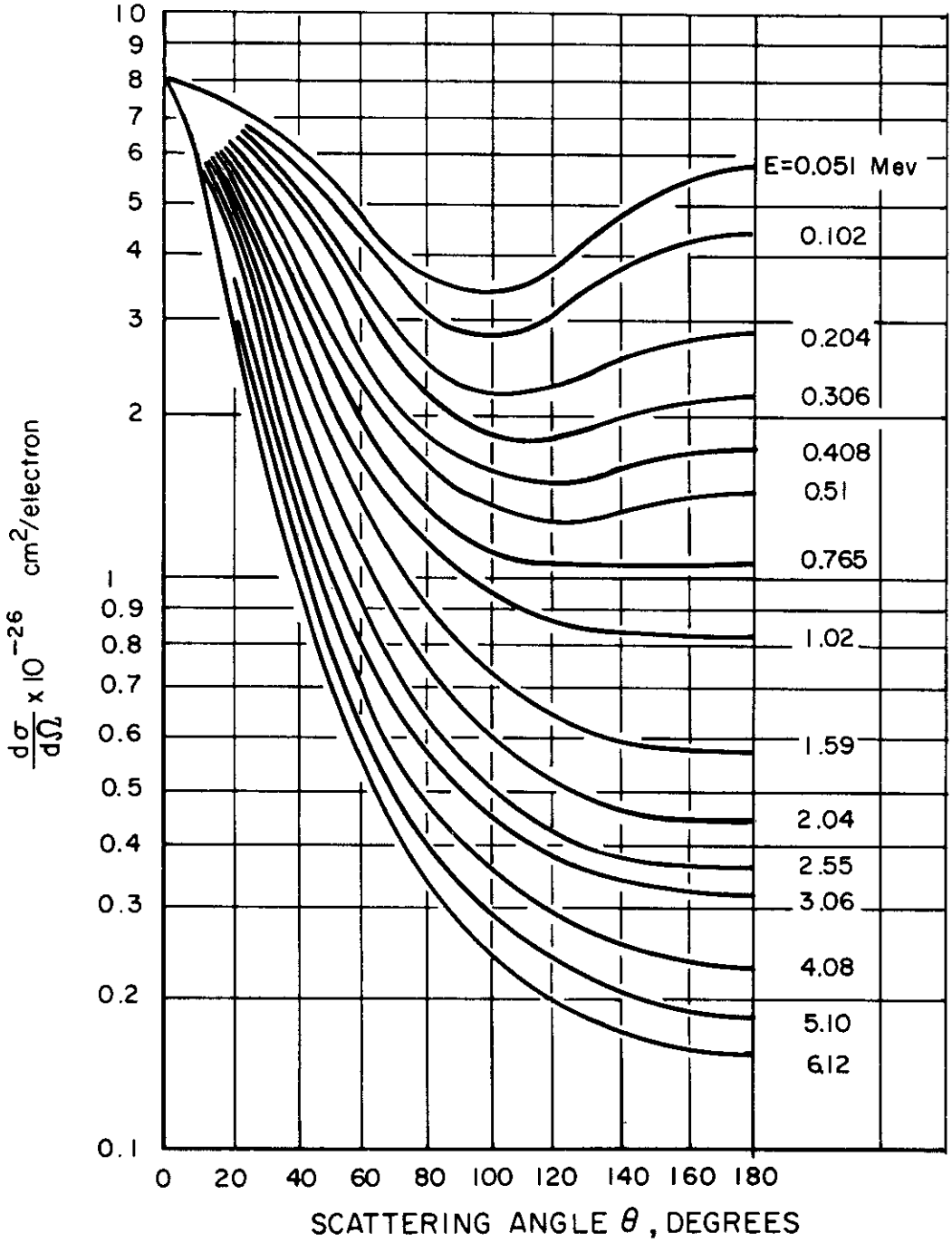

Figure 3-11. Gamma-Ray Differential Klein-Nishina Cross Section

3.7 Shielding Materials

Materials used in shielding may be divided into three categories according to their functions:

1. High density materials to absorb gamma radiation, and slow down fast neutrons to below 0.5 Mev by inelastic scattering.
2. Hydrogenous materials to slow down neutrons to thermal energies.
3. Materials containing thermal neutron suppressors, to capture thermal neutrons without producing high-energy capture gamma rays.

It should be noted that some shield materials may serve two or three functions at the same time.

Selection of a shield material cannot be made solely on the basis of its primary function, that of radiation attenuation. In addition to the nuclear characteristics of the shield material, such factors as structural characteristics, physical and chemical properties, cost, availability, etc., must be considered.

In the space application, heat rejection is by thermal radiation, necessarily at elevated temperatures. High temperature shield materials are therefore mandatory unless one is willing to undertake the excessive effort of refrigerating a shield. Lack of a gravitational field — in the ordinary sense — is apt to lead to unusual and undesirable bubble formations in a liquid shield. Solid materials are therefore preferable. The containment vessel will desirably be light and consequently subject to damage by moderately large pressure differentials. Since a vacuum will be on the outside the shield material should have a low vapor pressure at operating conditions.

The following sections give a brief description of shielding properties of various shield materials.

3.7.1 Gamma-Ray Shielding

The shield thickness required to achieve a specific gamma-ray attenuation decreases with an increase in the linear gamma-ray absorption coefficient, which is equal to the mass absorption coefficient (cm^2/gm) multiplied by the density of the material (gm/cm^3). Therefore in order to have a high linear absorption coefficient, a material must have a high mass absorption coefficient and a high density. The mass absorption coefficient of elements, generally,

increases with an increase in atomic number. Therefore, in order to achieve a specified gamma-ray attenuation with a minimum thickness, materials with a high atomic number and high density should be used. It should be noted that in addition to the gamma-ray attenuating properties of materials, the neutron interactions which produce high energy secondary gamma rays should be considered. This additional source usually complicates the reactor shielding problem.

Figure 3-3 gives mass absorption coefficients for various materials.

3.7.2 Fast Neutron Shielding

The most effective way to attenuate fast neutrons (> 0.5 Mev) is by slowing them down to thermal energies and then absorbing them. Hydrogen is a very desirable component in a neutron shield, because of the large energy degradation that accompanies a neutron collision with a hydrogen nucleus. At high energies, however, the scattering cross section of hydrogen is very small and it decreases as the energy increases. Thus considerable thicknesses of hydrogen would be required to thermalize fast neutrons. This situation may be improved, however, by introducing elements of high mass number, which will reduce the neutron energy by inelastic scattering to an energy where the cross section for hydrogen is much higher. Hence, a combination of high-mass number elements with hydrogen make very effective fast neutron shields.

Table 3-8 and Figure 3-9 give fast neutron removal cross sections for various materials. It should be emphasized that removal cross sections can only be used when they are followed by $\sim$2 feet of water or other hydrogenous media.

3.7.3 Thermal Neutron Suppressors

After the neutrons have slowed down by inelastic scattering and then by elastic scattering from light elements, the next aspect of shielding to consider is that of capturing these neutrons. The capture process may result in the emission of high-energy gamma rays or charged particles such as alpha particles or protons. Since the gamma rays are much more penetrating than charged particles, the ideal shield material for capturing slow neutrons would be one that emits charged particles. Boron and to a lesser extent lithium are widely used as thermal neutron suppressors.

The reaction with boron is $B^{10}(n, \alpha)Li^{7}$. In this reaction, 6% of neutron captures in B^{10} result in a 2.79 Mev alpha particle, and 94% of neutron captures result in a 2.31 Mev alpha particle and a 0.48 Mev gamma ray. The reaction with lithium is $Li^{6}(n, \alpha)H^{3}$. In this case all neutron captures result in a 4.78 Mev alpha particle. These values are important in heat generation calculations in shields.

Boral is a widely used thermal neutron suppressor. It is composed of a mixture of boron carbide (B_4C) and aluminum, and clad with aluminum. It usually comes in sheets 1/8 or 1/4 inch thick and has a density of about 2.5 g/cm^3. The amount of B_4C ranges from 10 to 50 wt %.

Another material which is a good neutron suppressor as well as an excellent neutron shield is lithium hydride (LiH). Due to its light weight and nuclear properties, LiH is an outstanding neutron shield material for nuclear powered aircraft and for SNAP reactors in space. Table 3-9 and Figure 3-10 give some of the important properties of lithium hydride. It should be noted that the fast-neutron dose attenuation coefficient as given in Table 3-9 applies to an isotropic point fission source in an infinite medium of LiH.

TABLE 3-9

PROPERTIES OF LITHIUM HYDRIDE

Molecular weight	7.95
Density (20°C)	0.775 gm/cc
Hydrogen density	5.86×10^{22} atoms/cc
Melting point	1270°F
Dissociation pressure	35 mm Hg at 1290°F
Specific heat at 20°C	1.03 cal/gm-°C
Coefficient of thermal expansion	4.2×10^{-5}/°C^{-1}
Thermal conductivity (powder form)	0.019 cal/cm-sec-°C
Vapor pressure at melting point	20 mm Hg
Fast-neutron removal cross section	0.1182 cm^{-1}
Fast-neutron dose attenuation coefficient	0.143 cm^{-1} (0 - 78 cm of LiH) 0.103 cm^{-1} (78 - 156 cm of LiH)

3.8 Structure Scattering

In some shield designs, the radiation level from structure scattering of gamma rays and neutrons may be important. For single scattering processes, the following equation holds:

$$D(E,\vec{r}) = \frac{NE}{K(E)} \iiint t(\vec{r}')j_o(E',\vec{r}') \frac{R(E,E',\theta)}{\ell^2(\vec{r},\vec{r}')} \frac{d\sigma(\theta)}{d\Omega} dA dE' d\Omega \qquad (3\text{-}26)$$

where

$D(E,\vec{r})$ = scattered dose at $\vec{r}$ carried by particles of energy E

$K(E)$ = conversion factor to suitable dose units

$t(\vec{r}')$ = thickness of scatterer at $\vec{r}'$

$j_o(E',\vec{r}')$ = primary radiation current of energy E' at $\vec{r}'$

N = number of atoms/cm^3 of scatterer

$R(E,E',\theta)$ = probability that primary particle of energy E' has energy E after scattering through angle θ

$\ell(\vec{r}',\vec{r})$ = separation of scatter point $\vec{r}'$ and target point $\vec{r}$

$\frac{d\sigma(\theta)}{d\Omega}$ = microscopic cross-section for scattering into a unit solid angle about the angle θ

θ = angle of scattering

The integrations indicated by dA, dE', $d\Omega$ are over the scattering surfaces, the range of incoming particle energies, and the target solid angle respectively.

This expression is appropriate for either neutrons or photons, provided that scatterers are thin enough to be represented by a single scattering calculation.

Figure 3-11 provides some useful information on photon scattering cross-sections.

REFERENCES

Section 3

1. F. E. Deloume, "Gamma-Ray Energy Spectra from Thermal Neutron Capture," DC-58-1-30, January 2, 1958
2. H. Goldstein, "The Attenuation of Gamma Rays and Neutrons in Reactor Shields," U.S. Government Printing Office, 1957
3. A. Foderaro and F. Obenshain, "Fluxes from Regular Geometric Sources," WAPD-TN-508, June 1955
4. T. Rockwell, "Reactor Shielding Design Manual," TID-7004, March 1956
5. J. Moteff, "Miscellaneous Data for Shielding Calculations," APEX-176, December 1, 1954
6. H. Goldstein and J. E. Wilkins, Jr., "Calculations of the Penetration of Gamma Rays," NYO-3075, June 30, 1954
7. "Activation Handbook for Aircraft Designers," NARF-57-50T, September 30, 1957
8. D. J. Hughesand R. B. Schwartz, "Nuclear Cross Sections," BNL-325, 2nd Edition, July 1, 1958
9. R. S. Rochlin, "Fission-Neutron Cross Sections for Threshold Reactions," Nucleonics 17, No. 1, 54 (1959)
10. R. J. Howerton, "Semi-Empirical Neutron Cross Sections," UCRL-5351, November 1958
11. D. J. Hughes and R. S. Carter, "Neutron Cross Sections, Angular Distribution," BNL-400, June 1956
12. J. A. Van Allen and L. A. Frank, "Survey of Radiation Around the Earth to a Radial Distance of 107,400 Kilometers," SUI-59-2, January 1959
13. J. A. Van Allen and L. A. Frank, "Radiation Measurements to 658,300 Kilometers with Pioneer IV," SUI-59-18, August 1959

RECOMMENDED ADDITIONAL REFERENCES

B. T. Price, C. C. Horton, and K. T. Spinney, "Radiation Shielding," Pergamon Press, New York, 1957

J. O. Blomeke and M. F. Todd, "U-235 Fission Product Production as a Function of Thermal Neutron Flux, Irradiation Time, and Decay Time," ORNL-2127, August 19, 1957

J. F. Perkins and R. W. King, "Energy Release from the Decay of Fission Products," Nuc. Sic. Eng., 3, No. 6, 726 (June 1958)

G. T. Chapman, and C. L. Storrs, "Effective Neutron Removal Cross Sections for Shielding," AECD-3978 (ORNL-1843), September 19, 1955

G. White Grodstein, "X-Ray Attenuation Coefficients from 10 kev to 100 Mev," NBS Circular 583, April 30, 1957

M. Grotenhuis, "Lecture Notes on Reactor Shielding," ANL-6000, March 1959

4. SAFETY

In considering the use of a nuclear auxiliary power system in space, the potential radiological hazards associated with its use must be evaluated. When anticipated by the appropriate design criteria, handling procedures, and operational limitations, it can be shown that these potential radiological hazards do not prevent the use of nuclear power in space. Throughout the design and development of SNAP 2, safety has provided the basis for many design decisions. In order to satisfy the objective of maximum possible safety of the SNAP space reactor systems, a set of safety design criteria for SNAP reactors was formulated. Compromises on the system design are necessary in order to obtain a suitable balance between the safety of the system and the operational characteristics of reliability, simplicity, and weight. The safety design criteria for the SNAP space reactor systems are outlined below:

1. Safety and Ease of Handling

   The reactor system will be designed so that personnel can handle, install, and repair the system before launch with safety and ease.

2. Prevention of Accidental Criticality

   The reactor systems will be designed to prevent criticality of the reactor under any condition except controlled operation.

3. Inherent Shutdown

   The reactor system will have inherent shutdown characteristics (i.e., negative temperature coefficient and fail-safe shutdown mechanisms to prevent reactor operation before or after mission time periods.

4. Orbital Startup

   Reactor system full power operation need not begin until after a suitably safe orbit has been established.

5. Orbital Shutdown

   After the mission has been completed and prior to re-entry, the reactor may be shut down.

6. Re-entry Burnup

Design of the reactor system and components will ensure the probability of high altitude re-entry burnup and dispersal of SNAP reactor components.

The four major periods of the operational sequence, the particular safety problems of each, and their evaluation and resolution are discussed below.

4.1 Shipment and Integration Period

During the shipment and integration of the NAPU into its payload and launch system, the possibility of accidental criticality and an uncontrolled power excursion must be prevented. The SNAP 2 reactor is specifically designed to allow the removal of the reactor's beryllium reflector and thus greatly increase the safety margin that must be overcome for accidental criticality. During shipment and integration the beryllium will be replaced with a thick solid aluminum jacket such that accidental immersion in water, liquid hydrogen, or kerosene cannot cause criticality. Likewise, the proximity of installation personnel will not cause accidental criticality. During the shipment and integration period the radioactivity remaining in the core from the factory checkout operations will have decayed to a sufficiently low level that personnel working on or around the APU will be subjected to radiation levels below the AEC established occupational dose rate of 7.5 mr/hr.

By supplementing these physical constraints with carefully planned procedures and trained personnel, the potential of accidental criticality and personnel injury during the shipment and integration period can be even further reduced.

4.2 Launch Pad Operations Period

It is not expected to be necessary to operate the reactor at full power on the launch pad. The SNAP 2 APU is designed such that system operation and performance can be checked out with electrical power supplying the heat in place of the reactor. If future requirements necessitate complete nuclear operation on the launch pad, it can be accomplished.

Figure 4-1 shows the dose rate as a function of distance from the operating SNAP 2 reactor with air and inverse square distance attenuation and with 3 feet of concrete shielding. It can be seen from inspection of Figure 4-1 that the dose outside of normal chemical exclusion radius or inside a normal blockhouse installation is within the AEC occupational dose rate of 7.5 mr/hr.

If the mission is "held" after 30 minutes of reactor power operation on the launch pad, the dose as a function of distance and decay time is shown in Figure 4-2. After a few hours of decay, short time access to the base of a typical booster is not prohibitive. If access to a payload section is necessary, a gantry mounted maintenance shield is required. A possible configuration is shown in Figure 4-3. The 4-inch thick lead maintenance shield is shown to reduce the dose at the payload region to about 100 mr/hr which allows several hours of payload access without excessive exposure.

If the mission is totally "scrubbed," the APU can be removed to a shielded storage well by means of a remotely operated manipulator and gantry.

In the case of a chemical accident after reactor operation or accompanied by an accidental power excursion, preliminary analysis indicates only minor hazards outside the normal exclusion radius. Deposition of radioactivity within the exclusion radius could lead to temporary evacuation, but the combination of decay time and emergency decontamination procedures can restore the launch pad area to usefulness.

Again, even the worst case of launch pad abort during reactor power operation can be handled if appropriate equipment and procedures are made available.

4.3 Launch to Orbit Period

The significant problem during the launch to orbit period is the possible chemical explosion accompanied by an uncontrolled reactor power excursion. Only during the early stages of launch does the missile path pass over land. For this period, the hazards analysis performed for the launch pad period is applicable, which indicated only

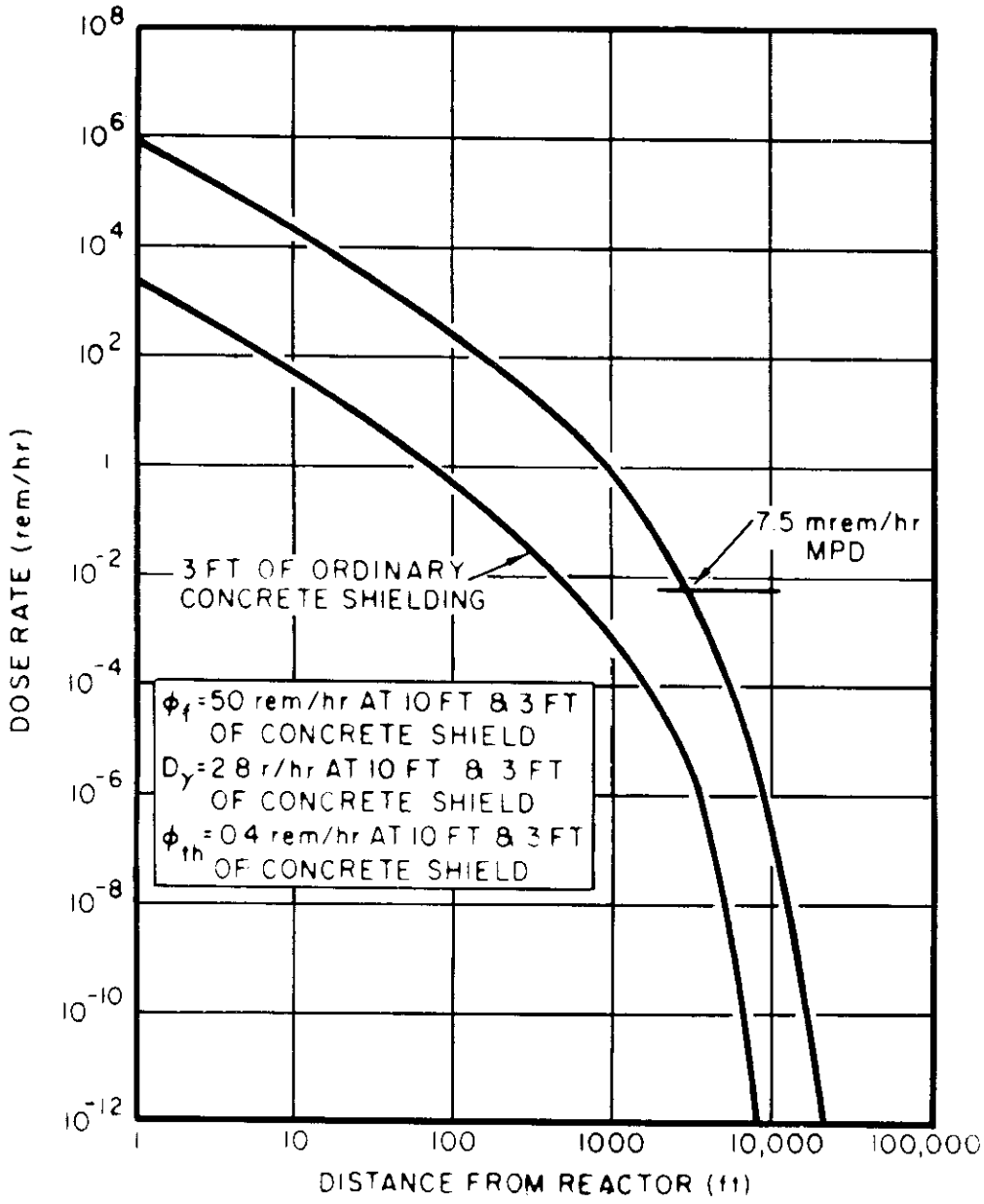

Figure 4-1. Total Dose Rate as a Function of Distance in Air from SNAP 2 APU During 50 kw Reactor Operation

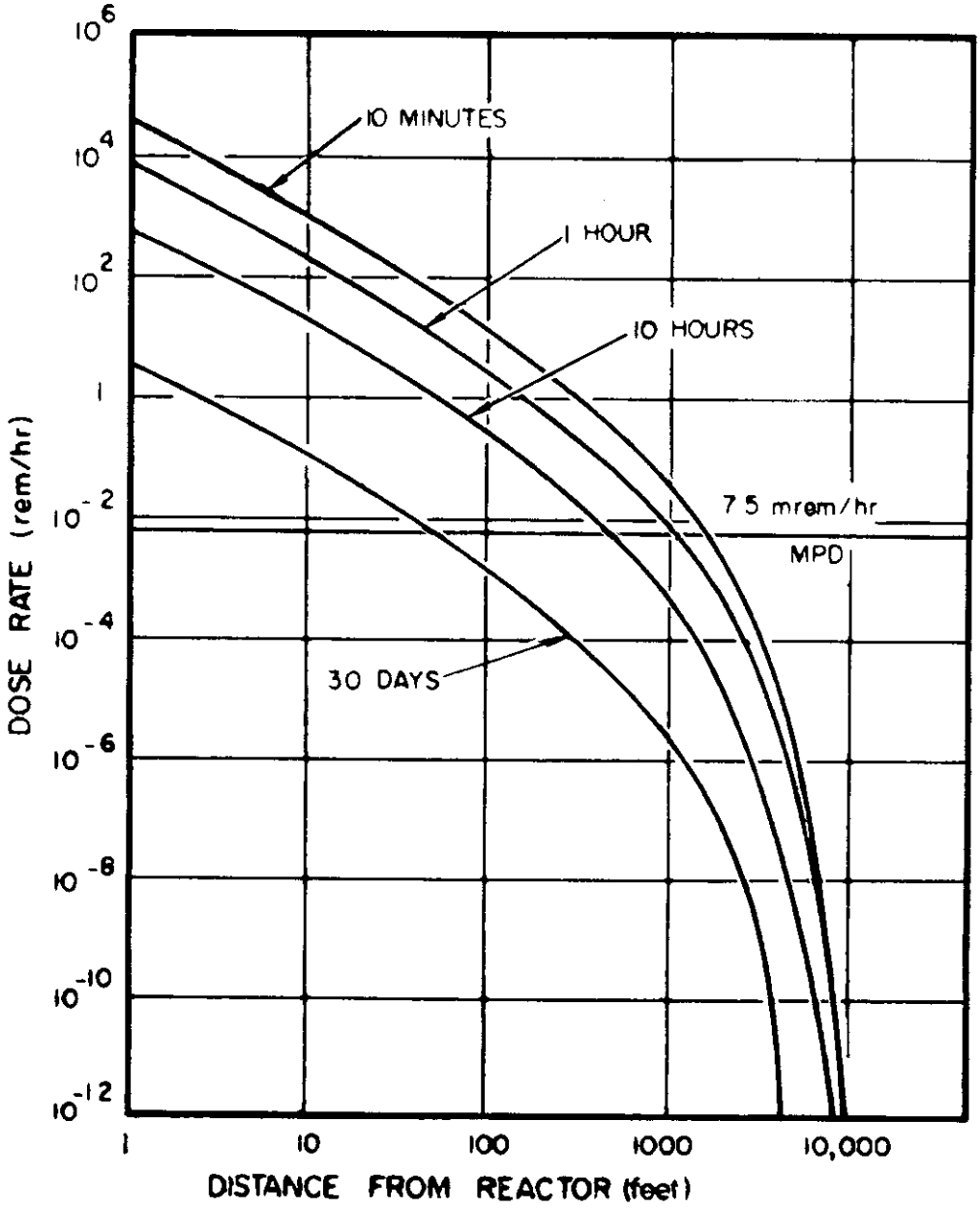

Figure 4-2. Gamma-Ray Dose Rate from SNAP 2 APU After 30 Minutes Operation at 50 kw

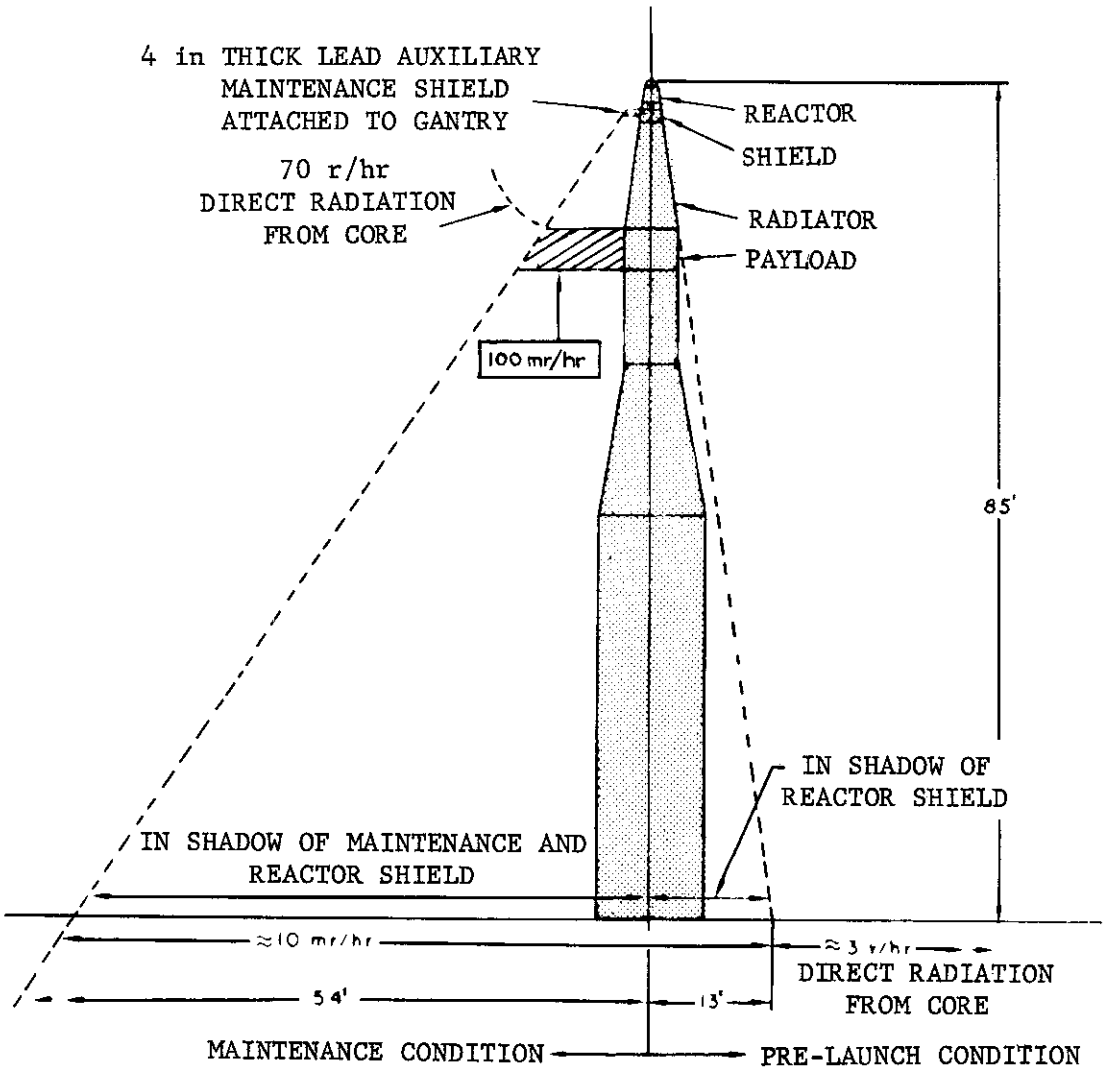

Figure 4-3. Dosage After 30 Minutes of Test Operation and 1 Hour Decay

minor hazards outside the normal exclusion radius. After lift off, the dispersal and dilution factors for the altitudes associated with the missile path over land will further decrease these minor hazards. The remainder of the abort conditions for the launch phase will exist over an ocean region in non-populated areas and far from inlands or major cities. Thus, the potential hazards to the general populace from a personnel as well as contamination standpoint is negligible over a complete range of possible abort conditions.

4.4 Re-entry Period

In the first three periods considered, the hazards are at all time subject to control through site selection, meteorological limitations, emergency procedures, range safety, etc. The unique problem associated with reactor re-entry results from the unpredictable location of re-entry and the fact that radiation is undetectable by an unaware populace.

The objective of the SNAP development program is to design for fuel element high altitude burnup and dispersal to result from re-entry heating. Preliminary calculations supplemented by arc-jet experiments indicate that this objective can be achieved. In order to evaluate the significance of contributing fission products to the earth's atmosphere through re-entry burnup and dispersal of SNAP systems, the resultant buildup of SR^{90} has been calculated. Figure 4-4 shows that the re-entry of one SNAP 2 system each year after one year of operation will, after 60 years, result in an equilibrium Sr^{90} concentration in the earth's atmosphere that is about 1/240 of the level then existing from bomb testing prior to 1960. Or, in other words, SNAP 2 systems could be employed at the rate of 240 per year for the next 60 years and only contribute an amount equal to the Sr^{90} level remaining then from the bomb testing prior to 1960.

Until complete re-entry burnup and high altitude dispersal have been demonstrated, there exists an immediately available solution to the hazards associated with the intact re-entry of a SNAP system. The problem can be solved by allowing sufficient time for radioactive

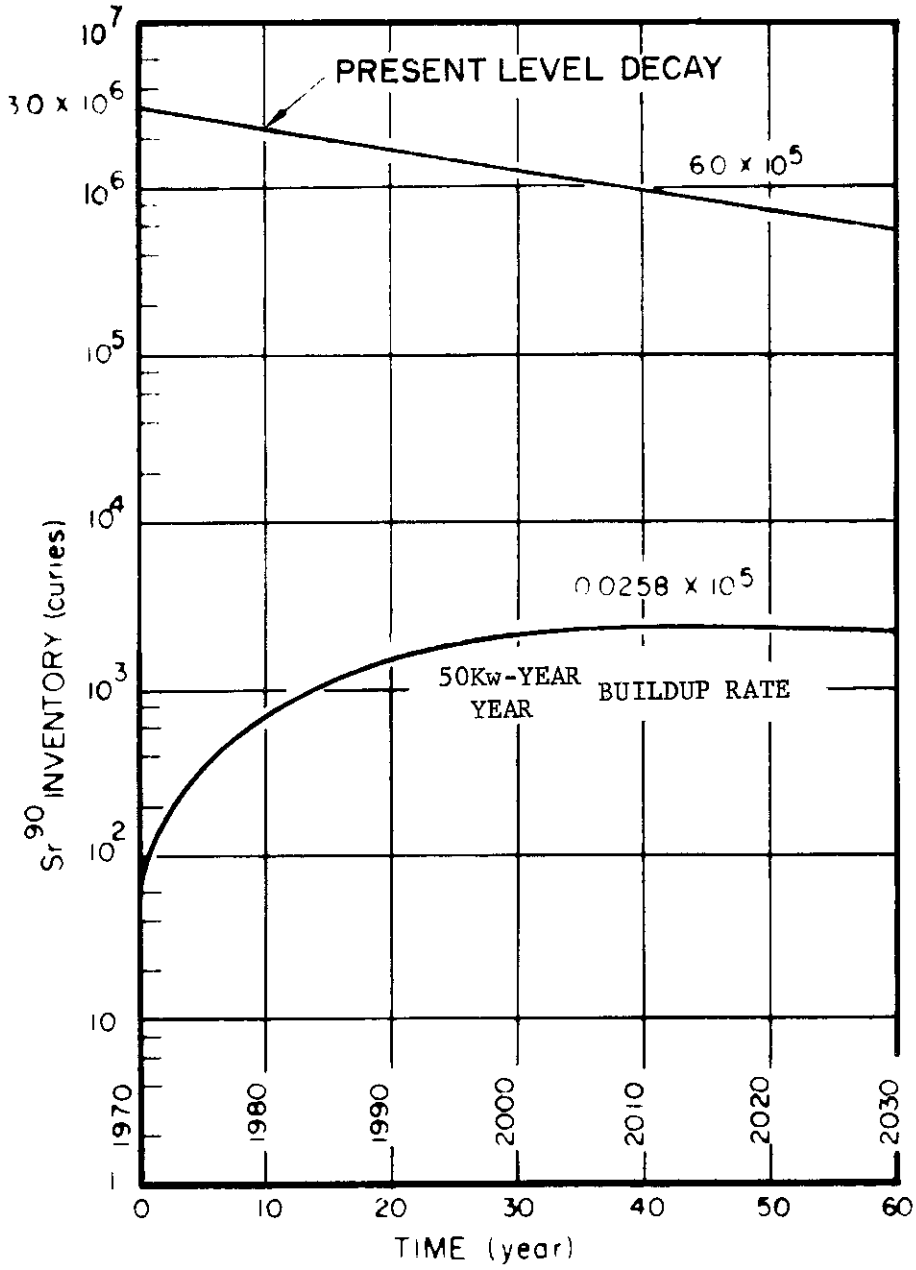

Figure 4-4. Comparison of Sr^{90} Inventory in Upper Atmosphere from PAST Nuclear Tests and Possible Space Programs

decay such that intact re-entry does not constitute a radiological hazard. This decay time is achieved by limiting the use of SNAP systems to orbital altitudes which have the requisite orbital lifetime for decay. This approach must be supplemented by orbital startup of the system. This capability, which is a SNAP 2 development objective, allows a complete safety appraisal of the orbit prior to system startup and fission product generation.

Figure 4-5 shows the relationship between dose rate, time for 25 r total dose, decay time, and orbital altitude as a function of distance from an intact SNAP 2 reactor. It can be seen that orbital lifetimes beyond 300 years, or about 600 miles for a typical large vehicle, lead to negligible dose rates. Therefore use of SNAP 2 in orbits of greater than 300 years duration coupled with orbital startup results in no re-entry radiological hazard.

In conclusion, it has been shown that radiological hazards do not significantly limit the use of SNAP 2 in space. The use of high altitude orbits and orbital startup eliminate the re-entry hazard by allowing long decay times prior to re-entry.

Re-entering systems with high altitude burnup and dispersal can be used in large numbers without appreciably contributing to the contamination of the earth's surface or atmosphere. The pre-launch and launch period hazards can be controlled through operational procedures and appropriate facilities and equipment.

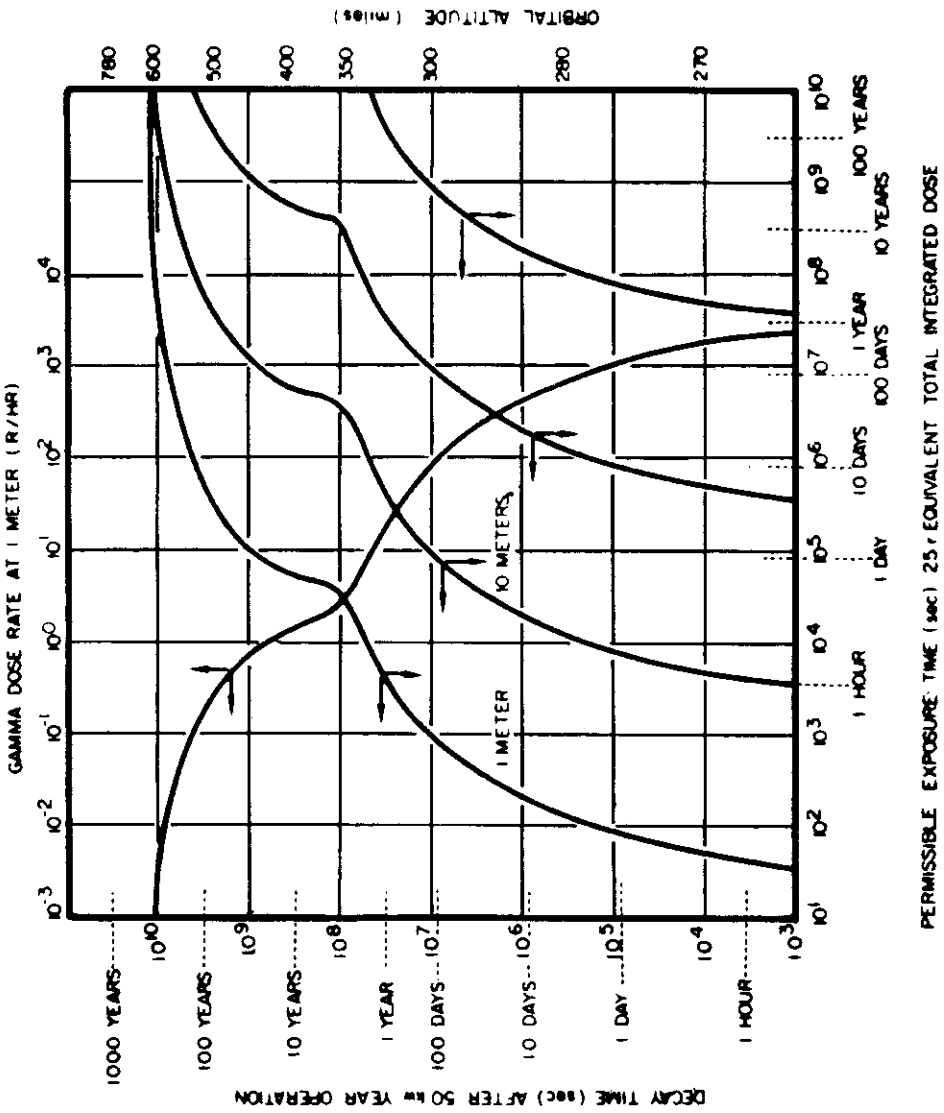

Figure 4-5. Permissible Exposure Time and Distance for Intact SNAP Re-entry vs Decay Time in Orbit and Orbital Altitude

REFERENCES

Section 4

1. R. Balent, "Nuclear Reactor Heat Source for Project Feed Back," NAA-AER-MEMO-896, February 13, 1954.

2. R. C. Brumfield and R. Balant, "Auxiliary Power Plant Prime Mover and Electrical Generator for Project Feed Back," NAA-AER-MEMO-897, February 13, 1954.

3. NAA-AER-1500, "A Proposed Nuclear Auxiliary Power Plant, 0.5-10 kw Net Electrical Capacity," October 15, 1955.

4. J. R. Wetch and R. L. Wallerstedt, "A 3 kw Nuclear Auxiliary Power Unit for the 117L Advanced Reconnaissance System," NAA-SR-1840, January 31, 1957.

5. RELIABILITY CONSIDERATIONS

5.1 Reliability Goals

The high costs associated with missile launching activities have made reliability a subject of pressing importance. If a satellite system has low reliability, several launchings will be required for success, thus increasing the cost of the successful satellites. If a satellite system has very high reliability, few launchings will be required to achieve successful satellites. However, if prohibitive development costs have been incurred in design and testing to achieve high reliability satellites, the cost of the successful satellites is increased. Thus an economic optimum value of satellite reliability exists. Unless military tactical considerations overrule, these economic optimum values of reliability may be estimated and used as developmental reliability goals.

The most difficult aspect to evaluate is the relation between development costs and achieved reliability. Reliability is achieved by judicious engineering design, yet environmental testing is required to demonstrate or prove the inherent reliability prior to acceptance. A development program will be assumed where engineering redesign efforts are conducted concurrently with reliability proof testing activity, so a feedback of test results guides redesign. With these conditions, it will be assumed that the achieved, or inherent, reliability increases with time and remains approximately equal to the statistically demonstrated or proven reliability accomplished by the steady accumulation of results from the testing program. The fact that the test statistician's samples are not constant but are redesigned and improved with time only makes his reliability results conservative. Of course, physical limitations of materials or production techniques put upper limits on the reliability that may be achieved.

Reliability is a statistical field with a literature containing its own vocabulary, and statistical results are as reliable as the input data. To facilitate understanding of this section, the following terms are defined:

t = service life of a nuclear power unit, (APU) (years)

θ = APU inherent mean time between failures (years)

θ_o = APU statistically proven mean time between failures (years)

θ_t = APU environmental test time required to prove θ_o (years)

$E = \frac{\theta_t}{\theta_o}$ = expectation of testing required to prove θ_o. (Under conditions of $\theta = \theta_o$ discussed above and in section on statistical test requirements, E = 2.7)

$R_a = E^{-t/\theta}$ = APU reliability

a = cost of required fabrication and operating expenses for environmentally testing 1 APU for 1 year

$A = a\theta_t$ = total cost of environmental testing program

$A = aE\theta_o$

$$A = aE \frac{t}{-\ln R_a}$$

For the launching expenses:

b = cost of fabrication and operating expenses for launching a complete missile including a satellite consisting of an APU and a payload

R_b = reliability of missile launching and payload

$C_n = N \frac{b}{R_a R_b}$ = cost of achieving N successful satellites

However, if the cost of the APU environmental testing program is amortized in the cost of N successful satellites, the total cost is the following:

$$C_n = N \frac{b}{R_a R_b} - \frac{aEt}{\ln R_a}$$

These costs are shown in Figure 5-1 for a 3 month satellite life, Figure 5-2 for a 1 year satellite life and in Figure 5-3 as a selected composite presentation. These curves indicate that the optimum APU reliability goal ranges from 70 to 95 percent depending primarily on the number of satellites desired.

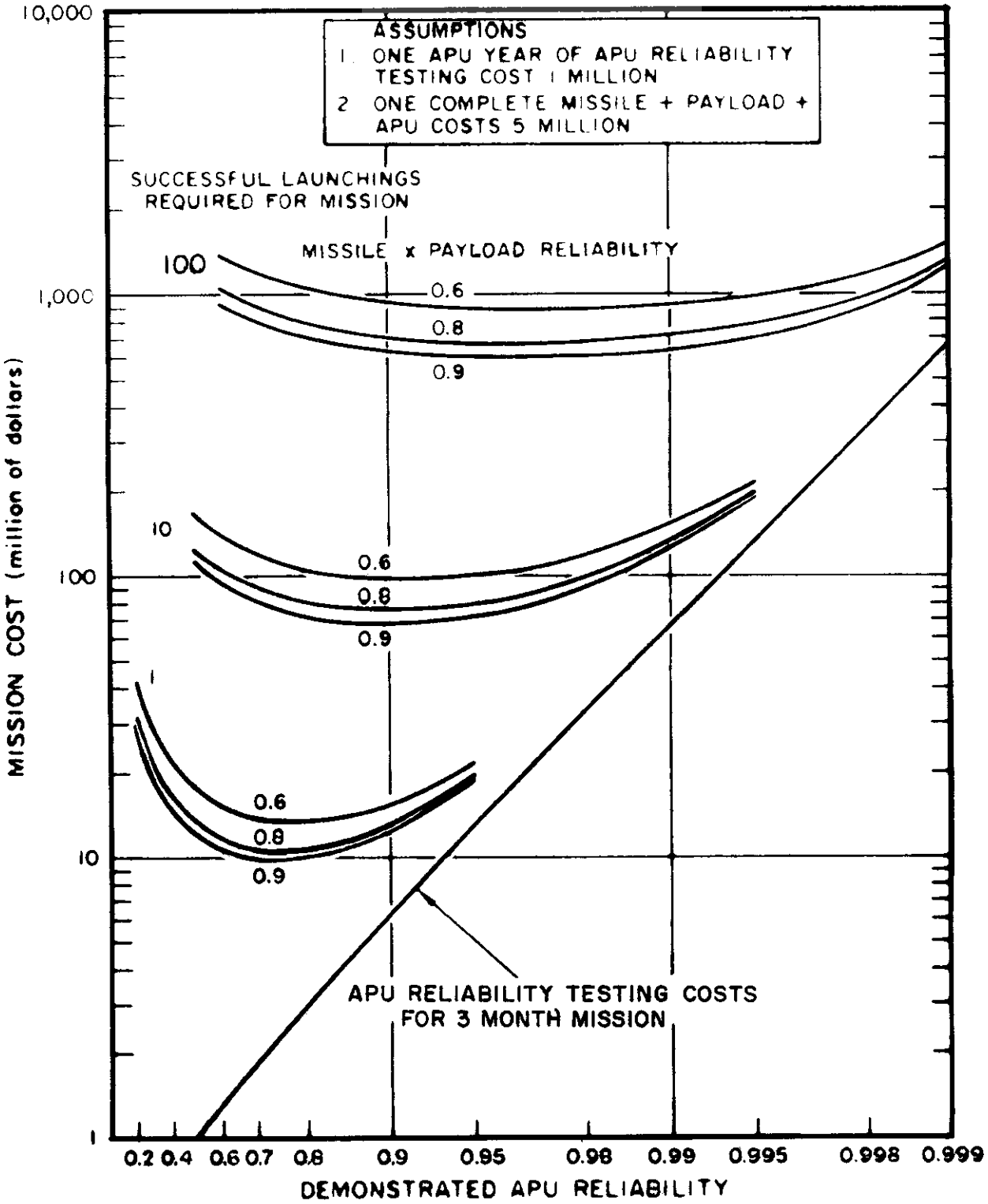

Figure 5-1. Optimum APU Reliability to Minimize 3 Month Mission Costs

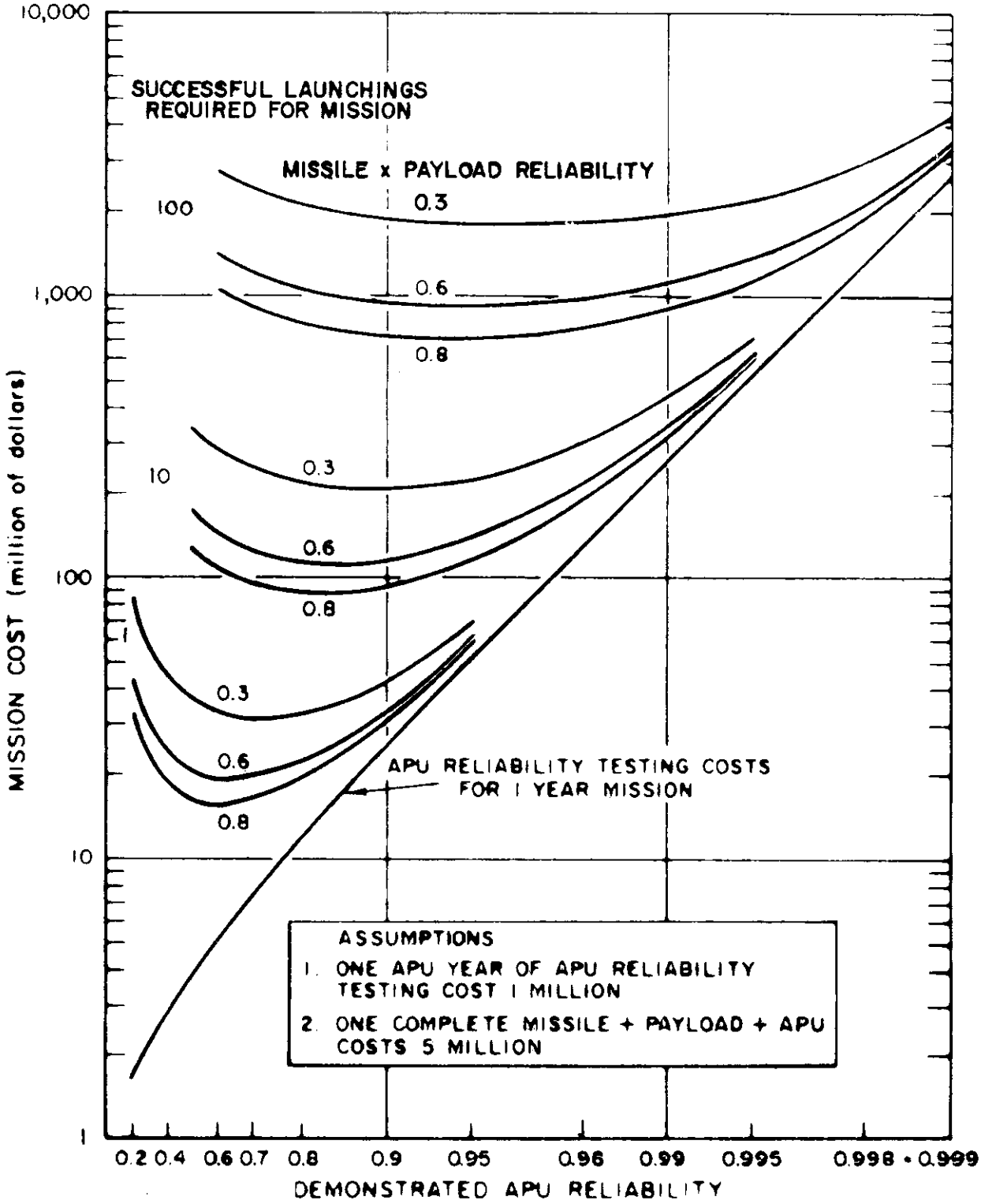

Figure 5-2. Optimum APU Reliability to Minimize 1 Year Mission Costs

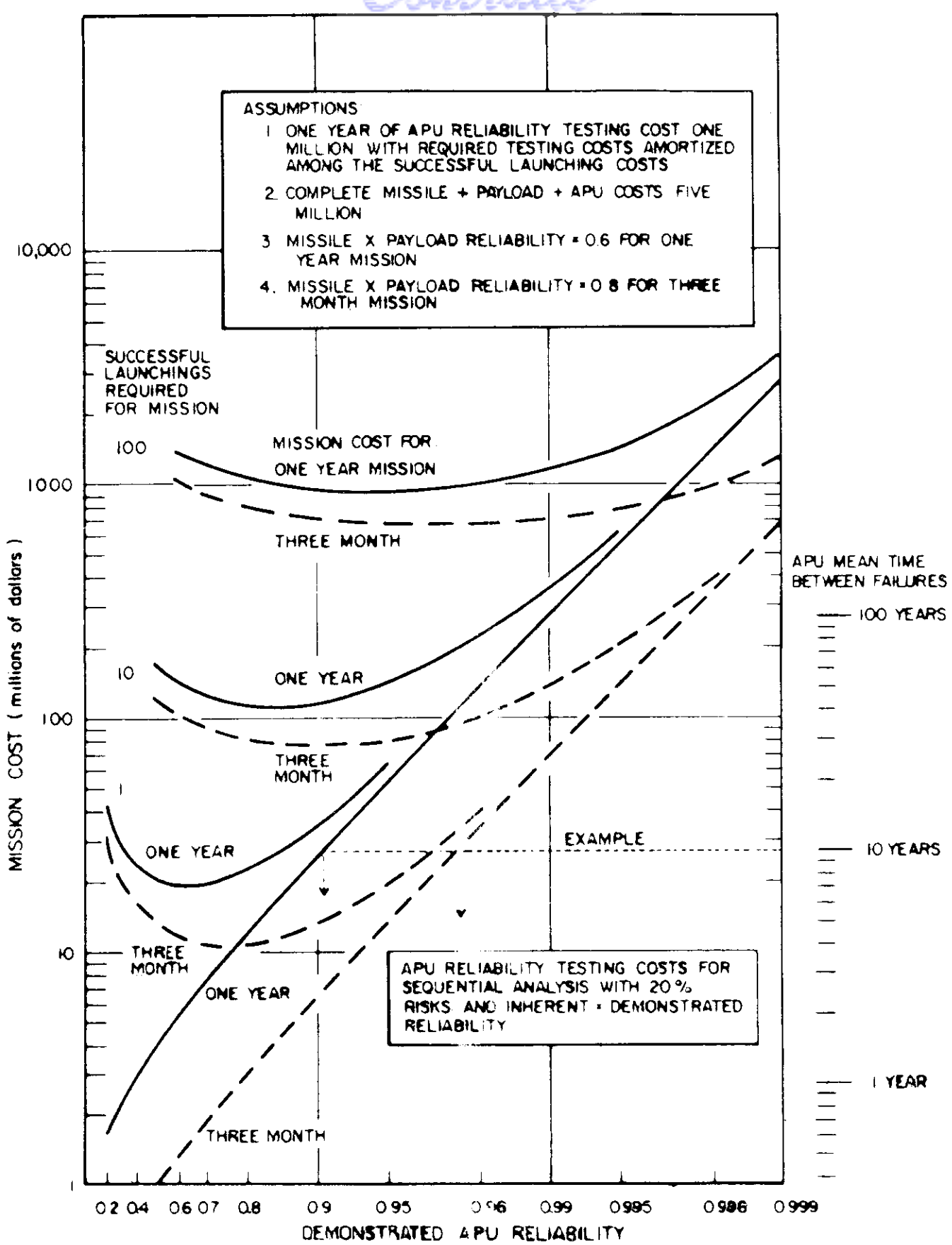

Figure 5-3. Optimum APU Reliability to Minimize Mission Costs

It is possible to estimate the optimum goals for space life of satellite systems from a similar formulation with the following substitutions in the definition of terms:

R_b = reliability of launching missile

R_s = reliability of satellite's APU and payload

a = cost of environmentally testing 1 satellite for 1 year

and

$$C_n = N \frac{b}{R_s R_b} - \frac{aEt}{\ln R_s}$$

at

$$\frac{dC_n}{dR_s} = 0$$

and

$$\frac{R_s}{(\ln R_s)^2} = \frac{Nb}{aEtR_b}$$

The optimum satellite reliability, R_s, is given by the last equation. By use of this solution to prepare Figure 5-4, the optimum satellite life, t, may be evaluated from Figure 5-4, as summarized in Table 5-1.

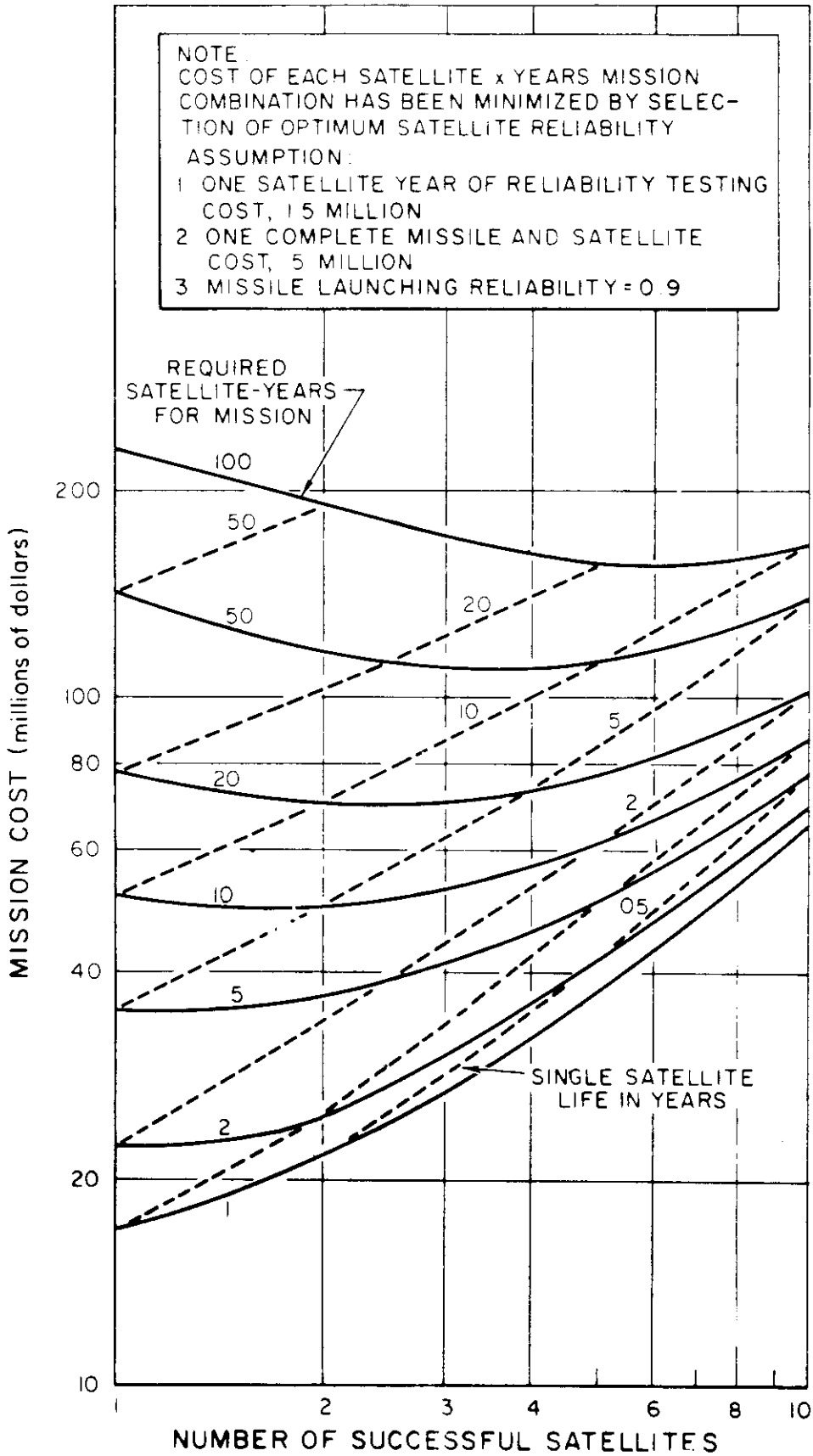

Figure 5-4. Mission Cost to Achieve a Given Satellite - Years Requirement

TABLE 5-1

OPTIMUM LIFE OF SATELLITE SYSTEMS

Number of Stations to be Filled	Total Mission in Satellite - Years	Minimum Cost Solution	
		Satellites	Single Satellite Life in Years
1	2	1	2
	5	1	5
	10	2	5
	20	3	6.7
	50	4	12.5
	100	6	16.7
3	5	3	1.7
	10	3	3.3
	20	3	6.7
	50	4	12.5
	100	6	16.7
6	20	6	3.3
	50	6	8.3
	100	6	16.7

It is clear that satellite systems with lives in excess of a year are reasonable economic goals.

5.2 Apportionment of Reliability

After the reliability goals of the system have been established, the individual reliability goals of the components in each environmental should be evaluated to guide the development and testing programs. For nuclear systems which are to be started up after achieving a stable orbit, there are three major unattended phases or environments which must be considered; launching, startup, and orbital life.

The first is the missile launch phase of which only the first 10 minutes is of importance in terms of possible damaging shock and vibrations. The shock and vibration testing may be conducted for many multiples of the 10 minutes boost phase, thereby permitting modifications and retests of failed components. Therefore, a high reliability apportionment should be allotted for this phase.

The startup phase may be time consuming with several functional steps in the startup procedure spaced by delays to achieve steady-state conditions. Several functions are of short duration and may be tested extensively; other functions are of a monitoring and control nature that must extend over the entire startup phase. Thus, the expectation of achieving and demonstrating reliability should be less for the startup phase than for the launch phase.

The last phase is the operation for extended time periods in space. This is the most difficult to demonstrate and as low a reliability as can be tolerated should be allotted to this phase.

It is convenient mathematically to use the expression failure rates, F, which are related to reliability, R, as follows:

$$R = e^{-Ft}$$

$$R = \prod_i R_i \text{ for series of i components}$$

$$e^{-Ft} = \prod_i E^{-F_i t}$$

and

$$F = \sum_i F_i$$

Thus, the failure rates are additive and are a quantity that may be allocated in proportion to estimates of the relative complexities or difficulties in achieving and demonstrating reliable components.

A further apportionment for particular components must be made for failure rates due to various modes of failure in order to guide design efforts. An example is the case of the radiator-condenser in which failure rates are apportioned by mode of failure as follows:

TABLE 5-2

RADIATOR-CONDENSER RELIABILITY

Radiator-condenser Mode of Failure in Orbital Life Environment	Failure Rate, F_3, (Failures/3 mo)
Micrometeorite tube penetration	0.020
Tube to header weld leakage	0.004
Significant subcooler tube blockages	0.001
	0.025

Of course, when the orbital life goals are increased beyond the initial 3 months, the tube shield design specifications would increase; e.g.:

Orbital Life	1 year probability for tube non-penetration by micrometeorites, P(O)
3 months	92 percent
6 months	96 percent
1 year	98 percent
2 years	99 percent

5.3 Effect of Redundancy

The reliability of systems with components that are functionally in series may be improved by adding components in parallel. However, in practice this often becomes difficult. If the parallel component is to be inactive until needed, a failure sensing and switching device which is itself very reliable must be provided. If the parallel component is to be active, the system must be able to tolerate both active components or both must operate at half capacity with a failure sensing and switching to full capacity device provided, as before.

Another difficulty is that to obtain any significant increase in reliability major sources of failure rates must be paralleled. The general description of reliability of n identical components in parallel, where x or fewer component failures may be tolerated, is as follows:

$$R = \sum_{x=0}^{x=X} \frac{n!}{(n - x)!\, x!} \; r^{n - x}(1 - r)^{x} \quad ,$$

Where r is the individual component reliability.

For two identical components in parallel (N = 2 and X = 1):

$$R = r^2 + 2r\,(1 - r)$$

Now consider the result if, for example, the SNAP-2 combined rotating unit, CRU, were paralleled with an identical unit and all necessary added switching devices had reliabilities of unity:

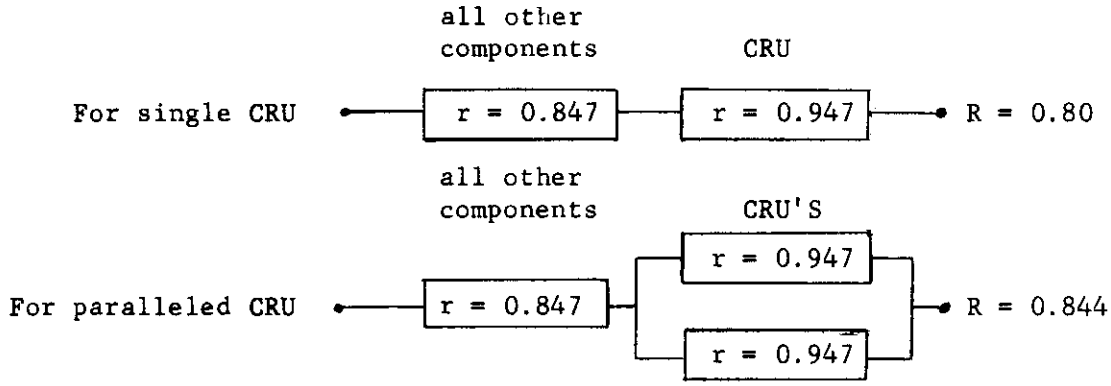

It would seem that redundant design for these systems is a difficult and weighty means to achieve a significant increase in reliability. Improved single component design is preferred.

5.4 Statistical Test Requirements to Demonstrate Reliability

The days of delivering a weapon system with ambiguous claims of quality and a firm handshake are gone. It is now necessary to present quantitative evidence of achieved quality or reliability. To provide this evidence requires extensive environmental testing. To minimize the expense of the testing program, sophisticated statistical techniques must be employed that allow statistical inference of the maximum amount of information from the minimum amount of test data.

The statistics in sequential analysis techniques have the desired sophistication and are well suited to monitoring testing programs on large systems. Sequential analysis is discussed extensively from the mathematician's viewpoint in a text by Wald[1] and briefly from the test engineer's viewpoint by Wilson[2]. Briefly, sequential analysis involves the following steps:

1. Assume a statistical distribution of failures like the binomial or Poisson. Distribution free procedures may be employed in sequential analysis to obtain more rigorous but more costly decisions.

2. Select two values of reliability, failure rates, or meantime between failures. One value should be at a level for satisfactory acceptance of the equipment and the other level that is intolerable; i.e., requires rejection of the equipment. The farther apart these values are selected, the more reliable will be the statistical decision as to which value is most likely to be correct.

3. Decide what fraction of the time decisions to accept must be correct, $1 - \alpha$; and what fraction of the time reject decisions must be correct, $1 - \beta$. The resulting sequential statistical analysis yields a test plan which may be presented graphically, as shown in Figure 5-5 for a particular set of conditions. The same conditions were used in Figure 5-6 to illustrate the relationship between three significant times; (1) environmental testing time with failures; (2) statistically demonstrated mean time between failures, θ_o; and (3) failure free service time with a particular reliability.

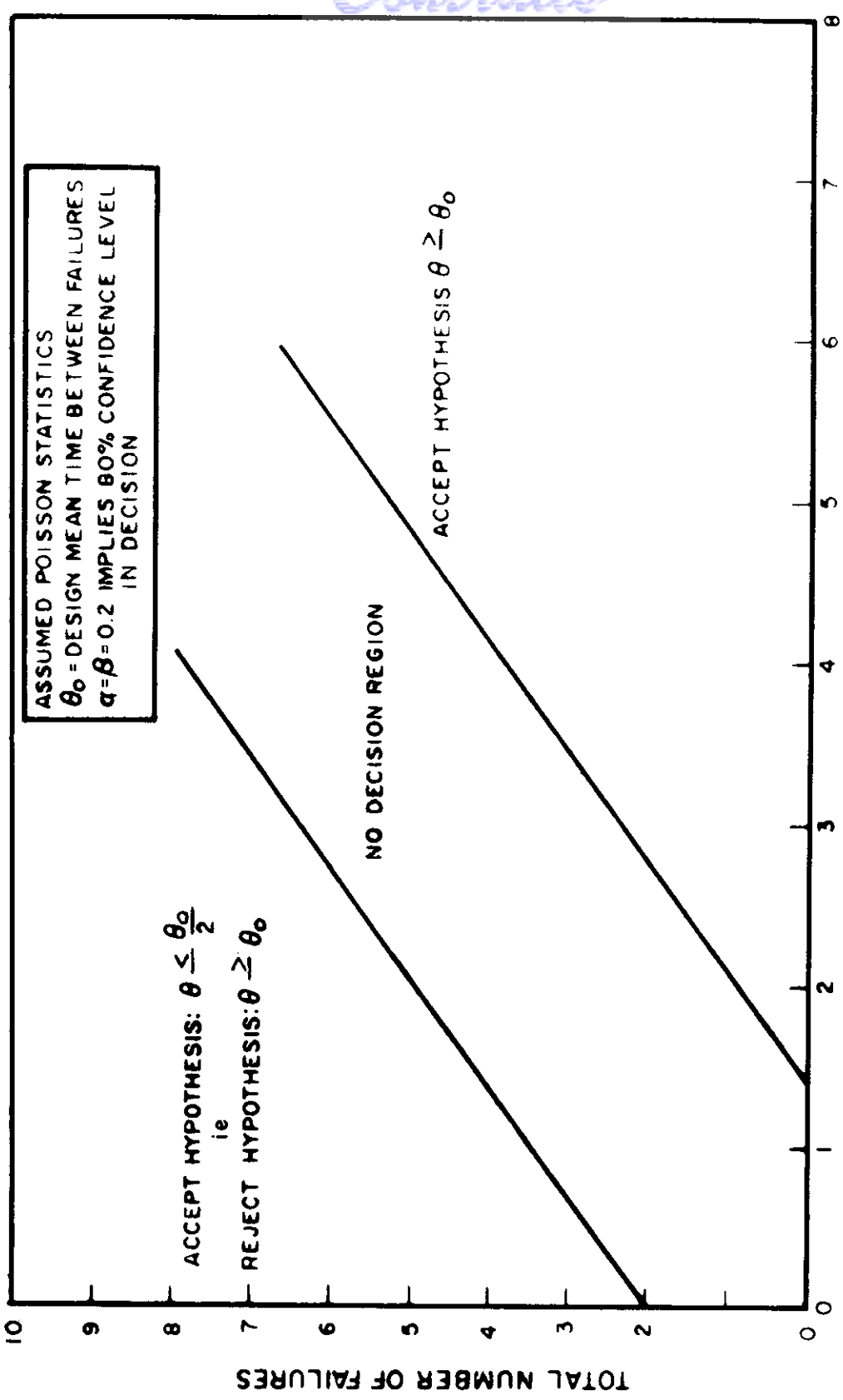

Figure 5-5. Sequential Test Plan

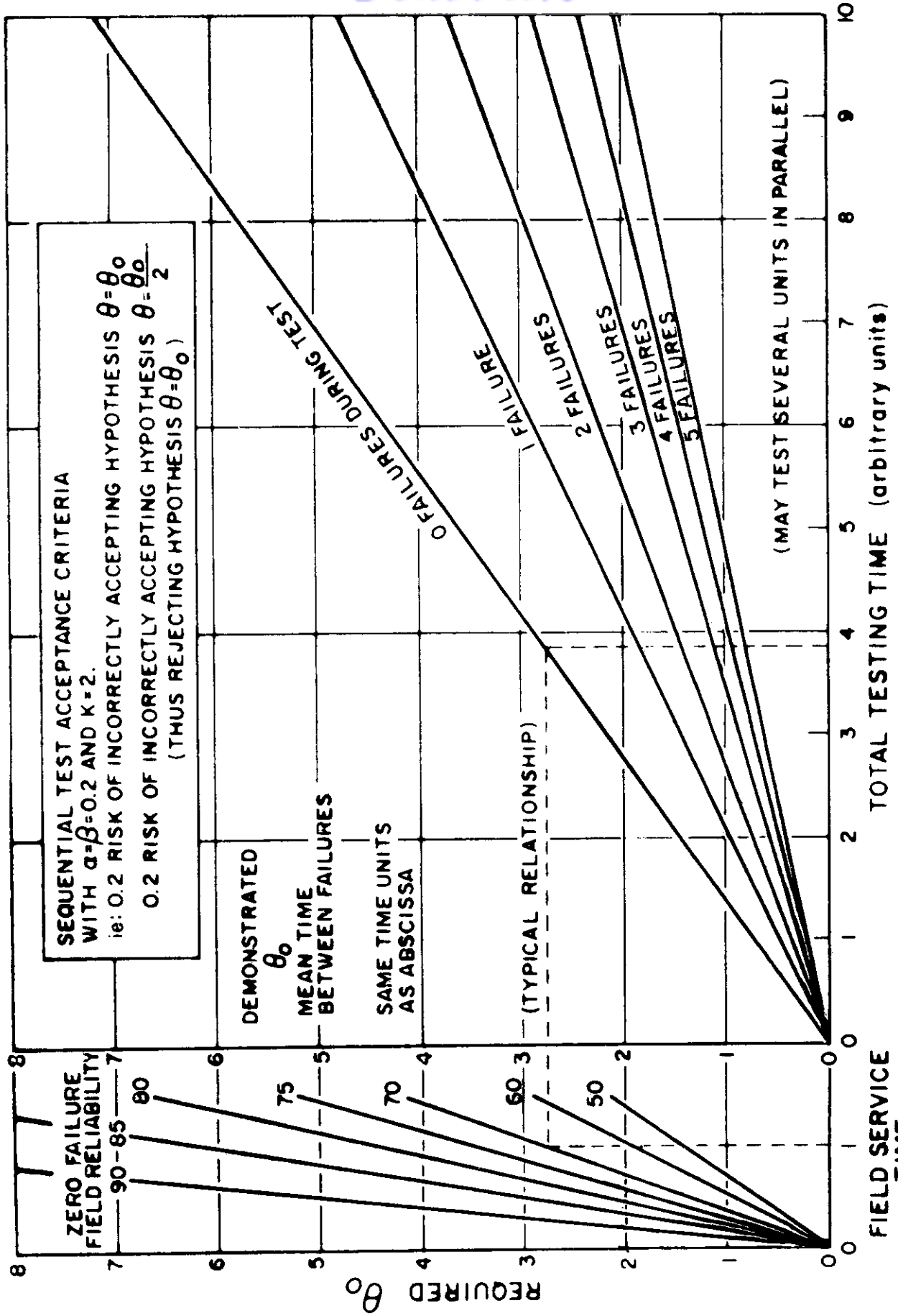

Figure 5-6. Relationship Between Field Service Time and Testing Time

According to Figure 5-5 it is possible for a particular set of test results to remain in the no-decision region indefinitely. Wald[1] has proven that the probability of arriving at a decision is unity if given infinite time, but this is not very gratifying. A more satisfactory solution is to truncate the testing after a certain amount of environmental operation and/or a certain number of failures. Wald[1] has developed the relation for the reduction in confidence of accept or reject decisions for truncated test plans.

There exists a certain expectation, E, for the magnitude of testing required to reach an accept or reject decision. The magnitude of E is dependent on the relation between inherent equipment reliability and statistically demonstrated reliability. For the test plan of Figure 5-5, the relation is as follows:

Inherent/Demonstrated Mean Time Between Failures	Expectation of Testing Time to Reach Accept Decision
θ/θ_o	$E = \theta_t/\theta_o$
1.0	2.7
1.5	2.25
0.0	1.4

The value of E = 2.7 was used in the estimate of reliability goals.

5,5 Present State of the Art of Reliability Design

In reliability design, what is desired is not arbitrarily beefed up designs but analytically controlled derating design procedures. An early engineering example of this is the determination of the required height of flood control dams. From a history of the randomness of weather conditions and consideration of local geographic conditions the dam height can be selected to contain any desired fraction of floods in a given time span.

Many components of electronic equipment now have test data on failure rates as a function of operation conditions in a particular environment.

For unique and complex mechanical and hydraulic equipment in a variety of launching and space environments, we have problems. What is needed is an extension and development of subjects such as the theory of extreme value. The variance of extreme stress conditions in an environment and extreme low strength conditions must be evaluated. Without such basic approaches reliability design will remain an empirical art.

REFERENCES

1. Abraham Wald, "Sequential Analysis," John Wiley and Sons, Inc., New York, 1947.

2. B. J. Wilson, "Reliability Evaluation of Aircraft and Missile Equipment I. Theory of Small Methods," U.S. Naval Research Laboratory, Washington, D.C., April 1958.